Applications of Functional Genomics in Studies of Yeast Signaling Networks and Genome Structure

by

Jun Ma

A dissertation submitted in partial fulfillment
of the requirements for the degree of
Doctor of Philosophy
(Molecular, Cellular and Developmental Biology)
in The University of Michigan
2008

Doctoral Committee:

Assistant Professor Anuj Kumar, Chair
Professor Arul M. Chinnaiyan
Professor Daniel J. Klionsky
Associate Professor Amy Chang

To my dad Longming Ma,

my mom Xiaorong Gu.

Acknowledgements

My greatest gratitude goes to my advisor and dissertation committee chair, Dr Anuj Kumar. His expertise and enthusiasm in scientific research led me into the field of functional genomics. Whenever I encountered difficulties in my research, I could go into Anuj's office and get instructions from him. Particularly I want to thank him for giving me freedom to explore the field I am interested in. Without his support I am not able to get training and knowledge in all aspects, which is essential for my future career.

I'd like to thank my dissertation committee members Dr. Daniel J. Klionsky, Dr. Amy Chang and Dr. Arul M. Chinnaiyan for their insightful criticism and valuable advice on my thesis.

I'd like to thank all the current and former members of the Kumar lab for their help and suggestions. Especially I want to thank Mr. Craig Dobry for his help and humorous.

I'd like to thank Dr. Daniel J. Klionsky and all the members in the Klionsky lab. Since the nature of my thesis project, Dr. Klionsky gave me a lot of detail guidance on my project and generously allowed me to use antibodies and equipments in his lab. The members in the Klionsky lab are all extremely nice and helpful. A special thank you to Zhifen Yang, Wei-lien Yan, Jiefei Geng, Congcong He, Yao Cao, Zhiping Xie, Heesung Cheong, Usha Nair and Ju Huang for providing me with protocols, helping me trouble

shooting experiments, discussing autophagy with me and letting me taste leftover from your group meeting. I also thank Mary Carr for her kindness and assistance.

I'd like to thank my friends Yanni Liu, Wei Zhao, Zhifen Yang, Xuan Wang, Hui Li, Jun Ni, Mengxi Jiang, Feng Wang, Brian Nord, Fidel Jimenez, Emmanuel Betrand and many others for their unconditional support.

This dissertation is dedicated to my parents for their endless love and support.

Chapter 2 of this dissertation has been published as:

Ma, J., Jin, R., Jia, X., Dobry, C.J., Wang, L., Reggiori, F., Zhu, J., and Kumar, A. (2007). An interrelationship between autophagy and filamentous growth in budding yeast. Genetics *177,* 205-214.

Chapter 3 of this dissertation has been published as:

Ma, J., Jin, R., Dobry, C.J., Lawson, S.K., and Kumar, A. (2007). Overexpression of autophagy-related genes inhibits yeast filamentous growth. Autophagy *3,* 604-609.

Chapter 4 of this dissertation has been published as:

Ma, J., Bharucha, N., Dobry, C.J., Frisch, R.L., Lawson, S., and Kumar, A. (2008). Localization of Autophagy-Related Proteins in Yeast Using a Versatile Plasmid-Based Resource of Fluorescent Protein Fusions. Autophagy *4,* 792-800.

Chapter 5 of this dissertation has been published as:

Ma, J., Dobry C.J., Krysan D.J. and Kumar, A. (2008) Unconventional genomic architecture in the budding yeast saccharomyces cerevisiae masks the nested antisense gene NAG1. Eukaryot Cell *7*, 1289-98.

Other publications:

Bharucha, N., Ma, J., Dobry, C.J., Lawson, S.K., Yang, Z., and Kumar, A. (2008). Analysis of the Yeast Kinome Reveals a Network of Regulated Protein Localization During Filamentous Growth. Mol. Biol. Cell *9*, 2708-17.

Geda, P., Patury, S., Ma, J., Bharucha, N., Dobry, C.J., Lawson, S.K., Gestwicki J.E., Kumar. A., (2008) A small molecule-directed approach to control protein localization and function. Yeast *25*, 577-94.

Table of Contents

List of Figures

List of Tables

Chapter 1

Introduction

The baker's yeast *Saccharomyces cerevisiae* has a long history of commercial utility and an equally important tradition as a workhorse for modern science. At present, *Saccharomyces cerevisiae* is the most thoroughly studied model organism in modern biological research due to its ease of manipulation and genetic tractability.

Several features of *Saccharomyces cerevisiae* make it an ideal model organism (Botstein, and Fink, 1988). It is non-pathogenic and has a rapid growth rate, with a doubling time of approximately 90 minutes. It is inexpensive to grow and maintain. It is stable in both the haploid and diploid state, thereby facilitating genetic analysis. Its haploid genome size is relatively small (1.2×10^7 bp) and is packaged into 16 well-characterized chromosomes (ranging in size from 230k bp to 2,352k bp)(Suter, Auerbach, and Stagljar, 2006). The yeast genome sequencing project, finished in 1996, estimated 6400 genes in the genome (Goffeau, Barrell, et al, 1996). The organization of the yeast genome is compact, with genes representing 70% of the total sequence. Only ~4% of yeast genes contain introns, which are usually close to the start of each coding sequence. Yeast genes and corresponding protein products are well annotated. Information regarding these genes is readily available through the Saccharomyces Genome Database (SGD) at www.yeastgenome.org. Compared against other eukaryotic model organisms, *S.*

cerevisiae has very active machinery for homologous recombination, allowing for the precise insertion of DNA sequence at specific genomic locations.

The budding yeast, as a unicellular organism, is obviously much less complex than a human being, whose genome has 25,000 coding genes classified into hundreds of cell types and arranged into multiple tissues and organs. Nonetheless, yeast has provided us with valuable information essential for the understanding of fundamental cellular processes, such as DNA repair mechanisms, protein metabolism, the cell cycle and even cancer signaling pathways. Since 40% of yeast proteins share amino acid sequence similarity with as least one human protein, the study of human disease related genes can also benefit from studies of orthologs in yeast (Bharucha, and Kumar, 2007). Although *Saccharomyces cerevisiae* normally doesn't cause infection, it can still be used as a model to learn more about pathogenic fungi; in particular, the study of yeast biology has informed our understanding of regulatory pathways and drug treatment, because *S. cerevisiae*, as a fungal species, shares many similar characteristics with its pathogenic relatives (Rappleye, and Goldman, 2006).

Yeast as a model for genomics

Upon completion of the yeast genome sequencing project, researchers could comprehensively study one organism at a number of levels for the first time in history. In addition to the basic genome itself, there are the transcriptome (the complete set of mRNA molecules), the kinome (the complete set of kinases), the proteome (the complete set of proteins) and the metabolome (the complete set of metabolites)(Oliver, 2002). The combination of information from all these levels will give us a whole picture of the

organism. Among these "omes", the genome is largely context independent and relatively stable, which makes it easier to be studied. A number of yeast genomic resources and technologies have been developed and have proven to be useful in discovering novel genes, revealing cellular mechanisms, and in identifying gene function and drug targets.

Yeast genome annotation and transposon mutagenesis

The first task to be done after completion of the yeast genome sequencing project was to accurately and completely annotate the genome. A number of computational and experimental approaches have been utilized to identify genes within genome sequence. Traditional computational methods for gene annotation include the comparison of sequence, motif, and structure with known proteins and translated expressed sequence tags (Wilson, Kreychman, and Gerstein, 2000). However, not every gene exhibits a clear ortholog or obvious motif. Experimental methods, such as gene cloning or microarray-based technologies to characterize expressed sequences from representative cDNA libraries were also used; however, weakly expressed genes or genes expressed only under certain conditions might be underrepresented in cDNA libraries. Since each method has its own shortcoming, none of them could provide comprehensive information for gene identification and annotation. To address this issue, an international consortium had set up standards for genome annotation (Mewes, Albermann, et al, 1997). The algorithm and criteria employed in this identification process tends to overlook open reading frames (ORFs) with a length less than 100 codons. Only small ORFs that correspond to known genes or have strong sequence similarity to known genes were annotated. ORFs nested

within longer ORFs on either the same or complementary strand were excluded. By this approach, some true genes may be overlooked, and other methods may be required to identify these genes.

Transposons are mobile genetic elements that can integrate themselves in the genome in a targeted or non-targeted manner. Because transposons can be used as effective lab tools for gene disruption and gene trapping, they can serve as part of a useful method for gene identification. In particular, transposon-based gene traps that insert without strong sequence bias into genomic DNA can be used to uncover genes, independent of previous conceptions regarding gene placement and organization. In yeast, transposons for genomic studies have been derived from either the endogenous yeast transposon Ty1 or from bacterial transposons. Since bacterial transposons exhibit less insertion site bias, they are particularly useful for large-scale genomic studies. The bacterial transposons used most extensively for genomic studies in yeast were derived from the transposon Tn3 or Tn7, containing a 5'-truncated *lacZ* reporter gene, a 3XHA epitope tag and selectable markers for yeast and bacteria (Vidan, and Snyder, 2001). Using these transposons, a yeast genomic library was mutagenized in *E. coli* first, followed by the excision of genomic DNA with the transposon insertion and transformation into yeast. The yeast transposon insertion mutants were then assayed for β-galactosidase activity to identify expressed sequences; by virtue of the promoter-less and 5'-truncated *lacZ* reporter, only insertions in frame with protein-coding sequence should yield β-galactosidase activity. By this approach, a collection of 28,428 yeast mutants with defined transposon insertion sites were generated, encompassing insertions affecting 3750 genes. (Craig, 1997) In addition to its utility as a simple gene trap, this

transposon-mutagenesis system can be used for various purposes, such as for detection of protein localization (Kumar, Agarwal, et al, 2002), and for the identification of phenotypes caused by the mutation. The transposon insertion point can be identified by sequencing outward from the insertion region. This transposon insertion mutant collection is uniquely useful as a tool for the discovery of novel genes. In Kumar *et al*. (Kumar, Harrison, et al, 2002), 137 novel genes were discovered using a similar method in combination with microarray analysis, such that coding sequence can be identified in a strand-specific manner. Among these genes, 107 of them were short, with a length of less than 100 codons. A previously overlooked class of genes nested antisense to other genes also emerged in this study. Similar kinds of antisense genes have been identified in other eukaryotes as protein-coding sequences or as naturally occurring RNA involved in regulatory processes. This novel group of genes could play some important roles in yeast as well. The principal shortcoming in these transposon-based approaches lies in the fact that transposon insertion is not completely random, and, thus, some regions of the genome may not be accessible to transposon mutagenesis.

Application of the yeast deletion strain collection

Through homologous recombination, a selected ORF in *S.cerevisiae* can be replaced by the precise and efficient integration of a cassette bearing a selectable marker (the *kanMX* cassette). The *kanMX* cassette itself has no phenotypic effect on yeast; it encodes resistance to the antifungal drug G418. In the 1990's, an international consortium of laboratories undertook a project to construct a collection of yeast deletion mutants, wherein each mutant would contain a precise start codon-stop codon

replacement of a gene with the *kanMX* cassette. In the final version of this collection, 5916 out of the approximately 6200 originally annotated yeast ORFs, including 1105 essential genes, were successfully deleted for the construction of a heterozygous diploid collection (Giaever, Chu, et al, 2002). Each deletion mutant is marked by a pair of molecular "barcodes" that identify the mutant uniquely. Because yeast cells are robust and fast growing, they are easy to be manipulated robotically in high-throughput format. Initially, this deletion collection was used to screen for drug sensitivity; the null strains that show growth defects in drug-containing medium are sensitive toward the cytotoxic or growth inhibitory effects of the specific compound. Since this deletion collection was first constructed; it has been tested under numerous drug treatments (Giaever, Flaherty, et al, 2004). The main advantage of the screens is to give us a comprehensive map of the chemical-genetic interactions between pathways targeted by the drug. The growth phenotype changes of deletion strains under different growth conditions including pH, high salt, sorbitol, minimal media, galactose, were also assayed. Several novel genes involved under specific growth conditions were identified. Functional groups of genes involved in the response to certain conditions were revealed as well.

In addition to haploid and homozygous deletion collections, the heterozygous gene deletion collection has proven to be a useful resource in identifying haploinsufficient genes under drug treatments or different conditions. The haploinsufficient profiling takes advantage of the fact that reducing gene dosage from two copies to one copy often increases sensitivity to the drug. In this way, researchers can identify previously missed targets of known inhibitors. Since viability is maintained even if an essential gene is deleted in heterozygous diploids, these haploinfufficiency screens

are also useful in studying the effects of compounds on essential genes (Giaever, Shoemaker, et al, 1999).

Another important application of the yeast deletion collection is in the synthetic genetic array (SGA) methodology, an approach involving the systematic construction of double mutants using the yeast deletion collection (Tong, and Boone, 2006). Synthetic lethality occurs when the deletion of non-essential genes combined within the same strain causes lethality. In this approach, a query strain with a specific mutation is mated with the entire haploid deletion collection of the opposite mating type. Through a tight sporulation condition and selection procedure, only haploid double mutants containing selection markers from the query and the deletion collection will be viable. The efficiency and reproducibility of the screen is enhanced by robotic high-density format pinning and replica printing. This method can reveal functionally redundant genes and pathways, subsequently linking them into networks (Davierwala, Haynes, et al, 2005; Ho, Gruhler, et al, 2002).

Furthermore, assuming that the toxicity of a drug mimics the loss-of –function mutation of the drug target, comparison of drug treatment profiles with a database of genetic interaction profiles may allow identification of the target pathway (Lum, Armour, et al, 2004) . The principle of SGA analysis can also be extended to look at the effect of gene overexpression in certain mutant backgrounds (Luesch, Wu, et al, 2005). As an alternative approach to investigate the functions of essential genes, a collection of tetracycline-regulated promoter replacement alleles was constructed for over two-thirds of all essential yeast genes, allowing for the analysis of cell cycle phenotypes upon

knockdown of essential gene expression (Sopko, Huang, et al, 2006; Zhu, Bilgin, et al, 2001).

Application of microarray technology

Perhaps not surprisingly, the budding yeast was an early test subject for DNA microarray technology. Presently, microarray technologies have become routine applications in molecular biology laboratories. Oligonucleotide and cDNA microarrays can simultaneously measure the expression of thousands of mRNAs, which has transformed the field of molecular biology from studying a few genes or pathways to more global investigations of cellular activity. This high throughput technique can be used to predict the function of unknown genes, to infer signaling networks, and to investigate the mechanisms by which a drug, disease mutation or environmental condition affects gene expression and cell function (Gasch, Spellman, et al, 2000; Hoheisel, 2006). For example, microarray technology has been used to measure gene expression in yeast under a variety of cell stress conditions. By comparing the expression pattern resulting from a given drug treatment with the expression patterns from treatments of drugs acting through known cellular mechanisms, one may infer mechanisms of drug action. Large databases have been produced to hold substantial quantities of gene expression information. Although transcription profiling only measures the quantity of mRNA, which is very volatile and prone to producing artifacts, this method still builds the foundation of systems biology. Designing adequately controlled experiments to draw biologically valid conclusions is crucial for the successful application of microarray technology (Curtis, Oresic, and Vidal-Puig, 2005). Since

different statistical data analysis methods may yield distinct results, a universal standard for data explanation is also needed to generate more reproducible and reliable data.

Applications of proteomics technology

Proteins are obviously an important class of functional entities in the cell. Therefore, among all levels of functional genomics analysis, proteomics stands as one of the most informative. Distinct from analysis of genome structure, which is quite stable, the proteome is context dependent and much harder to study.

One aspect that is critical for the understanding of protein function is protein localization within distinct subcellular compartments. Initial efforts for large-scale protein localization in yeast relied on transposon-mediated random epitope tagging and immunolocalization of overexpressed tagged proteins (Kumar, Agarwal, et al, 2002). To overcome potential errors caused by the random insertion strategy and fixation procedure, Erin O'Shea and colleagues constructed a collection of 6029 yeast strains, with each strain containing chromosomally integrated green fluorescent protein (GFP)-coding sequence at the 3' end of a target gene (Huh, Falvo, et al, 2003). This collection of carboxy-terminal GFP fusions allows for the visualization of protein localization in live yeast cells by expression from native promoters. Using this collection, the localization of 75% of the proteome was assigned to 23 localization categories based on subcellular compartments and organelles(Huh, Falvo, et al, 2003).

In complement to the chromosomally integrated GFP fusions collection, plasmid-based fluorescent protein fusion collections can be introduced into various genetic backgrounds easily for the analysis of protein localization (Bharucha, Ma, et al,

2008a)(Ma, Bharucha, et al, 2008). In combination with other existing collections, such protein localization studies can be used to identify examples of regulated protein localization in mutant alleles or in cells under conditions of stress. The GFP localization information can be combined with data from other functional genomics studies to confirm and extend predictions about protein functions. These predictions are especially useful in the case of proteins for which little or no functional data exist.

Another major focus of proteomics is the analysis of protein-protein interactions and the analysis of interactions leading to multi-protein complexes. Originally, the yeast two-hybrid system was developed to discover novel protein interactions among several proteins (Fields, and Song, 1989). The yeast two-hybrid system is very amenable to robotic platforms, and, despite the high rate of nonspecific interaction associated with this approach, high-throughput platforms have been develop to implement the yeast two-hybrid assay on a large scale (Krogan, Cagney, et al, 2006). The so-called "interactome" data suggests that there could be at least 12,000-18,000 possible protein interactions in yeast. Protein interactions and protein complex formation have also been assessed through approaches in which protein complexes are systematically isolated prior to the analysis of their components by mass spectrometry (Gavin, Aloy, et al, 2006) . By this approach, protein complexes are isolated by affinity purification of a tandem affinity (TAP)-tagged protein within the complex (Puig, Caspary, et al, 2001). The TAP-tagging method uses two tags instead of one to decrease the likelihood of nonspecific protein interaction. The TAP-tagged protein is expressed from its normal chromosomal locus to avoid the artifacts caused by protein overexpresion. After sequential purification over two high-affinity columns, the purified protein complex is eluted and separated by gel

electrophoresis, then identified by matrix assisted laser desorption/ionization time-of-flight MS (MALDI-TOF MS)(Wigge, Jensen, et al, 1998). A collection of carboxy-terminal TAP-tagged yeast strains has been constructed, and the level of expression of each protein was determined by sensitive Western-blotting that could detect low amounts of protein (Ghaemmaghami, Huh, et al, 2003). The purification of all yeast proteins and the identification of complex components by MALDI-TOF or LC-MS/MS are underway.

Although the development of commercially available proteome arrays is still in its infancy, protein microarray technology should be very beneficial for biochemical analysis and drug discovery procedures in the near future (Michaud, Salcius, et al, 2003).

As a summary for this section, functional genomics and proteomics have started a new era of biological research, with the promise of deep impact on the future of medical research. None of the methods presented above are without disadvantages, and, obviously, none of the technology is sufficient to explain the complexity of life in even a single-celled organism. The integration of information from all levels to create a "vertical" view is the prerequisite for the elucidation of the complex and interrelated processes that occur in biological systems. To make the most of current data, with the help of information technology, existing databases need to be refined and combined. Throughout these processes, the budding yeast will very likely continue to serve as an important testing ground for new technologies.

Nutrient sensing in yeast

Just like any living organism, *S.cerevisiae* cells possess the ability to sense the availability of nutrients in their surroundings and to make corresponding adjustments to transcriptional, metabolic, and developmental programs. Under conditions of nutrient limitation, these adjustments will minimize the energy spent in the cell, thereby maximizing the possibilities for survival (Bahn, Xue, et al, 2007).

Carbon source signaling

S.cerevisiae can grow on a variety of fermentable carbon sources (glucose, fructose, sucrose, galactose, etc) and non-fermentable carbon sources (glycerol, ethanol and lactate). Yeast cells prefer to use glucose and fructose rather than other sugars that need to be converted into glucose or fructose; yeast cells prefer any fermentable carbon source to any non-fermentable carbon source as well. The addition of glucose to cells growing in a non-fermentable carbon source initiates massive metabolic and transcriptional reprogramming. More than 40% of genes in yeast alter their expression level upon the addition of glucose. These changes increase the expression of genes functioning in ribosome biogenesis, allowing cells to use glucose as the sole carbon source (Schneper, Duvel, and Broach, 2004). Three signaling pathways function redundantly in the sensing process, protein kinase A (PKA), the Snf1p protein kinase, and Rgt2p, Snf3p glucose sensors.

The PKA pathway plays critical roles in growth, in cellular response to glucose and in cell cycle progression to mass accumulation (Kraakman, Lemaire, et al, 1999a).

Three genes, Tpk1p, Tpk2p and Tpk3p encode the catalytic subunits of PKA, with each gene product capable of monitoring somewhat overlapping sets of target proteins. Bcy1p is the regulatory subunit in PKA. The binding of Cyclic AMP (cAMP) to Bcy1p releases the catalytic subunits to perform their functions. The synthesis of cAMP is catalyzed by adenylate cyclase Cyr1p, and its degradation is catalyzed by phophodiesterases encoded by Pde1p and Pde2p. These genes function coordinately to control the balance of cAMP concentration. Two signaling pathway activate PKA, one mediated by Ras GTPase and the other through the G-protein coupled receptor Gpr1p and Gα homolog Gpa2p. (Jiang, Davis, and Broach, 1998)Only the GTP-bound Ras2p can bind to and stimulate adenylate cyclase Cyr1p(Colombo, Ma, et al, 1998; Colombo, Ronchetti, et al, 2004). The balance of GTP loading and GTP hydrolysis is controlled by guanine nucleotide exchange factor Cdc25p and GTPase activating proteins (GAPs), Ira1p and Ira2p. The addition of glucose results in a rapid increase in cAMP production, but the mechanism by which glucose increases Ras-GTP is still elusive. Just like other GPCR systems, Gpa2p functions as the Gα subunit, coupled with Gpr1p to activate cellular responses (Xue, Batlle, and Hirsch, 1998b). Since the defect in the *gpr1* and *gpa2* deletion strains can be suppressed by exogenous cAMP, this phenotype might indicate that Gpr1p and Gpa2p activate PKA through the activation of adenylate cyclase. (Kraakman, Lemaire, et al, 1999b)The β subunits might be Gpb1p/Krh1p and Gpb2p/Krh1p, with Gpg1p serving as the γ subunit. Although both pathways are associated with the modulation of PKA, some evidence shows that Ras2p play a more important role in mediating glucose-induced gene expression changes than Gpr1p-Gpa2p.

The Snf1p network is essential for growth on less preferred fermentable carbon sources and non-fermentable carbon sources. Snf1p is a member of the AMP-activated protein kinase family. The complete activation of Snf1p requires the phosphorylation of conserved residues and the association with β and γ regulatory subunits. The β subunit regulates substrate specificity. The binding with γ subunit causes a conformational change relieving Snf1p from autoinhibition. Once activated, the Snf1p complex phosphorylates numerous substrates, such as the transcriptional repressor Mig1p, the transcription factor Adr1p, Cat8p and Sip4p to regulates the expression of genes involved in use of alternate carbon sources. (Honigberg, and Lee, 1998)

Rgt2p and Snf3p encode transmembrane proteins that act as low and high affinity glucose sensors. Theses sensors bind to Mth1p and Std1p in conjunction with the transcription factor Rgt1p to repress transcription of hexose transporter genes, which import glucose or fructose into cells by diffusion along a gradient (Polish, Kim, and Johnston, 2005).

Nitrogen source signaling

As with carbon sources, *S.cerevisiae* doesn't use all nitrogen sources with equal efficiency. In order to use any nitrogen-containing compound, the yeast cell has to convert the compound into either glutamine or glutamate. Ammonia acts as a nitrogen donor for the synthesis of glutamate and glutamine. Ammonia can be converted into glutamate by glutamate dehydrogenase, or converted into glutamine by glutamine synthetase(Bahn, Xue, et al, 2007). Most amino acids can be catabolised and subsequently used as sources of nitrogen. While the favorable nitrogen source is used

rapidly and optimally, the utilization of less favorable nitrogen sources is repressed. This phenomenon is termed nitrogen catabolite repression. Good nitrogen sources, such as glutamine, glutamate or ammonium, support much higher growth rates.

The Gpr1p-Gpa2p GPCR system and the cAMP cascade were shown to form an important regulatory mechanism in response to the availability to ammonium. The Ssy1p-Prt3p-Ssy5p signaling system acts as a sensor for external amino acid concentrations (Andreasson, and Ljungdahl, 2004; Klasson, Fink, and Ljungdahl, 1999). Ssy1p is an amino acid sensor resembling an amino acid permease with the ability to activate downstream transcription factors. There are also three ammonium transporters, Mep1p, Mep2p and Mep3p, with Mep1p and Mep2p encoding high-affinity ammonium transporters and Mep3 encoding a lower affinity ammonium transporter. Deletion of all three ammonium transporters renders the yeast non-viable when grown on medium containing ammonium as the sole nitrogen source.

The internal amino acid concentration is sensed by the general control of amino acid biosynthesis (GCN) pathway. The signal for activation of the GCN pathway is uncharged tRNAs, which are bound by the kinase Gcn2p (Dong, Qiu, et al, 2000). The transcription factor Gcn4p is induced upon limitation of any amino acid and activates the expression of approximately 500 genes functioning in amino acid biosynthesis (Hinnebusch, 2005).

The Nitrogen Discrimination Pathway (NDP) is activated when there is no favorable nitrogen source available. The associated transcriptional network is complex and involves GATA family zinc-finger transcriptional activators and repressors, with the transcriptional activator Gln3p acting as the master regulator. When cells grow on poor

nitrogen sources, Gln3p localizes to the nucleus where it can bind to the promoters of NDP genes (Carvalho, Bertram, et al, 2001). When ammonium is available, Gln3p is in the cytoplasm. It is unclear, however, by which means the cytoplasmic glutamate and glutamine levels influence Gln3p localization and subsequent NDP gene activation. Yeast cells assimilate nitrogen from sources other than glutamate and glutamine by conversion to ammonium and the condensation with α-ketoglurarate to form glutamate. Therefore nitrogen regulation is tightly linked to the retrograde (RTG) response, regulating target genes that encode key enzymes of the TCA cycle necessary for the production of α-ketoglurarate (Magasanik, 2003).

The TOR signaling pathway

The *S.cerevisiae* targets of rapamycin, Tor1p and Tor2p, are functionally conserved PI3-like protein kinases that control growth related genes in response to nutrient condition. Tor2p and five other proteins comprise TORC2, which functions in regulating organization of the actin cytoskeleton and cell polarity. Tor1p or Tor2p, along with four other proteins, comprise TORC1, which regulates cell proliferation and the transition between growth and quiescence. Rapamycin treatment or lack of TOR shows a similar phenotype as cells starved for a carbon or nitrogen source. This phenotype includes inhibition of translation initiation, inhibition of ribosome biogenesis, sorting and turnover of nutrient permease, accumulation of glycogen, and induction of autophagy. The yeast TORs regulates downstream targets through a phosphatase switch composed of the type 2A-related phosphatase Sit4p, the PP2A/Sit4p-associated protein Tap42p, and the Tap42p-interacting protein Tip41p. Upon inactivation of the TOR complex, Sit4p

dissociates from its inhibitor Tap42p and gets activated (Yan, Shen, and Jiang, 2006). Activated Sit4p dephophorylates and activates several transcription factors, including Gln3p and Tip41p (Beck, and Hall, 1999; Bertram, Choi, et al, 2000). Under normal conditions, TOR represses starvation-specific transcription by keeping nutrient-responsive transcription factors, such as Gln3p, and stress-responsive transcription factors, Msn2p and Msn4p, in the cytoplasm.

The mechanism of filamentous growth

S.cerevisiae typically grows as single budding cells. In response to certain conditions of nutrient limitation, however, yeast cells, particularly those derived from Σ1278b, undergo a dimorphic transition from yeast-form growth to invasive-form growth (in a haploid strain), or pseudohyphal growth (in a diploid strain). This adaptation allows yeast cells to search for nutrient-rich substrates optimal for growth. Both haploid and diploid yeast strains can undergo filamentous growth as mentioned above, although there are some differences in the resulting phenotypes. Haploid filaments don't extend as significantly as do filaments in a diploid. In addition, diploids invade agar more strongly than haploids (Palecek, Parikh, and Kron, 2002). The signaling pathways for the two programs overlap significantly. In the rest of this section, pseudohyphal growth will be used to describe both programs.

In S.cerevisiae, nitrogen limitation induces pseudohyphal growth. Low concentrations of mating pheromone and short-chain alcohols such as butanol can also induce haploid pseudohyphal growth. Since this dimorphic transition is directly related with the virulence of human pathogens such as *Candida albicans* and *Cryptococcus*

neoformans, insight into virulence mechanisms can be gained from research on *S.cerevisiae*. Furthermore, the reorientation and polarization of the actin cytoskeleton in response to environmental signals during pseudohyphal growth are similar to rearrangements observed during the transition of cancer cells to a metastatic state. During pseudohyphal growth, the cells are elongated, budding occurs synchronously in a unipolar fashion, and the mother and daughter cells remain physically attached, producing chains of cells (Pan, Harashima, and Heitman, 2000). As a consequence, smaller cells spend more time in the G1 phase before reaching critical size for entry into S phase. An extended G2/M phase is also needed for the separation of mother and daughter cells. Branching filaments permit wider exploration of surroundings with lower energy cost. Highly polarized growth promotes invasion into the substrate. The high-surface-to-volume ratio of filaments also facilitates nutrient transport.

There are at least two major signaling pathways involved in yeast pseudohyphal growth. The first pathway is a MAP kinase pathway; this pseudohyphal growth MAPK pathway shares many components with the pheromone-induced MAPK mating pathway in haploid cells. The second pathway is a cAMP-dependent pathway, which has been mentioned previously. Initial studies suggested that Ras2p might be the central switch for both pathways; however, there is still no information on the mechanism by which Ras2p is activated in conditions leading to pseudohyphal growth (Pan, Harashima, and Heitman, 2000).

MAP kinase pathway

Upon receiving appropriate environmental cues, Ras2p is activated; this activates the guanine nucleotide exchange factor Cdc42p, which, in turn, activates GTP-Cdc24p. Activated Cdc24p interacts with the protein kinase Ste20p, targeting it towards the site of growth. Ste20p subsequently activates the MAP kinase cascade formed by the MAPKKK Ste11p, the MAPKK Ste7p and the MAPK Kss1p. The unphosphorylated form of Kss1p binds to the transcription factor Ste12p and the negative regulators Dig1p and Dig2p (Madhani, and Fink, 1997). After Kss1p is phosphorylated, Ste12p is phosphorylated by Kss1p, causing the dissociation of the Dig proteins. The target genes of Ste12p are then released from repression. One common feature of these genes is an element called FRE (for Filamentous and invasive Response Element) present in their promoter regions. These are composite elements with two adjacent binding sites for the binding of transcription factors Ste12p and Tec1p. Since the MAP kinase pathway shares elements with other regulatory pathways, such as the mating pathway and high osmolarity response pathway, yeast has developed mechanisms to prevent inappropriate cross talk between the pathways. Each pathway utilizes a specific MAPK: Kss1p is involved in pseudohyphal growth, Hog1p in osmotic stress, and Fus3p in mating. The scaffolding proteins and interacting transcription factors for each response are also different (Flatauer, Zadeh, and Bardwell, 2005).

cAMP-PKA pathway

Since pseudohyphal growth is the cellular response to nutrient deprivation, it is not surprising that the nutrient-sensing cAMP pathway regulates pseudohyphal growth. As mentioned before, this pathway involves the G-protein-coupled receptor Gpr1p, the α subunit Gpa2p, the cAMP-depended protein kinases, and the downstream transcription factors Flo8p and Sfl1p. The Gpr1p-Gpa2p system which regulates cAMP production in response to glucose is required for pseudohyphal growth (Xue, Batlle, and Hirsch, 1998a). Exogenous cAMP enhances pseudohyphal growth; mutation of the negative regulatory subunit Bcy1p dramatically increases filamentation (Pan, and Heitman, 1999).

The three catalytic subunit of PKA also play important roles in pseudohyphal growth, with Tpk2p activating pseudohyphal growth, and Tpk1p and Tpk3p repressing filamentation. The target of Tpk2p is the transcription factor Flo8p, which is mutated in the common lab strain S288C; accordingly, S288C and its derivatives do not undergo pseudohyphal growth (Liu, Styles, and Fink, 1996). It has also been reported that the Ras2p/cAMP pathway is overactive in the Σ1278b strain. Flo8p regulates the expression of the surface floculin Flo11p (also called Muc1p), which contributes to agar invasion. Flo11p is a common target for both the cAMP pathway and MAP kinase pathway. Tpk2p relieves the inhibitory effect of transcription factor Sfl1p on the expression of Flo11p. The *FLO11* promoter is much larger than most yeast promoters, and the expression level of *FLO11* has a direct link with the pseudohyphal growth phenotype (Halme, Bumgarner, et al, 2004).

Other genes involved in the regulation of filamentous growth

Distinct from the two pathways described above, there are a number of additional genes involved in the regulation of pseudohyphal growth, such as the transcription factors Phd1p, Sok2p and Ash1p (Gagiano, Bauer, and Pretorius, 2002; Pan, Harashima, and Heitman, 2000). Since the absence of the transcriptional activator Msn1p and Mss11p could be partially compensated by the expression of Flo11p, these two genes may bind to the promoter of *FLO11*. Ammonium permease Mep2p is also needed for pseudohyphal growth (Lorenz, and Heitman, 1998). A mutation in the glutamine $tRNA_{CUG}$ allows pseudohyphal growth in a nitrogen-rich medium where cells grow exclusively in the yeast form (Murray, Rowley, et al, 1998).

Since the regulation of cell shape is coupled to the cell cycle, recent studies indicate that both the G1 cyclins Cln1p, Cln2p, and Cln3p and the Clb2p mitotic cyclin may play roles in pseudohyphal growth. In particular, *cln1* and *cln2* mutations inhibit filament formation, whereas *cln3* mutations enhance filamentation. The *ure2* and *gln3* mutants, functioning in the nitrogen discrimination pathway, fail to exhibit pseudohyphal growth in response to nitrogen starvation. Mutations in genes required for bipolar budding in diploids such as Bud1p, Bud5p or Bud8p prevent pseudohyphal growth (Cullen, and Sprague, 2002). Pseudohyphal growth could be inhibited by sublethal concentration of rapamycin, which indicate a role for the TOR pathway in the regulation of pseudohyphal growth (Schmelzle, Beck, et al, 2004).

The mechanism of autophagy

Another mechanism for yeast cells to survive under conditions of nutrient deprivation is autophagy. Autophagy is a vacuolar degradation pathway for bulk proteins and organelles, in contrast to the ubiquitin-proteasome system which degrades specific short-lived proteins (Nair, and Klionsky, 2005). Upon nutrient starvation, a double-membrane vesicle, termed the autophagosome, is generated to sequester cytoplasmic material. The formation of the autophagosome takes place at the perivacular, pre-autophagosomal structure (PAS). The autophagosome then fuses with the vacuole, delivering the inner single-membrane vesicle into the vacuolar lumen. The resulting autophagic body is lysed; small molecules are released back into the cytosol and reused for the synthesis of new proteins required for cell survival. Autophagy also occurs in other eukaryotes such as in mammals, insects and worms. In higher eukaryotes, autophagy is induced in response to conditions of nutrient depletion as well. Autophagy is also involved in other cellular processes such as cellular development and differentiation. Autophagy has been related to the protective mechanism of several diseases, such as cancer, muscular disorders and neurodegenerative diseases (Yorimitsu, and Klionsky, 2005).

To date, approximately 30 autophagy related genes (ATG) have been shown to function in the process of autophagy. The biosynthetic cytoplasm-to-vacuole targeting (Cvt) and pexophagy pathways are very similar to the autophagy pathway. Some ATG genes are shared among these pathways (Harding, Hefner-Gravink, et al, 1996; Scott, Hefner-Gravink, et al, 1996). The difference is that the Cvt and pexophagy pathway are

selective processes. Two vacuolar hydrolases, Ape1p and Ams1p, are transported within Cvt vesicle into the vacuole through the Cvt pathway. Compared with the autophagosome, the Cvt vesicle is much smaller in size.

In addition to nitrogen, carbon and auxotrophic depletion, autophagy can be induced by the antibiotic rapamycin whose effects mimic starvation. TOR1C and PKA have been shown to participate in the induction of autophagy (Noda, and Ohsumi, 1998). Under nutrient deprivation conditions or upon addition of rapamycin, the Tor kinase is inactivated, and autophagy is enhanced. Constitutive activation of PKA could prevent the induction of autophagy. Rapamycin treatment or nitrogen starvation leads to a rapid dephosphorylation of Atg13p that facilitates the interaction of Atg13p with Atg1p and Atg17p (Kabeya, Kamada, et al, 2005). Atg1p is a kinase. Its kinase activity is stimulated by the formation of the complex, but the role of Atg1p kinase activity and its relationship with the PKA pathway is still not clear(Kamada, Funakoshi, et al, 2000). The formation of the Atg1p-Atg13p-Atg17p complex may regulate autophagosome formation. As for the Cvt pathway, Atg11p and Atg19p play an important role in the formation of Cvt vesicles. Neither Atg11p nor Atg19p is required for bulk nonselective autophagy. The Atg19p-Atg8p-phosphatidylethanolamine (Atg8-PE) interaction might function to exclude the entry of nonspecific cytosolic components into Cvt vesicles.

The building material for the autophagosome is not from pre-existing organelles. The site for vesicle formation is the PAS. Most ATG genes are involved in this process, more or less. The PtdIns 3-kinase complex I might generate phosphatidylinositol 3-phosphate (PtdIns(3)P), which recruits several ATG genes to the PAS, including Atg18p, Atg20p, Atg21p, Atg24p and Atg27p. Two ubiquitin-like conjugation systems, Atg8p-PE

and Atg12p-Atg5p are involved in the generation of autophagic vesicles as well (Ohsumi, 2001). The formation of the Atg12p-Atg5p conjugation system is helped by the E1 ubiquitin-activating enzyme homolog Atg7p and the homolog of the E2 ubiquitin-activating enzyme Atg10p. The conjugation of Atg8p to PE also occurs by a ubiqutin-like procedure with the help of the E1-like Atg7p and E2-like enzyme Atg3p. Atg9p is required for their localization to the PAS. These two complexes function in the expansion and curvature formation of the membrane. The Atg12p-Atg5p-Atg16p complex seems to dissociate from vesicles before or immediately after completion of the autophagosome; Atg8p-PE remains associated with the autophagosome and is finally degraded in the vacuole. Actually, most of the core machinery ATG genes are excluded from the completed vesicle.

Since the localization of Atg9p is distributed among several punctate structures across the cell, including the PAS, it has been proposed to play some roles in the delivery of lipid membrane to vesicles; this process is essential for vesicle expansion (He, Song, et al, 2006). The source of the membrane might be the mitochondria. The retrieval of Atg9p from the PAS depends on the Atg1p-Atg13p complex, Atg2p and Atg18p. The absence of any of these proteins causes the accumulation of Atg9p at the PAS.

After completion of the vesicle, the autophagosome fuses with the vacuole. The inner membrane of the autophagosome is delivered into the vacuole, and the content material is degraded by the vacuolar hydrolases. Atg15p is involved in the intravascular lysis process. After degradation, monomeric units are exported to the cytosol for reuse. Atg22p has been identified as an amino acid effluxer that functions together with other vacuolar permeases to export amino acids (Yang, Huang, et al, 2006).

Thesis Summary

As described in this chapter, a substantial amount of knowledge has been acquired about the networks mediating yeast cell responses to various quantities and qualities of nutrients. Although the intracellular signaling pathway of each of these cellular processes has been characterized to some degree, a major task still remains to connect these pathways into one system. Some of the overlapping components among different pathways have been mentioned above; for example, the PKA, MAPK and TOR signaling pathways activated by various extracellular stimuli elicit the activation of completely different group of genes, yet the survival of yeast cells depends on all of them. Obviously, other inter-connections exist between pathways to provide responses to different levels of nutrient combinations. However, focused studies in each pathway may not help us view the response network as a whole. More global and large-scale methods may need to be applied to gain this information. Meanwhile, the nutrient response network also provides a good model system to test the usability of novel genomic collections and approaches.

Although autophagy and pseudohyphal growth are both responsive to nitrogen stress, a link between these processes has not been investigated. So in the first part of my thesis, I consider a possible link between these processes, detecting extensive upregulation of the pathway governing autophagy during early pseudohyphal growth by microarray-based expression profiling(Ma, Jin, et al, 2007b). Both processes are active under conditions of nitrogen stress. The inhibition of autophagy results in increased pseudohyphal growth. This result suggests a model in which autophagy mitigates nutrient

stress, delaying the onset of pseudohyphal growth. On the other hand, inhibition of autophagy exacerbates nitrogen stress, resulting in precocious and overactive pseudohyphal growth.

Next, we extended our studies to encompass a phenotypic analysis of pseudohyphal growth upon overexpression of ATG genes(Ma, Jin, et al, 2007a). Several ATG genes were shown to inhibit pseudohyphal growth upon overexpression. This result indicates that there might be additional undefined regulatory mechanisms linking autophagy and pseudohyphal growth, possibly independent of the upstream nitrogen-sensing machinery.

We have constructed a plasmid-based collection of yeast gene fusions with fluorescent proteins to facilitate systematic studies of protein localization under different genetic background and under varying conditions of nutrient availability. A suite of low-copy destination vectors containing different fluorescent proteins have been generated as part of this work. A sub-collection of 276 genes encoding caboxy-terminal fusions to yellow fluorescent protein (vYFP) has been constructed; this collection includes genes functioning as kinases, transcription factors and signaling proteins. In particular, the kinase collection has been used to observe protein localization shifts under pseudohyphal growth-inducing condition (Bharucha, Ma, et al, 2008b). The localization of 14 autophagy-related genes in wild type and *atg11* deletion strain have also been investigated(Ma, Bharucha, et al, 2008). This plasmid-based resource of yeast gene-vYFP fusions provides an initial toolkit for a variety of systematic and large-scale localization studies exploring pathway biology in the budding yeast.

In the last part of this thesis, I describe the identification and analysis of a novel yeast gene, *NAG1*. Previous genome-wide transposon-tagging studies putatively identified a 19-kDa protein nested entirely within the coding sequence of YGR031W in an antisense orientation on the opposite strand. We have characterized this gene, *NAG1*, further through a variety of studies. Phenotypic analysis of a site-directed mutant (*nag1-1*) disruptive of Nag1 but silent with respect to YGR031W, defines a role for Nag1 in yeast cell wall biogenesis; microarray profiling of *nag1-1* indicates decreased expression of genes contributing to cell wall organization, and the *nag 1-1* mutant is hypersensitive to the cell wall perturbing agent Calcofluor white. Furthermore, production of Nag1p is dependent upon the presence of the cell wall integrity pathway MAPK Slt2p and its downstream transcription factor Rlm1p (Ma, Bharucha, et al, 2008). Thus, *NAG1* represents the first identified nested antisense protein-coding gene in yeast, with an interesting function in yeast cell wall biogenesis. Furthermore, the identification of this gene raises the possibility that additional nested genes may reside in the yeast genome.

References

Andreasson, C., and Ljungdahl, P.O. (2004). The N-terminal regulatory domain of Stp1p is modular and, fused to an artificial transcription factor, confers full Ssy1p-Ptr3p-Ssy5p sensor control. Mol. Cell. Biol. *24,* 7503-7513.

Bahn, Y.S., Xue, C., Idnurm, A., Rutherford, J.C., Heitman, J., and Cardenas, M.E. (2007). Sensing the environment: lessons from fungi. Nat. Rev. Microbiol. *5,* 57-69.

Beck, T., and Hall, M.N. (1999). The TOR signalling pathway controls nuclear localization of nutrient-regulated transcription factors. Nature *402,* 689-692.

Bertram, P.G., Choi, J.H., Carvalho, J., Ai, W., Zeng, C., Chan, T.F., and Zheng, X.F. (2000). Tripartite regulation of Gln3p by TOR, Ure2p, and phosphatases. J. Biol. Chem. *275,* 35727-35733.

Bharucha, N., and Kumar, A. (2007). Yeast genomics and drug target identification. Comb. Chem. High Throughput Screen. *10,* 618-634.

Bharucha, N., Ma, J., Dobry, C.J., Lawson, S.K., Yang, Z., and Kumar, A. (2008a). Analysis of the Yeast Kinome Reveals a Network of Regulated Protein Localization During Filamentous Growth. Mol. Biol. Cell

Bharucha, N., Ma, J., Dobry, C.J., Lawson, S.K., Yang, Z., and Kumar, A. (2008b). Analysis of the Yeast Kinome Reveals a Network of Regulated Protein Localization During Filamentous Growth. Mol. Biol. Cell

Botstein, D., and Fink, G.R. (1988). Yeast: an experimental organism for modern biology. Science *240,* 1439-1443.

Carvalho, J., Bertram, P.G., Wente, S.R., and Zheng, X.F. (2001). Phosphorylation regulates the interaction between Gln3p and the nuclear import factor Srp1p. J. Biol. Chem. *276,* 25359-25365.

Colombo, S., Ma, P., Cauwenberg, L., Winderickx, J., Crauwels, M., Teunissen, A., Nauwelaers, D., de Winde, J.H., Gorwa, M.F., Colavizza, D., and Thevelein, J.M. (1998). Involvement of distinct G-proteins, Gpa2 and Ras, in glucose- and intracellular acidification-induced cAMP signalling in the yeast Saccharomyces cerevisiae. EMBO J. *17,* 3326-3341.

Colombo, S., Ronchetti, D., Thevelein, J.M., Winderickx, J., and Martegani, E. (2004). Activation state of the Ras2 protein and glucose-induced signaling in Saccharomyces cerevisiae. J. Biol. Chem. *279,* 46715-46722.

Craig, N.L. (1997). Target site selection in transposition. Annu. Rev. Biochem. *66,* 437-474.

Cullen, P.J., and Sprague, G.F.,Jr. (2002). The roles of bud-site-selection proteins during haploid invasive growth in yeast. Mol. Biol. Cell *13,* 2990-3004.

Curtis, R.K., Oresic, M., and Vidal-Puig, A. (2005). Pathways to the analysis of microarray data. Trends Biotechnol. *23,* 429-435.

Davierwala, A.P., Haynes, J., Li, Z., Brost, R.L., Robinson, M.D., Yu, L., Mnaimneh, S., Ding, H., Zhu, H., Chen, Y. *et al*. (2005). The synthetic genetic interaction spectrum of essential genes. Nat. Genet. *37,* 1147-1152.

Dong, J., Qiu, H., Garcia-Barrio, M., Anderson, J., and Hinnebusch, A.G. (2000). Uncharged tRNA activates GCN2 by displacing the protein kinase moiety from a bipartite tRNA-binding domain. Mol. Cell *6,* 269-279.

Fields, S., and Song, O. (1989). A novel genetic system to detect protein-protein interactions. Nature *340,* 245-246.

Flatauer, L.J., Zadeh, S.F., and Bardwell, L. (2005). Mitogen-activated protein kinases with distinct requirements for Ste5 scaffolding influence signaling specificity in Saccharomyces cerevisiae. Mol. Cell. Biol. *25,* 1793-1803.

Gagiano, M., Bauer, F.F., and Pretorius, I.S. (2002). The sensing of nutritional status and the relationship to filamentous growth in Saccharomyces cerevisiae. FEMS Yeast Res. *2,* 433-470.

Gasch, A.P., Spellman, P.T., Kao, C.M., Carmel-Harel, O., Eisen, M.B., Storz, G., Botstein, D., and Brown, P.O. (2000). Genomic expression programs in the response of yeast cells to environmental changes. Mol. Biol. Cell *11,* 4241-4257.

Gavin, A.C., Aloy, P., Grandi, P., Krause, R., Boesche, M., Marzioch, M., Rau, C., Jensen, L.J., Bastuck, S., Dumpelfeld, B. *et al*. (2006). Proteome survey reveals modularity of the yeast cell machinery. Nature *440,* 631-636.

Ghaemmaghami, S., Huh, W.K., Bower, K., Howson, R.W., Belle, A., Dephoure, N., O'Shea, E.K., and Weissman, J.S. (2003). Global analysis of protein expression in yeast. Nature *425,* 737-741.

Giaever, G., Chu, A.M., Ni, L., Connelly, C., Riles, L., Veronneau, S., Dow, S., Lucau-Danila, A., Anderson, K., Andre, B. *et al*. (2002). Functional profiling of the Saccharomyces cerevisiae genome. Nature *418,* 387-391.

Giaever, G., Flaherty, P., Kumm, J., Proctor, M., Nislow, C., Jaramillo, D.F., Chu, A.M., Jordan, M.I., Arkin, A.P., and Davis, R.W. (2004). Chemogenomic profiling: identifying the functional interactions of small molecules in yeast. Proc. Natl. Acad. Sci. U. S. A. *101,* 793-798.

Giaever, G., Shoemaker, D.D., Jones, T.W., Liang, H., Winzeler, E.A., Astromoff, A., and Davis, R.W. (1999). Genomic profiling of drug sensitivities via induced haploinsufficiency. Nat. Genet. *21,* 278-283.

Goffeau, A., Barrell, B.G., Bussey, H., Davis, R.W., Dujon, B., Feldmann, H., Galibert, F., Hoheisel, J.D., Jacq, C., Johnston, M. *et al*. (1996). Life with 6000 genes. Science *274,* 546, 563-7.

Halme, A., Bumgarner, S., Styles, C., and Fink, G.R. (2004). Genetic and epigenetic regulation of the FLO gene family generates cell-surface variation in yeast. Cell *116,* 405-415.

Harding, T.M., Hefner-Gravink, A., Thumm, M., and Klionsky, D.J. (1996). Genetic and phenotypic overlap between autophagy and the cytoplasm to vacuole protein targeting pathway. J. Biol. Chem. *271,* 17621-17624.

He, C., Song, H., Yorimitsu, T., Monastyrska, I., Yen, W.L., Legakis, J.E., and Klionsky, D.J. (2006). Recruitment of Atg9 to the preautophagosomal structure by Atg11 is essential for selective autophagy in budding yeast. J. Cell Biol. *175,* 925-935.

Hinnebusch, A.G. (2005). Translational regulation of GCN4 and the general amino acid control of yeast. Annu. Rev. Microbiol. *59,* 407-450.

Ho, Y., Gruhler, A., Heilbut, A., Bader, G.D., Moore, L., Adams, S.L., Millar, A., Taylor, P., Bennett, K., Boutilier, K. *et al*. (2002). Systematic identification of protein complexes in Saccharomyces cerevisiae by mass spectrometry. Nature *415,* 180-183.

Hoheisel, J.D. (2006). Microarray technology: beyond transcript profiling and genotype analysis. Nat. Rev. Genet. *7,* 200-210.

Honigberg, S.M., and Lee, R.H. (1998). Snf1 kinase connects nutritional pathways controlling meiosis in Saccharomyces cerevisiae. Mol. Cell. Biol. *18,* 4548-4555.

Huh, W.K., Falvo, J.V., Gerke, L.C., Carroll, A.S., Howson, R.W., Weissman, J.S., and O'Shea, E.K. (2003). Global analysis of protein localization in budding yeast. Nature *425,* 686-691.

Jiang, Y., Davis, C., and Broach, J.R. (1998). Efficient transition to growth on fermentable carbon sources in Saccharomyces cerevisiae requires signaling through the Ras pathway. EMBO J. *17,* 6942-6951.

Kabeya, Y., Kamada, Y., Baba, M., Takikawa, H., Sasaki, M., and Ohsumi, Y. (2005). Atg17 functions in cooperation with Atg1 and Atg13 in yeast autophagy. Mol. Biol. Cell *16,* 2544-2553.

Kamada, Y., Funakoshi, T., Shintani, T., Nagano, K., Ohsumi, M., and Ohsumi, Y. (2000). Tor-mediated induction of autophagy via an Apg1 protein kinase complex. J. Cell Biol. *150,* 1507-1513.

Klasson, H., Fink, G.R., and Ljungdahl, P.O. (1999). Ssy1p and Ptr3p are plasma membrane components of a yeast system that senses extracellular amino acids. Mol. Cell. Biol. *19,* 5405-5416.

Kraakman, L., Lemaire, K., Ma, P., Teunissen, A.W., Donaton, M.C., Van Dijck, P., Winderickx, J., de Winde, J.H., and Thevelein, J.M. (1999a). A Saccharomyces cerevisiae G-protein coupled receptor, Gpr1, is specifically required for glucose activation of the cAMP pathway during the transition to growth on glucose. Mol. Microbiol. *32,* 1002-1012.

Kraakman, L., Lemaire, K., Ma, P., Teunissen, A.W., Donaton, M.C., Van Dijck, P., Winderickx, J., de Winde, J.H., and Thevelein, J.M. (1999b). A Saccharomyces cerevisiae G-protein coupled receptor, Gpr1, is specifically required for glucose activation of the cAMP pathway during the transition to growth on glucose. Mol. Microbiol. *32,* 1002-1012.

Krogan, N.J., Cagney, G., Yu, H., Zhong, G., Guo, X., Ignatchenko, A., Li, J., Pu, S., Datta, N., Tikuisis, A.P. *et al*. (2006). Global landscape of protein complexes in the yeast Saccharomyces cerevisiae. Nature *440,* 637-643.

Kumar, A., Agarwal, S., Heyman, J.A., Matson, S., Heidtman, M., Piccirillo, S., Umansky, L., Drawid, A., Jansen, R., Liu, Y. *et al*. (2002). Subcellular localization of the yeast proteome. Genes Dev. *16,* 707-719.

Kumar, A., Harrison, P.M., Cheung, K.H., Lan, N., Echols, N., Bertone, P., Miller, P., Gerstein, M.B., and Snyder, M. (2002). An integrated approach for finding overlooked genes in yeast. Nat. Biotechnol. *20,* 58-63.

Liu, H., Styles, C.A., and Fink, G.R. (1996). Saccharomyces cerevisiae S288C has a mutation in FLO8, a gene required for filamentous growth. Genetics *144,* 967-978.

Lorenz, M.C., and Heitman, J. (1998). The MEP2 ammonium permease regulates pseudohyphal differentiation in Saccharomyces cerevisiae. EMBO J. *17,* 1236-1247.

Luesch, H., Wu, T.Y., Ren, P., Gray, N.S., Schultz, P.G., and Supek, F. (2005). A genome-wide overexpression screen in yeast for small-molecule target identification. Chem. Biol. *12,* 55-63.

Lum, P.Y., Armour, C.D., Stepaniants, S.B., Cavet, G., Wolf, M.K., Butler, J.S., Hinshaw, J.C., Garnier, P., Prestwich, G.D., Leonardson, A. *et al*. (2004). Discovering modes of action for therapeutic compounds using a genome-wide screen of yeast heterozygotes. Cell *116,* 121-137.

Ma, J., Bharucha, N., Dobry, C.J., Frisch, R.L., Lawson, S., and Kumar, A. (2008). Localization of Autophagy-Related Proteins in Yeast Using a Versatile Plasmid-Based Resource of Fluorescent Protein Fusions. Autophagy *4,*

Ma, J., Jin, R., Dobry, C.J., Lawson, S.K., and Kumar, A. (2007a). Overexpression of autophagy-related genes inhibits yeast filamentous growth. Autophagy *3,* 604-609.

Ma, J., Jin, R., Jia, X., Dobry, C.J., Wang, L., Reggiori, F., Zhu, J., and Kumar, A. (2007b). An interrelationship between autophagy and filamentous growth in budding yeast. Genetics *177,* 205-214.

Madhani, H.D., and Fink, G.R. (1997). Combinatorial control required for the specificity of yeast MAPK signaling. Science *275,* 1314-1317.

Magasanik, B. (2003). Ammonia assimilation by Saccharomyces cerevisiae. Eukaryot. Cell. *2,* 827-829.

Mewes, H.W., Albermann, K., Bahr, M., Frishman, D., Gleissner, A., Hani, J., Heumann, K., Kleine, K., Maierl, A., Oliver, S.G., Pfeiffer, F., and Zollner, A. (1997). Overview of the yeast genome. Nature *387,* 7-65.

Michaud, G.A., Salcius, M., Zhou, F., Bangham, R., Bonin, J., Guo, H., Snyder, M., Predki, P.F., and Schweitzer, B.I. (2003). Analyzing antibody specificity with whole proteome microarrays. Nat. Biotechnol. *21,* 1509-1512.

Murray, L.E., Rowley, N., Dawes, I.W., Johnston, G.C., and Singer, R.A. (1998). A yeast glutamine tRNA signals nitrogen status for regulation of dimorphic growth and sporulation. Proc. Natl. Acad. Sci. U. S. A. *95,* 8619-8624.

Nair, U., and Klionsky, D.J. (2005). Molecular mechanisms and regulation of specific and nonspecific autophagy pathways in yeast. J. Biol. Chem. *280,* 41785-41788.

Noda, T., and Ohsumi, Y. (1998). Tor, a phosphatidylinositol kinase homologue, controls autophagy in yeast. J. Biol. Chem. *273,* 3963-3966.

Ohsumi, Y. (2001). Molecular dissection of autophagy: two ubiquitin-like systems. Nat. Rev. Mol. Cell Biol. *2,* 211-216.

Oliver, S.G. (2002). Functional genomics: lessons from yeast. Philos. Trans. R. Soc. Lond. B. Biol. Sci. *357,* 17-23.

Palecek, S.P., Parikh, A.S., and Kron, S.J. (2002). Sensing, signalling and integrating physical processes during Saccharomyces cerevisiae invasive and filamentous growth. Microbiology *148,* 893-907.

Pan, X., Harashima, T., and Heitman, J. (2000). Signal transduction cascades regulating pseudohyphal differentiation of Saccharomyces cerevisiae. Curr. Opin. Microbiol. *3,* 567-572.

Pan, X., and Heitman, J. (1999). Cyclic AMP-dependent protein kinase regulates pseudohyphal differentiation in Saccharomyces cerevisiae. Mol. Cell. Biol. *19,* 4874-4887.

Polish, J.A., Kim, J.H., and Johnston, M. (2005). How the Rgt1 transcription factor of Saccharomyces cerevisiae is regulated by glucose. Genetics *169,* 583-594.

Puig, O., Caspary, F., Rigaut, G., Rutz, B., Bouveret, E., Bragado-Nilsson, E., Wilm, M., and Seraphin, B. (2001). The tandem affinity purification (TAP) method: a general procedure of protein complex purification. Methods *24,* 218-229.

Rappleye, C.A., and Goldman, W.E. (2006). Defining virulence genes in the dimorphic fungi. Annu. Rev. Microbiol. *60,* 281-303.

Schmelzle, T., Beck, T., Martin, D.E., and Hall, M.N. (2004). Activation of the RAS/cyclic AMP pathway suppresses a TOR deficiency in yeast. Mol. Cell. Biol. *24,* 338-351.

Schneper, L., Duvel, K., and Broach, J.R. (2004). Sense and sensibility: nutritional response and signal integration in yeast. Curr. Opin. Microbiol. *7,* 624-630.

Scott, S.V., Hefner-Gravink, A., Morano, K.A., Noda, T., Ohsumi, Y., and Klionsky, D.J. (1996). Cytoplasm-to-vacuole targeting and autophagy employ the same machinery to deliver proteins to the yeast vacuole. Proc. Natl. Acad. Sci. U. S. A. *93,* 12304-12308.

Sopko, R., Huang, D., Preston, N., Chua, G., Papp, B., Kafadar, K., Snyder, M., Oliver, S.G., Cyert, M., Hughes, T.R., Boone, C., and Andrews, B. (2006). Mapping pathways and phenotypes by systematic gene overexpression. Mol. Cell *21,* 319-330.

Suter, B., Auerbach, D., and Stagljar, I. (2006). Yeast-based functional genomics and proteomics technologies: the first 15 years and beyond. BioTechniques *40,* 625-644.

Tong, A.H., and Boone, C. (2006). Synthetic genetic array analysis in Saccharomyces cerevisiae. Methods Mol. Biol. *313,* 171-192.

Vidan, S., and Snyder, M. (2001). Large-scale mutagenesis: yeast genetics in the genome era. Curr. Opin. Biotechnol. *12,* 28-34.

Wigge, P.A., Jensen, O.N., Holmes, S., Soues, S., Mann, M., and Kilmartin, J.V. (1998). Analysis of the Saccharomyces spindle pole by matrix-assisted laser desorption/ionization (MALDI) mass spectrometry. J. Cell Biol. *141,* 967-977.

Wilson, C.A., Kreychman, J., and Gerstein, M. (2000). Assessing annotation transfer for genomics: quantifying the relations between protein sequence, structure and function through traditional and probabilistic scores. J. Mol. Biol. *297,* 233-249.

Xue, Y., Batlle, M., and Hirsch, J.P. (1998a). GPR1 encodes a putative G protein-coupled receptor that associates with the Gpa2p Galpha subunit and functions in a Ras-independent pathway. EMBO J. *17,* 1996-2007.

Xue, Y., Batlle, M., and Hirsch, J.P. (1998b). GPR1 encodes a putative G protein-coupled receptor that associates with the Gpa2p Galpha subunit and functions in a Ras-independent pathway. EMBO J. *17,* 1996-2007.

Yan, G., Shen, X., and Jiang, Y. (2006). Rapamycin activates Tap42-associated phosphatases by abrogating their association with Tor complex 1. EMBO J. *25,* 3546-3555.

Yang, Z., Huang, J., Geng, J., Nair, U., and Klionsky, D.J. (2006). Atg22 recycles amino acids to link the degradative and recycling functions of autophagy. Mol. Biol. Cell *17,* 5094-5104.

Yorimitsu, T., and Klionsky, D.J. (2005). Autophagy: molecular machinery for self-eating. Cell Death Differ. *12 Suppl 2,* 1542-1552.

Zhu, H., Bilgin, M., Bangham, R., Hall, D., Casamayor, A., Bertone, P., Lan, N., Jansen, R., Bidlingmaier, S., Houfek, T. *et al*. (2001). Global analysis of protein activities using proteome chips. Science *293,* 2101-2105.

Chapter 2

An Interrelationship Between Autophagy and Filamentous Growth in Budding Yeast

Introduction

From the human pathogen *Candida albicans* to the corn smut fungus *Ustilago maydis*, many diverse fungal species possess the ability to switch between a cellular yeast form and a filamentous invasive form in response to appropriate environmental cues (Gimeno et al. 1992; Madhani and Fink 1998). Constituting an essential determinant of fungal pathogenicity in both plants and humans (Lo et al. 1997), this morphogenetic switch has garnered increased attention over the last fifteen years, particularly in the budding yeast *Saccharomyces cerevisiae* (Gimeo et al. 1992). Like its pathogenic counterparts, certain strains of *S.cerevisiae* also undergo a shift to a filamentous growth form (Gancedo 2001; Kron 1997; Madhani and Fink 1998). Presumably as a means of foraging for nutrients, diploid yeast cells grown under conditions of nitrogen starvation differentiate into branching chains of elongated cells (Gimeno et al. 1992; Liu et al. 1993). The morphogenetic changes associated with filamentous differentiation are extensive; during filamentous growth, yeast cells delay in G2/M, exhibit an elongated morphology, bud in a unipolar fashion, remain physically attached, and invade their growth substrate (Gimeno et al. 1992; Kron et al. 1994). The resulting filaments are called pseudohyphae, and hence this form of growth is referred to as pseudohyphal

growth (PHG).

In *S. cerevisiae*, PHG is regulated by at least two signaling pathways: 1) the nutrient-sensing cyclic AMP-protein kinase A (PKA) pathway, and 2) a mitogen-activated protein kinase (MAPK) pathway. During filamentous growth, the GTP-binding protein Ras2p is activated through a sensor system that is not well characterized at present. Activated Ras2p, in turn, stimulates the synthesis of cAMP, which activates protein kinase A (Robertson and Fink 1998). The yeast PHG MAPK cascade also functions downstream of Ras2p (Mosch et al. 1996). Activated Ras2p acts through the G-protein Cdc42p to stimulate the p21-activated kinase Ste20p (Peter et al. 1996). Ste20p, in turn, initiates a MAPK signaling cascade consisting of Ste11p, Ste7p, and the MAPK itself Kss1p (Cooket al. 1997).

These well characterized signaling modules act upstream of a diverse and incompletely defined set of genes, including many transcription factors such as Ste12p, Tec1p, Phd1p, Flo8p, and Mss11p (Baredwell et al. 1998; Borneman et al. 2006; Gagiano et al. 2003; Kobayashi et al. 1996; Liu et al. 1996; Madhani and Finkand 1997; Prinz et al. 2004; Vandyk et al. 2005; Webber et al. 1997). The PHG PKA and MAPK pathways have been linked with pathways governing cell polarity, bud site selection, and cell cycle progression (Rua et al. 2001), but the extensive changes associated with PHG likely encompass additional pathways as well.

Like PHG in yeast, autophagy is also a stress response initiated under conditions of nutrient deprivation. Autophagy is an intracellular catabolic pathway conserved among all eukaryotes in which cytosol, organelles, and other structures are sequestered within double membrane vesicles (autophagosomes) for delivery to the

vacuole/lysosome, where they are consumed by resident hydrolases (Levine and Klionsky 2004; Reggiori and Klionsky 2002; Reggiori and Klionsky 2005). Autophagy plays a principal role in the degradation and recycling of long-lived proteins and organelles; as such, it is an important cellular stress response, enabling eukaryotic cells to survive starvation conditions by generating an internal pool of nutrients (Reggiori and Klionsky 2002). In addition, autophagy plays an important role in various developmental pathways, in tumor suppression, in innate immunity, and in lifespan extension (Levine and Klionsky 2004; Reggiori and Klionsky 2005; Shintani and Klionsky 2004a). Autophagy has also been associated with several myopathies and neurodegenerative diseases (Shintani and Klionsky 2004a).

As mentioned above, autophagy is a cellular response to conditions of nutrient stress. Although nitrogen deprivation is the most common stimulus for autophagy in laboratory studies, carbon stress (Takeshiget et al. 1992), amino acid stress (Yang et al. 2006) and organelle stress, in the form of endoplasmic reticulum stress and mitochondrial dysfunction (Yorimitsu et al. 2006; Abeliovich 2007), also result in activation of the autophagy pathway. Through extensive studies, this pathway is known to encompass more than 20 autophagy-related (ATG) genes in the budding yeast (Levine and Klionsky 2004). In particular, Atg1p is a serine/threonine kinase essential for autophagy (Matsuura et al. 1997; Stephan and Herman 2006). Atg1p is required for the induction of autophagy and is thought to function as part of a protein complex with several other components of the autophagy pathway (Klionsky 2005; Reggiori et al. 2004). ATG7 encodes an activating enzyme (E1) that is part of two ubiquitin-like systems essential for vesicle expansion and completion (Ichimura et al. 2000; Mizushima et al. 1998). While the

majority of these autophagy-related genes have been studied explicitly, functional relationships between autophagy and other cell signaling pathways remain to be determined.

To date, autophagy has not been investigated in a filamentous strain of S. cerevisiae, and thus, no connection between autophagy and PHG has been considered. Here, we present several studies indicating a physiological interrelationship between these processes. Through microarray-based expression profiling, assays for autophagic induction, filamentous growth analyses, and cell survival assays, we derive a model of yeast PHG and autophagy in which PHG is responsive to the degree of nitrogen stress, and autophagy plays a critical role in determining the degree of this stress.

Materials and Methods

Strains: All non-filamentous lab strains are of the S288c genetic background and are derived from those used by the Yeast Deletion Consortium (e.g., BY4743 described in Winzeler et al. (Winzeler et al. 1999)). All filamentous lab strains are derived from the Σ1278b genetic background (Gimeno et al. 1992). The filamentous strains Y825 and Y826 were used to generate homozygous diploid deletion strains. The genotype of Y825 is as follows: MATa ura3-52 leu2Δ0. Y826 is a haploid strain of opposite mating type otherwise isogenic to Y825. Modified forms of Y825 and Y826 were constructed containing URA3 (Y825 Ura^+) and LEU2 (Y826 Leu^+) for the subsequent generation of Y825/6 diploid mutants.

Media and growth conditions: PHG was induced according to standard protocols using low-nitrogen growth media (Gimeno et al. 1992), except as noted. Briefly, a 50 ml yeast culture was grown at 30°C to an OD 600 of 0.6 (cell density of approximately 4.3 x 10^6) in YPD medium (1% yeast extract, 2% peptone, 2% glucose). Cells were harvested by centrifugation and washed twice before being transferred to SLAD medium (2% glucose, 50 μm ammonium sulfate, 0.17% yeast nitrogen base without amino acid and ammonium sulfate, supplemented with essential amino acids for nutritional auxotrophies) for varying times as indicated (Gimeno et al. 1992).

PHG was assessed in autophagy mutants by growth in SLAD medium and by growth in SLAD medium supplemented with 1% ethanol. Strains were incubated on plates at 30°C for approximately 5-6 days, followed by continued growth at room temperature for an additional 3-4 days as needed.

Gene deletions and ATG1 overexpression: Gene deletions were performed using the one-step gene replacement strategy of Baudin et al. (Baudin et al. 1993) with the KanMX6 disruption cassette from plasmid pFA6a-KanMX6 (Longtine et al. 1998). To generate homozygous diploid deletion mutants, gene replacement was performed individually in Y825 Ura^+ (MATa) and in Y826 Leu^+ (MATα); transformants were selected on YPD plates containing 200 μg/ml G418. These strains were subsequently mated and selected on SC -Ura -Leu medium to generate homozygous diploid deletion mutants. In all cases, correct integration was verified by PCR.

ATG1 overexpression was achieved using the pRS416-derived plasmid pCUP1-ATG1 carrying a gene fusion between the copper-inducible CUP1 promoter and ATG1

(Sikorski and Hieter 1989). Expression was induced using media supplemented with 10, 50, or 100 μM copper sulfate. To achieve gentler overexpression of ATG1, we have also used this plasmid in the absence of copper sulfate; by Western blot analysis, expression from Pcup1 in pRS416 without copper sulfate results in 2-3-fold overexpression of ATG1.

Microarray experiments and data analysis: Yeast strains were cultured as described above. RNA was prepared according to standard protocols using the Poly(A) Purist kit (Ambion, Austin, TX). RNA concentration and purity were determined spectrophotometrically and by gel electrophoresis. Microarray hybridization was performed with the Yeast Genome S98 Array using standard protocols (Affymetrix, Inc, Santa Clara, CA). All microarray experiments were performed in quadruplicate (four biological replicates) for each strain and indicated time point. Differentially expressed genes were identified by significance analysis of microarrays (SAM) (Rieger and Chu2004; Tusher et al. 2001). Briefly, SAM computes a nonparametric score for each gene by dividing the between-group difference of (normalized log) gene expression levels and the within-group difference of gene expression levels. The score is then compared with random permutation scores. The random permutation scores for a gene are computed in the same manner as the original score, but based on randomly sampled gene expressions. If the difference between the original score and the random permutation score is larger than a chosen threshold value, the corresponding change in gene expression is claimed to be significant. Each threshold value corresponds to a false discovery rate (FDR), indicating the percentage of genes

identified as being significant by chance alone. Thus, increasing the threshold value decreases the number of claimed significant genes, but also decreases the FDR, yielding a greater degree of confidence. Here, we have used SAM's multi-class analysis function, with the threshold value chosen so that the corresponding FDR was 0.

Western blotting and GFP-Atg8p processing assay: GFP-Atg8p transport and processing was monitored by microscopy and biochemical means as previously described (Kim et al. 2001; Shintani and Klionsky 2004b). The plasmid expressing the GFP-Atg8p fluorescent chimera (pCU-GFP-ATG8) (Kim et al. 2001) was introduced by standard DNA transformation into the non-filamentous yeast strain BY4743 (WIinzeler et al. 1999) and into the filamentous Y825/6 strain. Fluorescent images of GFP- Atg8p were acquired using the DeltaVision Spectris inverted epifluorescence microscope (Applied Precision, Issaquah, WA).

For Western blot analysis, strains carrying pCU-GFP-ATG8 were grown in SC-Ura medium with 50 μM of $CuSO_4$ to an OD 600 of 0.8. Two OD 600 equivalents of cells were transferred into SLAD medium with 0, 50, or 100 μM ammonium sulfate and were incubated at the same temperature for an additional three hours. Cells were successively collected by centrifugation before precipitating proteins with 10% trichloroacetic acid (TCA) followed by two washings with 100% acetone. Finally, proteins were resuspended in 80 μl of SDS-PAGE sample buffer [72 μl of Laemmli sample buffer and 8 μl of 1M dithiothreitol (DTT)] by sonication and vortexing in the presence of glass beads. Samples were incubated at 75 ^{o}C for 10 minutes and 0.5 OD 600 equivalents of cells were resolved by SDS-PAGE. After Western blotting, membranes

were probed with both anti-GFP (Covance Research Products, Berkeley, CA) and anti-Pgk1p (Invitrogen, Carlsbad, CA).

Cell survival assays: Nitrogen starvation experiments were performed essentially as described previously (Scott et al. 1996). Briefly, wild-type and deletion strains were grown in 5 ml YPD to 0.6 OD 600. Cells were collected and washed twice, before being transferred to SLAD medium. After growth for the indicated periods of time, samples were collected and diluted 10,000-fold. 100 µl of each diluted culture was spread on a YPD plate. Viable colonies were counted after two days growth at 30°C. All platings were performed in triplicate.

Results

Increased transcription of the autophagy pathway during early pseudohyphal growth: In *S. cerevisiae*, the transition to filamentous growth is striking, encompassing morphological and cellular changes driven, in part, by an extensive transcriptional regulatory network. By microarray-based expression profiling of the yeast genome, we investigated the scope of genes and cell processes transcriptionally regulated during PHG. As previous studies suggest that the transcriptional program of PHG is initiated quickly within the first few hours upon nitrogen limitation (Prinz et al. 2004), we specifically chose to profile the early onset of pseudohyphal growth, identifying genes differentially expressed after 20 minutes, one hour, and two hours (approximately one generation) of nitrogen deprivation in a filamentous strain of budding yeast. Note that the Σ1278b strain

serves as the genetic background for our studies; unlike most laboratory strains of *S. cerevisiae*, Σ1278b undergoes an extensive and easily controlled transition to PHG and, as a result, is the preferred background for studies of yeast filamentous growth.

In total, this microarray analysis reveals an extensive transcriptional program encompassing a wide variety of genes and cell pathways. In particular, this transcriptional profile reveals an interesting and previously undocumented point: The pathway mediating autophagy is extensively upregulated during early PHG (Figure 2.1 A and B). In yeast, the process of nonselective bulk autophagy requires 19 genes (Nair and Klionsky 2005); 11 of these genes were transcriptionally induced during PHG (ATG1, ATG3, ATG4, ATG5, ATG6, ATG7, ATG8, ATG9, ATG14, ATG17, and ATG22).

Specifically, mRNAs for these genes were identified as being differentially abundant in at least one of the time points examined, with increased abundance evident upon 1-2 hours nitrogen stress in filamentous yeast. Microarray results were confirmed by real-time PCR (Table 2.1). Formally, this reflects either increased transcription of a given gene and/or decreased RNA turnover, and we use the general terms "induction" or "upregulation" to indicate this point.

In addition to the genes responsible for bulk autophagy, we also find three autophagy-related genes specific for the cytoplasm to vacuole targeting (Cvt) pathway (ATG19, ATG20, and ATG21) upregulated during our microarray time course analysis of early PHG (Figure 1A and B). The Cvt pathway is a type of selective autophagy, in which oligomers formed by the resident vacuolar protease Lap4p/Ape1p are transported directly from the cytoplasm into the vacuole lumen (Reggiori and Klionsky 2002). Thus, we identify transcriptional upregulation of genes encoding components of both yeast

trafficking pathways mediating protein delivery directly from the cytoplasm to the vacuole. In total, 29 autophagy-related genes have been identified in yeast (He and Klionsky 2006; Klionsky and Kumar 2006), and we find 14 of these genes transcriptionally induced during early filamentous growth in *S. cerevisiae*.

Induction of autophagic activity during filamentous growth: Although approximately half of all known autophagy-related genes are transcriptionally upregulated during PHG, it is possible that autophagy itself may not be active during filamentous growth due to post-transcriptional regulatory mechanisms. To consider this possibility more explicitly, we used the GFP-Atg8p processing assay developed by Shintani and Klionsky (Shintani and Klionsky 2004b) as an indication of autophagic induction. Atg8p is a ubiquitin-like protein essential for autophagy that is unconventionally linked to the lipid phosphatidylethanolamine (Ichimura et al. 2000). Part of Atg8p remains associated with autophagosomal structures from the stage of initial formation to complete breakdown in the vacuole; therefore, GFP-Atg8p is an optimal marker to follow the itinerary of double membrane vesicles (Kirisako et al. 1999). As a result, the delivery of Atg8p to the vacuole serves as a useful measure of autophagosome formation and autophagic induction. To visualize this process, we use a GFP-Atg8p chimera. Upon delivery to the vacuole, Atg8p is degraded, while GFP, which is relatively stable in the presence of vacuolar hydrolases, accumulates in the vacuolar lumen. Therefore, the presence of the free GFP moiety in the vacuole indicates Atg8p delivery and autophagic induction (Shintani and Klionsky 2004b).

As indicated in Figure 2.2 A, using the GFP-Atg8p processing assay, we detect induction of autophagy during filamentous growth in *S. cerevisiae*. By Western blot analysis, we detect free GFP resulting from cleavage of GFP-Atg8p in the vacuole during nitrogen stress (concentrations of 0, 50, and 100 μM ammonium sulfate) in the filamentous yeast strain Σ1278b. For comparison, we repeated this analysis in the standard non-filamentous S288c-derived genetic background BY4743; autophagy is known to occur in non-filamentous yeast during nitrogen stress, and we observe comparable levels of autophagic induction in filamentous yeast as compared to non-filamentous yeast. These results are confirmed by fluorescence microscopy of yeast cells carrying GFP-Atg8p under conditions of nitrogen stress and sufficiency (Figure 2.2 B). Under normal growth conditions, GFP-Atg8p is localized to a perivacuolar punctate spot, indicating the pre-autophagosomal structure (the PAS). The PAS is believed to be the site where double-membrane vesicles are formed (Kim et al. 2002; Suzuki et al. 2001). Under conditions of nitrogen deprivation, however, GFP staining is evident in the vacuole in filamentous and non-filamentous strains of yeast, indicative of Atg8p transport to the vacuole and autophagic activity. Thus, we conclude that autophagy is induced during nitrogen stress in filamentous yeast.

Phenotypic analysis of PHG in autophagy-impaired mutants: Since pseudohyphal growth and autophagy are active stress responses in a filamentous strain of yeast, with nitrogen deprivation acting as a common stimulus, we sought to further investigate a relationship between these processes. For this purpose, we generated a homozygous diploid strain of the Σ1278b genetic background deleted for ATG1.

Atg1p is a serine/threonine kinase essential for autophagy (Matsuura et al. 1997; Stephan and Herman 2006). Atg1p is required for the induction of autophagy, and it is thought to function as part of a protein complex with several other components of the autophagy pathway (Klionsky 2005; Reggiori et al. 2004). Using the standard assay of Gimeno et al. (Gimeno et al. 1992), we examined homozygous diploid atg1Δ mutants for filamentous growth under conditions inducing PHG. Interestingly, we found increased PHG in atg1Δ relative to the filamentous wild-type strain (Figure 2.3). Conversely, inhibition of filamentous growth does not affect autophagy appreciably (data not shown); this is consistent with the volume of studies characterizing active autophagy in strains of budding yeast deficient in filamentous growth.

The increased growth of the homozygous diploid atg1Δ strain is evident in its colony morphology (Figure 2.3A) and at the cellular level as well (Figure 2.3B). Yeast cells undergoing PHG are characteristically elongated and can be distinguished from cells undergoing normal vegetative growth by this fact; however, a colony is a heterogeneous cell population, and even during PHG, not all cells within a colony will be elongated. The relative fraction of elongated cells, though, does provide a confirming measure of the extent of PHG in a given strain under given growth conditions. To assess this more quantitatively, we measured the length and width of cells from atg1Δ and wild-type colonies under PHG-inducing growth conditions; this analysis is indicated in Figure 2.3B and C. PHG cells exhibit a length:width ratio of approximately 1.5-2.0 or greater, and we find a larger fraction of these elongated cells in atg1Δ relative to wild-type. Specifically, four times as many atg1Δ cells as compared to wild- type cells exhibit a length:width ratio of 2.0 or greater under identical PHG-inducing conditions. Other than the increased

fraction of elongated cells, we do not detect significant differences in cell morphology between the atg1Δ mutants and wild-type Σ1278b strains; both strains exhibit large vacuoles indicative of growth under conditions of nutrient stress (Figure 2.3 B).

The phenotype observed upon deletion of ATG1 may be specific to this gene or may result from general inhibition of the autophagy pathway. To distinguish between these possibilities, we generated a homozygous diploid strain of the Σ1278b background deleted for ATG7. ATG7 encodes an activating enzyme (E1) that is part of two ubiquitin-like systems essential for autophagy (Ichimura et al. 2000; Mizushima et al. 1998). Atg7p is required for vesicle expansion and completion; it is not thought to function in complex with Atg1p. As indicated in Figure 2.3, homozygous diploid atg7Δ mutants also exhibited increased filamentous growth under PHG-inducing conditions. Colonies of atg7Δ mutant display increased surface-spread filamentation, and approximately five times as many cells from atg7Δ colonies are elongated (length:width ratio of greater than 2.0) relative to wild-type Σ1278b cells. Thus, we observed exaggerated PHG in both atg1Δ and atg7Δ mutants.

Phenotypic analysis of PHG upon ATG1 overexpression: In complement to phenotypic studies of *atg* deletion mutants, we also overexpressed ATG1 and assessed pseudohyphal growth. For this study, we expressed ATG1 from the copper-inducible CUP1 promoter carried on a low-copy yeast shuttle vector derived from pRS416 (Scott et al. 2007). Even in the absence of copper sulfate, expression of Pcup1-ATG1 yields 2-3-fold overexpression of ATG1 (as confirmed by Western blot analysis). It is important to note that overexpression of ATG1 is insufficient to activate autophagy under non-

inducing conditions in yeast; however, it is difficult to quantify autophagic activity, and, thus, it is difficult to assess whether the process occurs more aggressively upon overexpression of ATG1 under conditions of nitrogen stress. Qualitatively, by the GFP-Atg8p assay described previously, autophagy is strongly activated by ATG1 overexpression under conditions of nitrogen stress. Also consistent with increased autophagic induction, a yeast strain of the Σ1278b background overexpressing ATG1 exhibits smaller colony size on low-nitrogen medium than a corresponding wild-type strain.

To assess pseudohyphal growth upon ATG1 overexpression, we assayed the strain described above for surface-spread filamentation at the colony level and for cell elongation/clustering at the single- cell level. As indicated in Figure 2.3, ATG1 overexpression is sufficient to markedly decrease pseudohyphal growth relative to a wild-type strain grown under identical conditions of nitrogen stress. This phenotype is consistent with results from the converse experiment in which hyperactive filamentous growth was observed upon deletion of ATG1.

Graded PHG during nitrogen stress in filamentous yeast: Considering the findings presented above, exaggerated filamentous growth during nitrogen deprivation in autophagy-impaired mutants may reflect the worsened state of nitrogen stress in these strains. Autophagy is a recycling process, acting, in part, to mitigate the effects of nitrogen starvation. In the absence of autophagy, nitrogen stress may be significantly increased relative to a wild-type strain grown under identical conditions of nitrogen deprivation; the exaggerated PHG in autophagy-deficient mutants may reflect this

condition. If so, PHG must be a graded response, with increased filamentous growth correlated with decreasing available nitrogen. As shown in the lower panel of Figure 2.4, we find that wild-type Σ1278b exhibits a graded increase in PHG in response to decreasing levels of exogenously supplied ammonium sulfate. Note that the growth medium for this analysis contains some amino acids to complement nutritional auxotrophies in the strain; thus, even the absence of ammonium sulfate generates a state of nitrogen stress rather than nitrogen starvation. We observe a similar graded response in atg7Δ mutants; however, PHG is induced at a higher concentration of exogenously supplied ammonium sulfate (top panel of Figure 2.4). In the presence of low-nitrogen growth medium supplemented with 100 μM ammonium sulfate, atg7Δ undergoes PHG, whereas a wild-type strain of the same genetic background does not. We observe identical results in mutants deleted for ATG1 (data not shown). We, therefore, suggest that exaggerated PHG in autophagy-deficient mutants may be a cellular response to an exacerbated condition of nitrogen stress in these strains.

Filamentous growth and autophagy facilitate cell survival during nitrogen stress: The findings above suggest that both filamentous growth and autophagy act to relieve nitrogen stress, presumably contributing to yeast cell survival. To consider this further, we have assessed the ability of wild type filamentous (Σ1278b) and non-filamentous yeast to survive during nitrogen starvation (Figure 2.5). In contrast to the non-filamentous yeast strain BY4743, wild type Σ1278b cells survive nitrogen deprivation fairly well for greater than 9 days, exhibiting only a 25% reduction in colony number. To assess the contributions of PHG and autophagy in a filamentous strain of S. cerevisiae, we generated

and assayed a homozygous diploid mutant impaired in autophagy (atg1Δ) and a homozygous mutant impaired in filamentous growth (muc1Δ) for cell viability under conditions of nitrogen starvation in the Σ1278b background. Muc1p is a GPI-anchored cell surface glycoprotein required for diploid pseudohyphal growth under conditions of nitrogen stress (Guo et al. 2000; Lambrechts et al. 1996; Rupp et al. 1999).

As shown in Figure 2.5, the autophagy-defective atg1Δ strain dies rapidly upon nitrogen removal, becoming inviable after 4-5 days. The homozygous diploid muc1Δ mutant survives the course of the assay, exhibiting an efficiency of survival comparable to that of a wild-type non-filamentous strain, although, after 5 days of starvation, the muc1Δ mutant cells begin to die more rapidly. Thus, both filamentous growth and autophagy contribute to cell survival during nitrogen starvation, but autophagy plays a more critical role.

Discussion

By microarray analysis of genes differentially expressed during early pseudohyphal growth in the filamentous Σ1278b strain of *S. cerevisiae*, we detect extensive upregulation of the autophagy pathway. Although both pseudohyphal growth and autophagy are active under conditions of nitrogen deprivation in filamentous strains of yeast, we find that inhibition of autophagy results in precocious and exaggerated filamentous growth. This phenotypic effect is not specific to a single autophagy-related gene; instead, it seems to reflect a requirement for wild-type function of the autophagy pathway as a whole. Collectively, these results suggest a model (Figure 2.6) in which both autophagy and filamentous growth mutually mitigate the effects of nutrient stress,

contributing positively to the available pool of nitrogen in the cell. In particular, the autophagy pathway strongly impacts the degree of nitrogen stress in the yeast cell, and the extent of filamentous growth is responsive to the severity of this nitrogen stress. This model explains the exaggerated degree of PHG evident in autophagy-impaired mutants: interruption of autophagy results in a heightened state of nitrogen stress, manifesting itself in the premature initiation of PHG and, thus, hyperactive filamentation.

Pseudohyphal growth and autophagy are interconnected stress responses:

Autophagy is involved in many important physiological processes, but has been studied most intensely as a cellular adaptation to starvation conditions (Reggiori and Klionsky 2005). As a stress response, therefore, its link with PHG is not surprising: nitrogen deprivation is a common stimulus inducing PHG and autophagy. Our results indicating transcriptional induction of the autophagy pathway are consistent with specific expression studies of the autophagy genes ATG8 and ATG14 (Chan et al. 2001; Kirisako et al. 1999), reported to be upregulated in non-filamentous yeast under conditions of nitrogen stress. It is unclear as to why transcriptional induction of autophagy is widespread over the pathway, encompassing the majority of autophagy genes. Possibly, autophagy proteins are required to sustain an intense autophagic activity. In agreement with this hypothesis, it has been shown that the induced expression of ATG8 and its subsequent translation are essential to generate normal-sized autophagosomes (Abeliovich et al. 2000). This extensive, but not comprehensive, complement of PHG-regulated autophagy genes may suggest the presence of many regulatory control points, rather than a single focus point. Computational analysis of the ATG promoter sequences does not reveal any

enrichment for known transcription factor binding sites, and, in particular, chromatin-immunoprecipitation/microarray studies of pseudohyphal growth transcription factors do not identify autophagy-related genes (Borneman et al. 2006). It is noteworthy that the 14 autophagy-related genes identified as being differentially regulated in this study were not identified as such in previous microarray-based studies of filamentous growth (Prinz et al. 2004), possibly due to the different time frames, growth conditions, and statistical measures employed in the respective analyses.

Transcriptional induction of both autophagy and pseudohyphal growth correlates with the activity of each process; both processes are active under conditions of nitrogen stress in a strain of yeast capable of filamentous growth, and autophagy is active in non-filamentous yeast under similar conditions. Therefore, we do not find that autophagy and PHG act as mutually exclusive pathways, but rather that both pathways contribute to the cellular response to nutrient stress. The role of autophagy in relieving nutrient stress is well documented (Klionsky and Kumar 2006; Wang and Klionsky 2003; Yang et al. 2006). Pseudohyphal growth plays a less substantial, but nonetheless tangible, role in this process as well: A cohort of genes mediating nitrogen utilization is upregulated during PHG (Prinz et al. 2004), and a strain of budding yeast capable of undergoing filamentous growth survives nitrogen stress better than a non-filamentous wild-type strain (Figure 2.5). Of course, as the filamentous and non-filamentous strains are non-isogenic, this observation must be interpreted cautiously.

The timing and onset of filamentous growth and autophagy: The activity of both autophagy and pseudohyphal growth during nitrogen stress raises an interesting question

as to the timing and onset of each process. This question is difficult to address directly, since we lack a well-defined indicator for the onset of pseudohyphal growth, other than cell morphological changes that require a period of two hours (one cell cycle) in order to become evident. With that qualification in mind, we speculate that autophagy might be initiated before pseudohyphal growth. The transition to filamentous growth is an extensive morphogenetic process that may be initiated when nutrient stress is sensed as being severe. In essence, autophagy may act to delay the onset of PHG by relieving initial nitrogen stress; note again that PHG occurs at higher concentrations of available nitrogen source in autophagy-deficient yeast (Figure 2.4). Our ATG1 overexpression results (Figure 2.3) suggest that the autophagy pathway represses filamentous growth. Again, during nitrogen stress, both autophagy and filamentous growth are active; however, the autophagy pathway may limit filamentous growth, preventing it from being maximally active and thereby contributing to the fine balance between these cellular processes. The fact that 2-3-fold overexpression of ATG1 is sufficient to repress filamentous growth suggests that the balance between autophagy and filamentous growth is indeed fine.

A possible direct connection between autophagy and pseudohyphal growth:

Although our model does not necessitate a direct link between autophagy and filamentous growth, it is likely that such a connection exists. Since the autophagy pathway is active under conditions of nitrogen stress irrespective of filamentous growth (Figure 2.2), but filamentous growth is affected by autophagy (Figure 2.3), it seems most likely that a component of the autophagy pathway might regulate PHG (this is indicated in Figure 2.6

by the horizontal arrow from autophagy to PHG). Several PHG or autophagy-related transcription factors and/or kinases may mediate cross talk between the processes; however, at present, chromatin immunoprecipitation/microarray studies of known PHG transcription factors do not indicate extensive regulation of autophagy-related genes (Borneman et al. 2006), and by the same token, we have yet to uncover an autophagy protein directly regulating a known component of the PHG pathways. In this regard, it is interesting to consider the decreased level of PHG evident upon overexpression of ATG1. By our current understanding of the pathway in yeast, and in contrast to the orthologous pathway in D. melanogaster (Scott et al. 2007), overexpression of ATG1 is not sufficient to induce autophagy under repressive growth conditions. While the colony morphology of ATG1 overexpression mutants and results from the GFP-Atg8p processing assay suggest that the rate of autophagy may be slightly increased upon overexpression of ATG1 under conditions of nitrogen stress, the effect is fairly marginal and is unlikely to affect the cellular nitrogen pool sufficiently to account for the marked filamentous growth phenotype. The results presented here indicate that Atg1p nevertheless plays a repressive role in limiting filamentous growth and that Atg1p may directly or indirectly affect activity of the filamentous growth pathways distinct from signals put forth by nitrogen-sensing transducers. Considering this possibility further, however, will be challenging, as many potential Atg1p targets exist in known PHG pathways (Stephan ad Herman 2006).

In total, this study describes an interrelationship between autophagy and pseudohyphal growth and therein raises two important points regarding these processes.

First, autophagy is a critical mechanism by which the cell can regulate or buffer its nutritional state from environmental stresses of nutrient deprivation. Second, PHG is finely tuned to the nutritional state of the cell, with the extent of PHG reflective of the degree of nitrogen stress to which the cell is subjected.

Acknowledgments

We thank Daniel Klionsky for providing plasmids pCU-GFP-ATG8 and pCUP1-ATG1; we also thank Damian Krysan, Robert Fuller, Anthony Borneman, and Michael Snyder for providing filamentous yeast strains. This work was supported by grant RSG-06-179-01-MBC from the American Cancer Society, grant DBI 0543017 from the National Science Foundation, and Basil O'Connor Award 5-FY05- 1224 from the March of Dimes. F.R. was supported by NIH grant GM53396.

Figure 2.1 Differential expression of autophagy-related genes during early pseudohyphal growth. (A) Red-green color scale indicating the mean change in expression (log scale) for a given gene relative to the standard deviation of repeated measurements for that gene; all experiments were performed with four biological replicates at each time point. In this heat map, the red coloring indicates increased mRNA abundance at the given time point. Statistical significance was determined by SAM (as described in Materials and Methods). The score provided alongside each gene is a statistical measure describing the degree of the observed change in gene expression; the higher the score, the greater the change in mRNA abundance for a given gene in the time course studied. Note that all autophagy-related genes shown here exhibit statistically significant changes in gene expression, as determined using a threshold cut-off score such that the false discovery rate is 0. (B) Listing of the autophagy-related process and specific function for each protein encoded by the ATG genes identified in this microarray study.

A

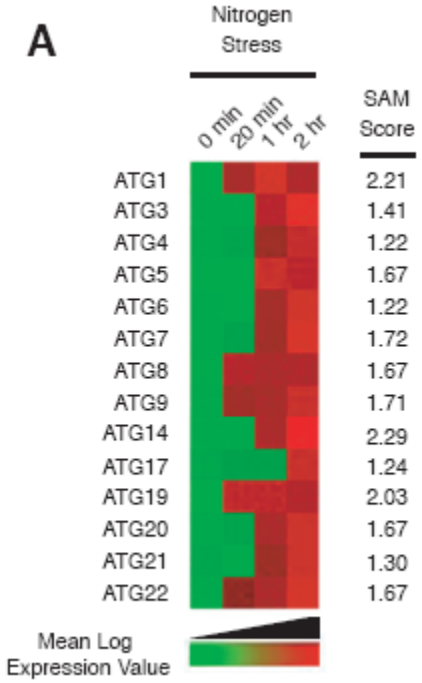

B

	Gene	Autophagy Process	Protein function / description
Autophagy	ATG1	Induction; retrieval	Protein kinase
	ATG3	Vesicle expansion and completion	Conjugation enzyme
	ATG4	Vesicle expansion and completion	Cysteine protease
	ATG5	Vesicle expansion and completion	Conjugation protein
	ATG6	Vesicle nucleation	PI3-kinase complex
	ATG7	Vesicle expansion and completion	Activation enzyme
	ATG8	Vesicle expansion and completion	Ubiquitin-like protein
	ATG9	Vesicle nucleation; retrieval	Integral membrane protein
	ATG14	Vesicle nucleation	PI3-kinase complex
	ATG17	Induction	Atg1p modulator
	ATG22	Macromolecular efflux from the vacuole/lysosome	Vacuolar permease
Cvt Pathway	ATG19	Cargo packaging	Receptor protein
	ATG20	Induction	PI3P binding
	ATG21	Cvt pathway	PI3P binding

Figure 2. 2 GFP-Atg8p processing assay of autophagic induction during nitrogen stress in filamentous and non-filamentous yeast strains. (A) Western blot of GFP-Atg8p processing; full-length GFP-Atg8p fusion and cleaved GFP are indicated. Pgk1p serves as a loading control. From these blots, autophagic induction is detected in both filamentous (Σ1278b) and non-filamentous (BY4743) yeast strains. (B) Analysis of GFP-Atg8p processing by fluorescence microscopy. In both filamentous and non- filamentous strains, staining of the perivacuolar pre-autophagosomal structure is evident under conditions of nitrogen sufficiency, and vacuolar staining is evident under conditions of nitrogen deprivation. By this assay, vacuolar GFP staining is not observed under conditions of nitrogen stress in yeast cells deficient in autophagy (data not shown). The scale bar represents 5 μm.

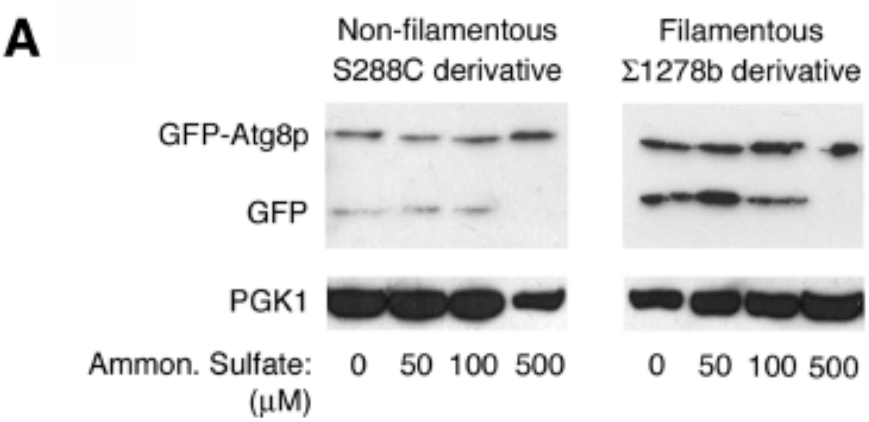
A
Non-filamentous
S288C derivative
Filamentous
Σ1278b derivative
GFP-Atg8p
GFP
PGK1
Ammon. Sulfate: (μM)
0 50 100 500
0 50 100 500

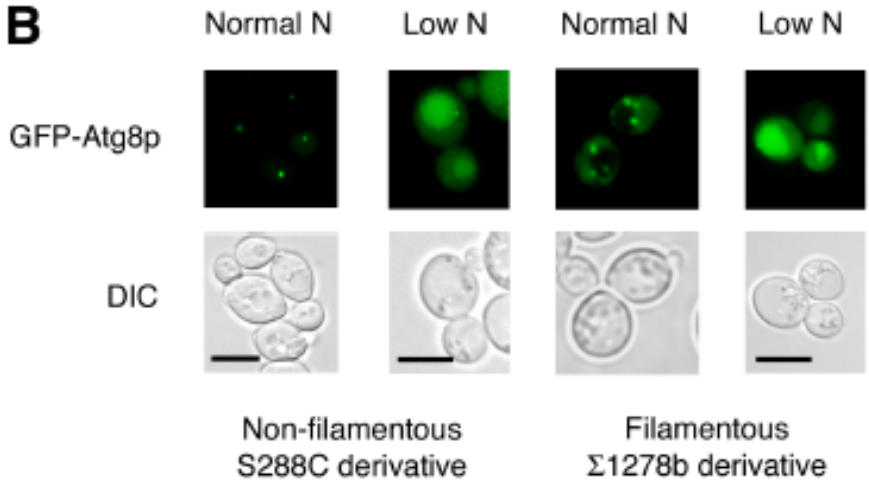
B
Normal N
Low N
Normal N
Low N
GFP-Atg8p
DIC
Non-filamentous
S288C derivative
Filamentous
Σ1278b derivative

Figure 2.3 Colony and cell morphology of autophagy mutants in a filamentous strain of budding yeast. (A) Low-magnification images of yeast colonies from wild-type, autophagy-deficient, and ATG1 overexpression strains in the filamentous Σ1278b genetic background. All strains were grown for 6 days at 30°C in SLAD medium (Materials and Methods) supplemented with 1% ethanol; this analysis was repeated using nitrogen deprivation (SLAD medium) alone to induce PHG, and observed results were identical. The scale bar represents 1 mm. (B) Cell morphology of wild-type, autophagy-deficient, and ATG1 overexpression strains of the filamentous Σ1278b genetic background as imaged by differential interference contrast (DIC) microsocopy. Strains were cultured as above; colonies were scraped into a solution for DIC microscopy. The scale bar represents 5 ∝m. (C) Pie charts indicating the observed cell length:width ratios of each strain. The cell sample number is indicated in the center of each chart.

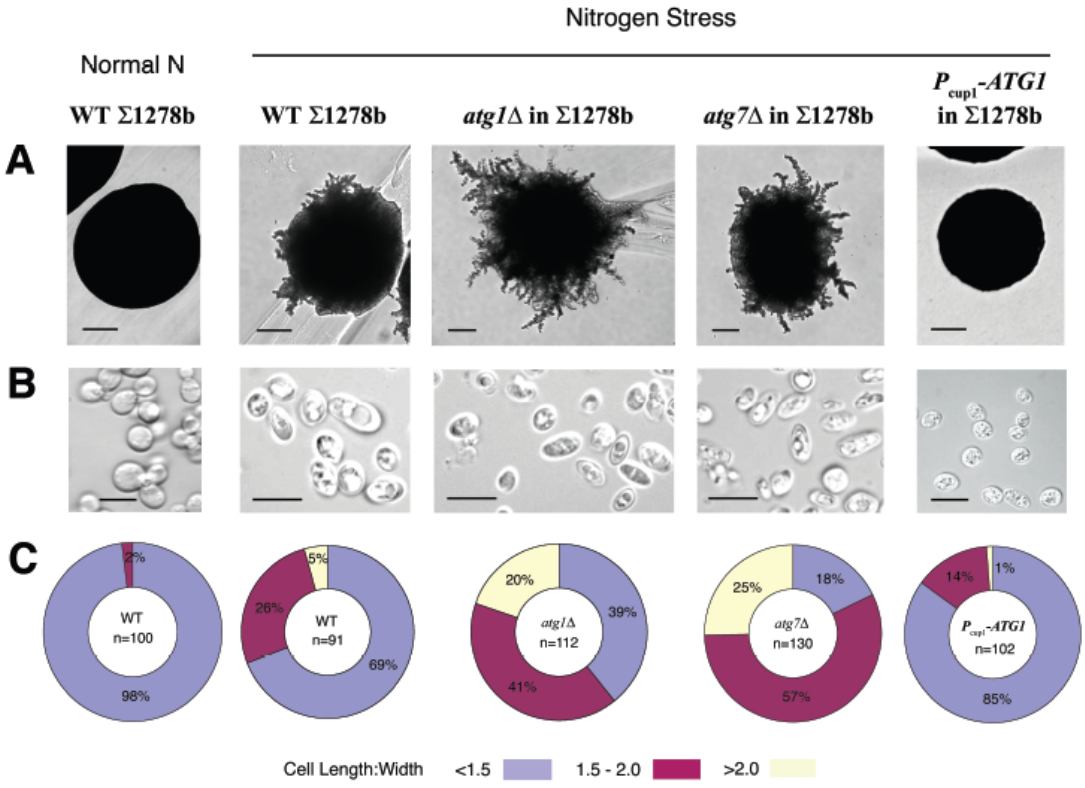
Nitrogen Stress
Normal N
WT Σ1278b
WT Σ1278b
atg1Δ in Σ1278b
atg7Δ in Σ1278b
Pcup1-ATG1 in Σ1278b
A
B
C
2%
98%
WT
n=100
5%
26%
69%
WT
n=91
20%
39%
41%
atg1Δ
n=112
25%
18%
57%
atg7Δ
n=130
14%
1%
85%
Pcup1-ATG1
n=102
Cell Length:Width
<1.5
1.5 - 2.0
>2.0

Figure 2.4 Graded PHG response during nitrogen stress in wild-type and autophagy-deficient filamentous yeast. Low-magnification images of diploid wild-type and homozygous diploid atg7Δ colonies of the Σ1278b genetic background under varying conditions of nitrogen stress. Strains were cultured 6 days at 30°C in SLAD medium prepared with the indicated concentrations of ammonium sulfate. Both strains were grown in medium supplemented with uracil and leucine to complement nutritional auxotrophies; thus, the absence of ammonium sulfate does not constitute complete nitrogen starvation. As indicated in the top and bottom panels, atg7Δ initiates PHG at a higher concentration of ammonium sulfate than does the wild-type strain. The scale bar represents 1 mm.

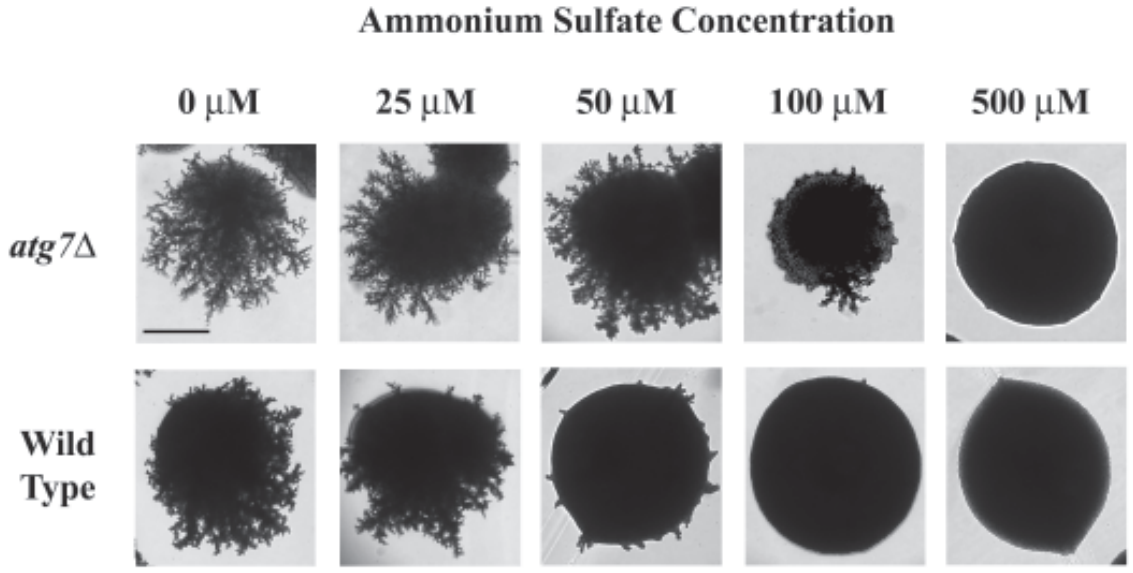
Ammonium Sulfate Concentration
0 μM
25 μM
50 μM
100 μM
500 μM
atg7Δ
Wild Type

Figure 2.5 Cell survival of Σ1278b mutants impaired in autophagy and pseudohyphal growth. The diploid wild type Σ1278b strain and diploid non-filamentous S288c-derivative BY4743 were assayed for cell viability under conditions of nitrogen stress. Briefly, cultures were grown to log-phase in YPD before being transferred to low-nitrogen growth medium. At the indicated days, aliquots of cells were diluted and plated on YPD. Percent survival was determined by counting the number of surviving colonies from triplicate platings and by dividing the number of colonies at each time point by the average number of colonies obtained at day 0. Homozygous diploid atg1Δ and muc1Δ mutants in the filamentous Σ1278b background were also assayed for cell viability as described above.

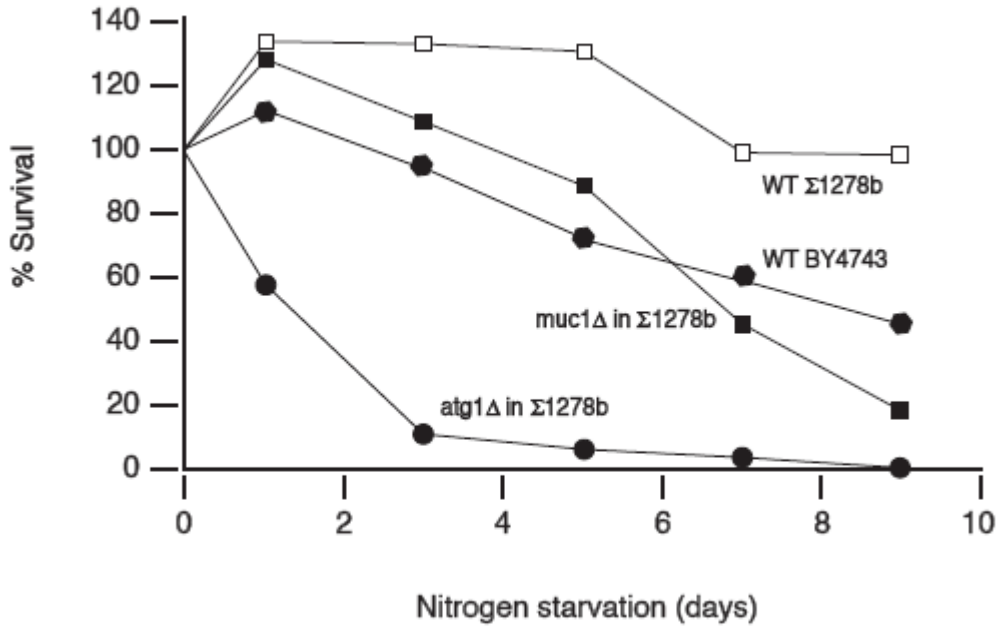
140
120
100
80
60
40
20
0
% Survival
0
2
4
6
8
10
Nitrogen starvation (days)
WT Σ1278b
WT BY4743
muc1Δ in Σ1278b
atg1Δ in Σ1278b

Figure 2.6 Model of the interrelationship between pseudohyphal growth and autophagy in yeast. In the filamentous strain Σ1278b, nitrogen stress induces both filamentous growth and autophagy, with both process contributing to cell survival and presumably to the relief of nitrogen stress, although autophagy plays a bigger role (indicated by the larger arrow). In the absence of autophagy, nitrogen stress is exacerbated, and the pseudophyphal growth response is increased. From our studies, autophagy regulates PHG as indicated; however, the molecular mechanism of this regulation remains to be determined.

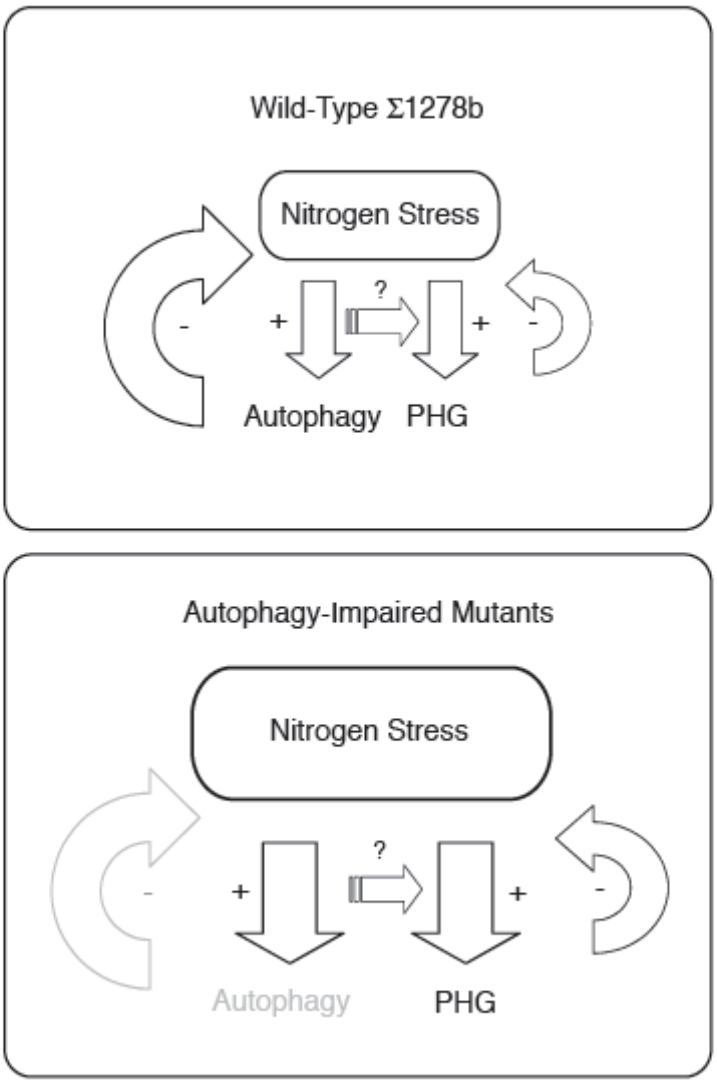
Wild-Type Σ1278b
Nitrogen Stress
?
-
+
+
-
Autophagy
PHG
Autophagy-Impaired Mutants
Nitrogen Stress
?
-
+
+
-
Autophagy
PHG

Table 2.1 Real-time RT-PCR analysis of autophagy gene induction during nitrogen stress. Systematic and standard gene names, and fold change measured by real time RT-PCR are listed.

Table S1. Real-time RT-PCR analysis of autophagic gene induction during nitrogen stress.

Gene[a]	Systematic Gene Name	Fold-Change[b]
ATG1	YGL180w	5.6-fold increase
ATG3	YNR007c	4-fold increase
ATG5	YPL149w	2.67-fold increase
ATG6	YPL120w	3.8-fold increase
ATG9	YDL149w	3-fold increase
ATG14	YBR128c	5.67-fold increase
ATG17	YLR423c	3.5-fold increase
ATG19	YOL082w	3.42-fold increase
ATG20	YDL113c	3.22-fold increase
ATG21	YPL100w	3.33-fold increase
ATG22	YCL038c	2.4-fold increase

[a]Results for *ATG4*, *ATG7*, and *ATG8* were inconclusive due to faint signal.

[b]RNA abundance was evaluated after two hours growth under conditions of nitrogen deprivation. Fold-change was calculated from expression levels determined by the comparative threshold method for relative quantitation of gene expression using actin in the control sample as a normalizer.

References

Abeliovich, H. 2007 Mitophagy: the life-or-death dichotomy includes yeast. Autophagy 3: 275-277.

Abeliovich, H., W. A. Dunn, J. Kim and D. J. Klionsky, 2000 Dissection of autophagosome biogenesis into distinct nucleation and expansion steps. J Cell Biol 151: 1025-1034.

Bardwell, L., J. G. Cook, D. Voora, D. M. Baggott, A. R. Martinez et al., 1998 Repression of yeast Ste12 transcription factor by direct binding of unphosphorylated Kss1 MAPK and its regulation by the Ste7 MEK. Genes Dev 12: 2887-2898.

Baudin, A., O. Ozier-Kalogeropouls, A. Denouel, F. Laroute and C. Cullin, 1993 A simple and efficient method for direct gene deletion in Saccharomyces cerevisiae. Nucleic Acids Res 21: 3329-3330.

Borneman, A. R., J. A. Leigh-Bell, H. Yu, P. Bertone, M. Gerstein et al., 2006 Target hub proteins serve as master regulators of development in yeast. Genes Dev 20: 435-448.

Chan, T. F., P. G. Bertram, W. Ai and X. F. Zheng, 2001 Regulation of APG14 expression by the GATA-type transcription factor Gln3p. J Biol Chem 276: 6463-6467.

Cook, J. G., L. Bardwell and J. Thorner, 1997 Inhibitory and activating functions forMAPK Kss1 in the S. cerevisiae filamentous growth signalling pathway. Nature 390: 85-88.

Gagiano, M., M. Bester, D. Van Dyk, J. Franken, F. F. Bauer et al., 2003 Mss11p is a transcription factor regulating pseudohyphal differentiation, invasive growth and starch metabolism in Saccharomyces cerevisiae in response to nutrient availability. Mol Microbiol 47: 119-134.

Gancedo, J. M., 2001 Control of pseudohyphae formation in Saccharomyces cerevisiae. FEMS Microbiol Rev 25: 107-123.

Gimeno, C. J., P. O. Ljungdahl, C. A. Styles and G. R. Fink, 1992 Unipolar cell divisions in the yeast S. cerevisiae lead to filamentous growth: regulation by starvation and RAS. Cell 68: 1077-1090.

Guo, B., C. A. Styles, Q. Feng and G. Fink, 2000 A Saccharomyces gene family involved in invasive growth, cell-cell adhesion, and mating. Proc Natl Acad Sci U S A 97: 12158-12163.

He, C., and D. J. Klionsky, 2006 Autophagy and neurodegeneration. ACS Chem Biol 23: 211-213.

Ichimura, Y., T. Kirisako, T. Takao, Y. Satomi, Y. Shimonishi et al., 2000 A ubiquitin-like system mediates protein lipidation. Nature 408: 488-492.

Kim, J., W. P. Huang and D. J. Klionsky, 2001 Membrane recruitment of Aut7p in the autophagy and cytoplasm to vacuole targeting pathways requires Aut1p, Aut2p, and the autophagy conjugation complex. J Cell Biol 152: 51-64.

Kim, J., W. P. Huang, P. E. Stromhaug and D. J. Klionsky, 2002 Convergence of multiple autophagy and cytoplasm to vacuole targeting components to a perivacuolar membrane compartment prior to de novo vesicle formation. J Biol Chem 277:

763-773.
Kirisako, T., M. Baba, N. Ishihara, K. Miyazawa, M. Ohsumi et al., 1999 Formation process of autophagosome is traced with Apg8/Aut7p in yeast. J Cell Biol 147: 435-446.
Klionsky, D. J., 2005 The molecular machinery of autophagy: Unanswered questions. J Cell Sci. 118: 7- 18.
Klionsky, D. J., and A. Kumar, 2006 A systems biology approach to learning autophagy. Autophagy 2: 12-23.
Kobayashi, O., H. Suda, T. Ohtani and H. Sone 1996 Molecular cloning and analysis of the dominant flocculation gene FLO8 from Saccharomyces cerevisiae. Mol. Gen. Genet. 251: 707-715.
Kron, S. J., 1997 Filamentous growth in budding yeast. Trends Microbiol 5: 450-454.
Kron, S. J., C. A. Styles and G. R. Fink, 1994 Symmetric cell division in pseudohyphae of the yeast Saccharomyces cerevisiae. Mol Biol Cell 5: 1003-1022.
Lambrechts, M. G., F. F. Bauer, J. Marmur and I. S. Pretorius, 1996 Muc1, a mucin-like protein that is regulated by Mss10, is critical for pseudohyphal differentiation in yeast. Proc Natl Acad Sci U S A 93: 8419-8424.
Levine, B., and D. J. Klionsky, 2004 Development by Self-Digestion: Molecular Mechanisms and Biological Functions of Autophagy. Devel. Cell 6: 463-477.
Liu, H., C. A. Styles and G. Fink, 1996 Saccharomyces cerevisiae S288C has a mutation in FLO8, a gene required for filamentous growth. Genetics 144: 967-978

Liu, H., C. A. Styles and G. R. Fink, 1993 Elements of the yeast pheromone response pathway required for filamentous growth of diploids. Science 262: 1741-1744.
Lo, W. S., E. I. Raitses and A. M. Dranginis, 1997 Development of pseudohyphae by embedded haploid and diploid yeast. Curr Genet 32: 197-202.
Longtine, M. S., A. MckenzieE III, D. J. Demarini, N. G. Shah, A. Wach et al., 1998 Additional Modules for Versatile and Economical PCR-based Gene Deletion and Modification in Saccharomyces cerevisiae. Yeast 14: 953-961.
Madhani, H. D., and G. R. Fink, 1997 Combinatorial control required for the specificity of yeast MAPK signaling. Science 275: 1314-1317.
Madhani, H. D., and G. R. Fink, 1998 The control of filamentous differentiation and virulence in fungi. Trends in Cell Biol. 8: 348-353.
Matsuura, A., M. Tsukada, Y. Wada and Y. Ohsumi, 1997 Apg1p, a novel protein kinase required for the autophagic process in Saccharomyces cerevisiae. Gene 192: 245-250.
Mizushima, N., T. Noda, T. Yoshimori, Y. Tanaka, T. Ishii et al., 1998 A protein conjugation system essential for autophagy. Nature 395: 395-398.
Mosch, H. U., R. L. Roberts and G. R. Fink, 1996 Ras2 signals via the Cdc42/Ste20/mitogen-activated protein kinase module to induce filamentous growth in Saccharomyces cerevisiae. Proc Natl Acad Sci U S A 93: 5352-5356.
Nair, U., and D. J. Klionsky, 2005 Molecular mechanisms and regulation of specific and nonspecific autophagy pathways in yeast. J Biol Chem 280: 41785-41788.
Peter, M., A. M. Nerman, H. O. Park, M. V. Lohuizen and I. Herskowitz, 1996 Functional analysis of the interaction between the small GTP inding protein Cdc42 and the Ste20 protein kinase in yeast. EMBO J 15: 7046-7059.

Prinz, S., I. Avila-Campillo, C. Aldridge, A. Srinivasan, K. Dimitrov et al., 2004 Control of Yeast Filamentous-Form Growth by Modules in an Integrated Molecular Network. Genome Research 14: 380-390.

Reggiori, F., and D. J. Klionsky, 2002 Autophagy in the eukaryotic cell. Eukaryot Cell 1: 11-21.

Reggiori, F., and D. J. Klionsky, 2005 Autophagosomes: biogenesis from scratch? Curr Opin Cell Biol 17: 415-422.

Reggiori, F., K. A. Tucker, P. E. Stromhaug and D. J. Klionsky, 2004 The Atg1-Atg13 complex regulates Atg9 and Atg23 retrieval transport from the pre-autophagosomal structure. Devel. Cell 6: 79-90.

Rieger, K. E., and G. Chu, 2004 Portrait of transcriptional responses to ultraviolet and ionizing radiation in human cells. Nucleic Acids Res 32: 4786-4803.

Robertson, L. S., and G. R. Fink, 1998 The three yeast A kinases have specific signaling functions in pseudohyphal growth. Proc Natl Acad Sci U S A 95: 13783-13787.

Rua, D., B. T. Tobe and S. J. Kron, 2001 Cell cycle control of yeast filamentous growth. Curr Opin Microbiol 4: 720-727.

Rupp, S., E. Summers, H. J. Lo, H. Madhani and G. Fink, 1999 MAP kinase and cAMP filamentation signaling pathways converge on the unusually large promoter of the yeast FLO11 gene. Embo J 18: 1257-1269.

Scott, R. C., G. Juhasz and T. P. Neufeld, 2007 Direct induction of autophagy by Atg1 inhibits cell growth and induces apoptotic cell death. Curr Biol 17: 1-11.

Scott, S. V., A. Hefner-Gravink, K. A. Morano, T. Noda, Y. Ohsumi et al., 1996 cytoplasm-to-vacuole targeting and autophagy employ the same machinery to deliver proteins to the yeast vacuole. Proc Natl Acad Sci U S A 93: 12304-12308.

Shintani, T., and D. J. Klionsky, 2004a Autophagy in health and disease: a double-edged sword. Science 306: 990-995.

Shintani, T., and D. J. Klionsky, 2004b Cargo Proteins Facilitate the Formation of Transport Vesicles in the Cytoplasm to Vacuole Targeting Pathway. J. Biol. Chem. 279: 29889-29894.

Sikorski, R. S., and P. Hieter, 1989 A system of shuttle vectors and yeast host strains designed for efficient manipulation of DNA in Saccharomyces cerevisiae. Genetics 122: 19-27.

Stephan, J., and P. K. Herman, 2006 The regulation of autophagy in eukaryotic cells: do all roads pass through Atg1? Autophagy 2: 146-148.

Suzuki, K., T. Kirisako, Y. Kamada, N. Mizushima, T. Noda et al., 2001 The pre-autophagosomal structure organized by concerted functions of APG genes is essential for autophagosome formation. EMBO J 20: 5971-5981.

Takeshige, K., M. Baba, S. Tsuboi, T. Noda, and Y. Ohsumi, 1992 Autophagy in yeast demonstrated with proteinase-deficient mutants and conditions for its induction. J Cell Biol 119: 301-311.

Tusher, V. G., R. Tibshirani and G. Chu, 2001 Significance analysis of microarrays applied to the ionizing radiation response. Proc Natl Acad Sci U S A 98: 5116-5121.

Van Dyk, D., I. S. Pretorius and F. F. Bauer, 2005 Mss11p is a central element of the regulatory network that controls FLO11 expression and invasive growth in Saccharomyces cerevisiae. Genetics 169: 91-106.

Wang, C.-W., and D. J. Klionsky, 2003 The Molecular Mechanism of Autophagy. Molecular Medicine 9: 65-76.
Webber, A. L., M. G. Lambrechts and I. S. Pretorius, 1997 MSS11, a novel yeast gene involved in the regulation of starch metabolism. Curr Genet 32: 260-266.
Winzeler, E. A., D. D. Shoemaker, A. Astromoff, H. Liang, K. Anderson et al., 1999 Fuctional characterization of the S. cerevisiae genome by gene deletion and parallel analysis. Science 285: 901-906.
Yang, Z., J. Huang, J. Geng, U. Nair and D. J. Klionsky, 2006 Atg22 recycles amino acids to link the degradative and recycling functions of autophagy. Mol Biol Cell 17: 5094-5104.
Yorimitsu, T., U. Nair, Z. Yang, and D. J. Klionsky, 2006 Endoplasmic reticulum stress triggers autophagy. J Biol Chem 281: 30299-30304.

Chapter 3

Overexpression of Autophagy-Related Genes Inhibits Yeast Filamentous Growth

Introduction

Eukaryotic cells respond to environmental stresses through an intricate interplay of signaling pathways mediating a broad array of biological processes. The scope of these processes is typically extensive, and the corresponding pathways engage in significant crosstalk to generate a concerted cellular response (Madhani et al. 1997; Kolch et al. 2005). This interconnection of pathways and stress responses is very evident in the budding yeast *S. cerevisiae* (Pan et al. 2000; Lengeler et al. 2000; Robers et al. 1994). In particular, here, we consider two potentially interrelated stress responses in yeast: autophagy and filamentous growth.

Autophagy is a ubiquitous process in eukaryotic cells, in which portions of the cytoplasm are sequestered in double-membrane vesicles for delivery to a degradative organelle (the vacuole or lysosome)(Levine et al. 2004; Reggiori et al. 2002; Klionsky et al. 2005). In yeast, autophagy is induced by a variety of stresses, including nitrogen deprivation. Under conditions of nitrogen stress, autophagy principally serves as a survival mechanism, replenishing internal nutrient pools by degrading cytoplasmic proteins and organelles, the constituent components of which are subsequently recycled to the cytosol (Shintani et al. 2004; He et al. 2007). In yeast, 30 autophagy-related genes have been identified (Levine et al. 2004; Nair et al. 2005), and functions within the

autophagy pathway have been ascribed to most of these genes (Klionsky et al. 2005); however, the mechanisms regulating this pathway and its crosstalk with other signaling networks remain to be defined.

In addition to autophagy, other cell processes are also induced by nitrogen stress in the budding yeast. Specifically, certain strains of *S. cerevisiae* undergo a dramatic change in growth form under conditions of nitrogen deprivation, transitioning from a typical "yeast-like" form to a filamentous form of growth (Gimeno et al. 1992; Madhani et al. 1998). During filamentous growth, yeast cells delay in G_2/M, exhibit an elongated morphology, invade their growth substrate, and remain physically connected after cytokinesis, collectively resulting in the formation of multicellular filaments, or pseudohyphae (Gimeno et al. 1992; Kron et al. 1994; Lo et al. 1997). This pseudohyphal growth is thought to be a type of foraging mechanism, allowing non-motile yeast to scavenge a wider area for nutrients (Gancedo et al. 2001). Yeast filamentous growth is now appreciated as a strong model of fungal pathogenicity, since similar growth transitions are required for virulence in *C. albicans* and in related pathogenic fungi (Lo et al. 1997).

The morphological and genetic changes underlying yeast filamentous growth are extensive, and the regulatory mechanisms controlling this process seem to be equally complex (Madhani et al. 1998; Kron et al. 1997). Presently, at least two signaling pathways are known to regulate yeast filamentous growth: 1) the nutrient-sensing cyclic AMP-protein kinase A (PKA) pathway (Mosch et al. 1996; Robertson et al. 1998), and 2) a mitogen-activated protein kinase (MAPK) pathway consisting of Ste11, Ste7, and the MAPK Kss1 (Liu et al. 1993). A large set of genes act downstream of these pathways,

encompassing components of pathways regulating polarized growth, cell cycle progression, and bud site selection in yeast (Kron et al. 1994; Madhani et al. 1999; Lo et al. 1998). This downstream gene set, however, is incomplete; many additional genes and pathways likely contribute to filamentous growth, and the identification of these genes will be a necessary step in clarifying our understanding of this cellular stress response.

Results

Autophagy and filamentous growth: interrelated stress responses: To consider the scope of genes and pathways contributing to filamentous growth, we profiled gene expression patterns in a filamentous strain of budding yeast under conditions of nitrogen stress in Chapter 2. From this analysis, we identified extensive upregulation of the autophagy pathway; 14 of 29 autophagy-related genes in yeast were transcriptionally induced during the first two hours of nitrogen stress. Through further analysis, we confirmed that the autophagy pathway is active in a filamentous strain of yeast during nitrogen starvation. In this same study, we constructed several yeast strains deleted for key autophagy-related genes and assayed these mutants for filamentous growth phenotypes. Surprisingly, these autophagy-impaired mutants were hyperfilamentous, exhibiting exaggerated filamentous growth both during nitrogen stress and in the presence of short-chain alcohols (known conditions for the induction of filamentous growth) (Gimeno et al. 1992; Lorenz et al. 2000). Filamentous growth is a graded response, and autophagy-deficient mutants initiated filamentous growth at higher concentrations of available nitrogen. Thus, from these studies, we developed a model

describing the interrelationship of autophagy and filamentous growth, wherein the level of autophagy contributes significantly to the degree of nitrogen stress in yeast, and filamentous growth is responsive to the state of this stress.

Inhibited filamentous growth upon overexpression of autophagy-related genes:

To further investigate this apparent link between autophagy and filamentous growth, we undertook the converse phenotypic analysis from that described above, assaying filamentous growth upon overexpression of *ATG* genes. Specifically, we previously performed an overexpression analysis of the autophagy gene *ATG1*. *ATG1* encodes a serine/threonine kinase required for the induction of autophagy (Matsuura et al. 1997; Stephan et al. 2006). Interestingly, overexpression of *ATG1* results in severely decreased filamentous growth. This finding raises several pertinent questions. Is the filamentous growth phenotype specific to the overexpression of *ATG1*, or does it represent a more general effect resulting from perturbation of the autophagy pathway? Furthermore, is autophagy significantly affected by overexpression of *ATG1*, and does this result affect our model of the interrelationship between autophagy and filamentous growth?

To address these questions, we present here an expanded phenotypic study of filamentous growth upon overexpression of autophagy-related genes. For this study, we used a collection of nine additional *ATG* genes (*ATG3*, *ATG4*, *ATG6*, *ATG7*, *ATG17*, *ATG19*, *ATG23*, *ATG24*, *ATG29*) cloned into a high-copy expression vector, such that each gene is under transcriptional control of a galactose-inducible promoter (Kumar et al. 2002). These overexpression constructs were generated as part of a larger cloning project, and the *ATG* gene collection reported here represents the full set of autophagy-

related genes successfully cloned during the initial stages of the project (Kumar et al. 2002; Kumar et al. 2003). Plasmids carrying the cloned *ATG* genes were introduced individually into a filamentous strain of yeast (derived from Σ1278b) by standard methods of DNA transformation (Ito et al. 1983). Gene overexpression was driven by galactose induction, and filamentous growth was assayed at the colony and cellular levels in low-nitrogen medium supplemented with 1% butanol (Figure 3.1).

Consistent with the phenotype observed upon overexpression of *ATG1*, overexpression of *ATG3*, *ATG7*, *ATG17*, *ATG19*, *ATG23*, *ATG24*, and *ATG29* also resulted in decreased filamentous growth (Table 3.1). Specifically, in these mutants, surface-spread filamentation was diminished, and a greater percentage of cells were round (Figure 3.1); yeast cells undergoing filamentous growth are characteristically elongated and can be distinguished from cells undergoing normal vegetative growth by this distinctive cell morphology (Gimeno et al. 1992). This phenotypic effect was not uniform over all mutants tested, however, as overexpression of *ATG4* and *ATG6* yielded no observable filamentous growth defects.

From these results, we conclude that the filamentous growth defect observed upon overexpression of *ATG1* is not specific to this gene; instead, overexpression mutants of at least eight additional autophagy-related genes each exhibit similar filamentous growth phenotypes. The outlying results from overexpression of *ATG4* and *ATG6* are interesting. *ATG4* encodes a cysteine protease that cleaves Atg8 to a form required for autophagosome and Cvt vesicle generation (Lang et al. 1998); thus, it does not function exclusively in the autophagy pathway. *ATG6/VPS30* encodes a protein involved in vacuolar protein sorting and, specifically, in the retrieval of the carboxypeptidase Y

receptor, Vps10, to the late Golgi body from the endosome (Seaman et al. 1997; Kametaka et al. 1998). It is, therefore, unclear whether overexpression of either gene would significantly impact upon autophagic activity, although a similar statement could be made regarding the autophagy-related genes yielding filamentous growth phenotypes as well.

To consider whether autophagic activity is indeed affected by overexpression of *ATG* genes, we assessed activity of the pathway upon overexpression of *ATG1*. In *D. melanogaster*, overexpression of *ATG1* is sufficient to induce high levels of autophagy under repressive conditions (Scott et al. 2007); thus, *ATG1* is the strongest candidate gene to affect autophagic activity in *S. cerevisiae*. To assess activity of the autophagy pathway, we used a chimera consisting of GFP fused to the amino terminus of Atg8, similar to the method developed by Shintani and Klionsky (Shintani et al. 2004).Briefly, Atg8 is a ubiquitin-like protein essential for autophagy (Ichimura et al. 2000). It is one of two proteins that remain associated with the completed autophagosome, allowing it to serve as an effective marker for this structure (Kirisako et al. 1999). In this assay, we use GFP-Atg8 to track delivery of Atg8 to the vacuole (Klionsky et al. 2006); upon trafficking to the vacuole, Atg8 is degraded, while GFP accumulates in the vacuolar lumen, due to its relative stability in the presence of vacuolar hydrolases. Thus, GFP fluorescence in the vacuole indicates autophagic activity, reflecting the net flux of GFP into/out of the vacuole (Shintani et al. 2004; Kim et al. 2001).

By this approach, we detect comparable levels of vacuolar GFP fluorescence during nitrogen stress in both wild type and *ATG1* overexpression mutants (Figure 3.2); for purposes of comparison, we also included the same background yeast strain deleted

for *ATG1*, as autophagy is inhibited in this mutant. Under normal growth conditions, GFP-Atg8 is localized to a perivacuolar spot representing the phagophore assembly site (PAS), and overexpression of *ATG1* in yeast is insufficient to induce autophagy under repressive conditions (DJ Klionsky, personal communication). As shown in Figure 3.2, after 10 minutes of nitrogen stress, GFP-Atg8 is localized largely to the PAS, although faint vacuolar fluorescence is visible in the wild type and *ATG1* overexpression strains. Autophagy is strongly active in all but the *atg1*Δ strain after 30 minutes of nitrogen stress. Thus, the autophagy pathway is clearly active upon overexpression of *ATG1* under conditions of nitrogen stress; however, by tracking GFP-Atg8, we do not detect noticeable differences in the kinetics of autophagic activation following *ATG1* overexpression as compared to wild type. Also, overexpression of any one *ATG* gene does not affect transcription of the remaining pathway (Nair et al. 2005). Possibly, *ATG* gene overexpression may subtly impact upon autophagic activity in a manner that is not apparent by the methods employed here; electron microscopy may be necessary to investigate autophagosome number and generation in *ATG* gene overexpression mutants as a more sensitive measure of pathway activity.

It is interesting to note that *ATG1* overexpression mutants do exhibit distinct colony morphologies, forming smaller colonies than corresponding wild type strains under conditions of nitrogen deprivation. *ATG1* overexpression mutants, however, are not petite; they grow normally on yeast growth medium with glycerol substituted for glucose, and, hence, are not obviously impaired in mitochondrial function. Similarly, we also do not observe morphological differences in colonies from other *ATG* overexpression strains.

Discussion

From the studies presented here, we find that the overexpression of autophagy-related genes can inhibit yeast filamentous growth, and we specifically report that this inhibition is not unique to a single *ATG* gene, but is instead widespread throughout much of the pathway. We, furthermore, find that *ATG* gene overexpression does not manifest itself in markedly altered autophagic activity.

These results hold significant implications regarding our understanding of the interrelationship between autophagy and yeast filamentous growth. In Chapter 2, we have developed a model linking these processes largely through their respective impact on, and response to, the available nitrogen pool in the yeast cell. The basic principles of this model are presented in Figure 3.3. Nitrogen stress activates autophagy, which mitigates the effects of nitrogen deprivation, contributing to internal pools of nitrogen through the breakdown and recycling of proteins and organelles. Filamentous growth is responsive to the state of this nitrogen pool, with increased filamentation correlated with decreased available nitrogen. Inhibition of autophagy exacerbates nitrogen stress, reducing the nitrogen pool and driving exaggerated filamentous growth. Accordingly, yeast mutants impaired in autophagy initiate filamentous growth at higher concentrations of externally supplied nitrogen. In developing this model, we also raised the possibility of a regulatory connection between autophagy and filamentous growth independent of the nitrogen pool and the mechanism discussed above.

Since the overexpression of autophagy-related genes inhibits filamentous growth with relatively little impact on the overall activity of the pathway, we expect that this regulatory effect is not dependent upon any autophagy-driven relief of nitrogen stress. In particular, this result supports a model highlighting crosstalk between the pathways (Figure 3.3). According to this hypothesis, components of the autophagy pathway drive events regulating filamentous growth. The converse does not appear to be true, as inhibition of filamentous growth does not affect autophagic activity. It is important to note that this mechanism of inter-pathway crosstalk is not at odds with the presence of regulatory effects mediated through the nitrogen pool; neither event is mutually exclusive of the other. Based on our findings, autophagy and filamentous growth are interrelated both as mutual responses to nitrogen stress and by regulatory crosstalk from the autophagy pathway.

At present, the mechanism of crosstalk between autophagy and filamentous growth remains unclear, and several possible regulatory connections could link the pathways. Most simply, a component of the autophagy pathway may directly regulate a gene controlling or contributing to filamentous growth. The kinase Atg1 is a candidate to fill such a role (Stephan et al. 2006), particularly since it is required for the induction of autophagy and is known to function as part of a larger protein complex (Matsuura et al. 1997). Atg1, however, is not known to target filamentous growth genes. Moreover, diminished filamentous growth is observed upon overexpresion of most autophagy-related genes; the effect is not specific to *ATG1*, as might be expected if Atg1 directly regulated filamentous growth. Autophagy-related genes downstream of *ATG1* may feed back to modulate Atg1 activity upon overexpression, but such a regulatory mechanism

has not been identified to date and seems unlikely based upon existing knowledge of the pathway.

Alternatively, overexpression of autophagy-related genes may result in a signal that feeds back to regulate filamentous growth through an upstream control point, such as the Tor protein kinases. The Tor kinases, Tor1 and Tor2, regulate cell growth in response to nutrient availability and function upstream of both autophagy and filamentous growth pathways in yeast (Zheng et al., 1997; Kamada et al., 2000). Specifically, the Tor kinases function in one of two distinct complexes; Tor complex 1 (TORC1) is sensitive to the natural product rapamycin and is thought to regulate autophagy and filamentous growth (Kamada et al. 2000; Loewith et al. 2002). It is unclear, however, as to how TORC1 contributes to the interrelationship of these processes; the inhibition of TORC1 activates autophagy and inhibits filamentous growth (Cutler et al. 2001), yet both autophagy and filamentous growth are active under conditions of nitrogen stress in filamentation-competent yeast. While TORC1 represents a potentially interesting shared control point upstream of both pathways, additional studies will be necessary to resolve its contributions to the activities of both autophagy and filamentous growth.

In total, this study adds to our knowledge concerning the interconnection between autophagy and filamentous growth. These two cellular processes both relieve nitrogen stress in yeast; autophagy contributes more significantly to the cell response under conditions of nitrogen deprivation, and filamentous growth is responsive to the degree of this stress. In addition, autophagy regulates the filamentous growth response independent of its general effect on the cellular nitrogen pool, but the specific genes mediating this regulatory control are unknown. The regulatory linkage between autophagy and

filamentous growth is likely unrelated to one particular *ATG* gene and may encompass components of the general cell machinery responsive to nutritional stress. In the near future, additional studies of the yeast *ATG* gene complement should reveal the molecular mechanism underlying the coordinated regulation of these processes.

Acknowledgements

This work was supported by grant RSG-06-179-01-MBC from the American Cancer Society, grant DBI 0543017 from the National Science Foundation, and Basil O'Connor Award 5-FY05-1224 from the March of Dimes.

Figure 3.1. Filamentous growth phenotypes of *ATG* overexpression mutants. (A) Low magnification images of yeast colonies upon overexpression of the indicated *ATG* gene under conditions inducing filamentous growth. All mutants were derived from the filamentous yeast strain Σ1278b. High-copy plasmids (with the *URA3* marker) carrying *ATG* genes cloned under transcriptional control of a galactose-inducible promoter were introduced into a haploid strain of Σ1278b; an empty vector was introduced into this strain as well to serve as the wild-type control. Gene overexpression was achieved by galactose induction according to standard methods (Kumar et al., 2002). Filamentous growth was observed on SC –Ura low-nitrogen medium (50 μM ammonium sulfate) with galactose as the carbon source and 1% (v/v) butanol (Lorenz et al., 2000). Mutants were grown for 3-5 days at 30ºC before examination by standard microscopy. The scale bar represents 1 mm. (B) Cell morphology of *ATG* overexpression strains imaged by differential interference contrast microscopy. Cells undergoing filamentous growth appear elongated relative to cells undergoing normal vegetative growth. Some mutants exhibit a greater degree of flocculence, or cell-cell adhesion, as well. The scale bar indicates 5 μm. (C) Pie charts indicating the observed cell length:width ratio of each strain. The cell sample number is indicated in the center of each chart.

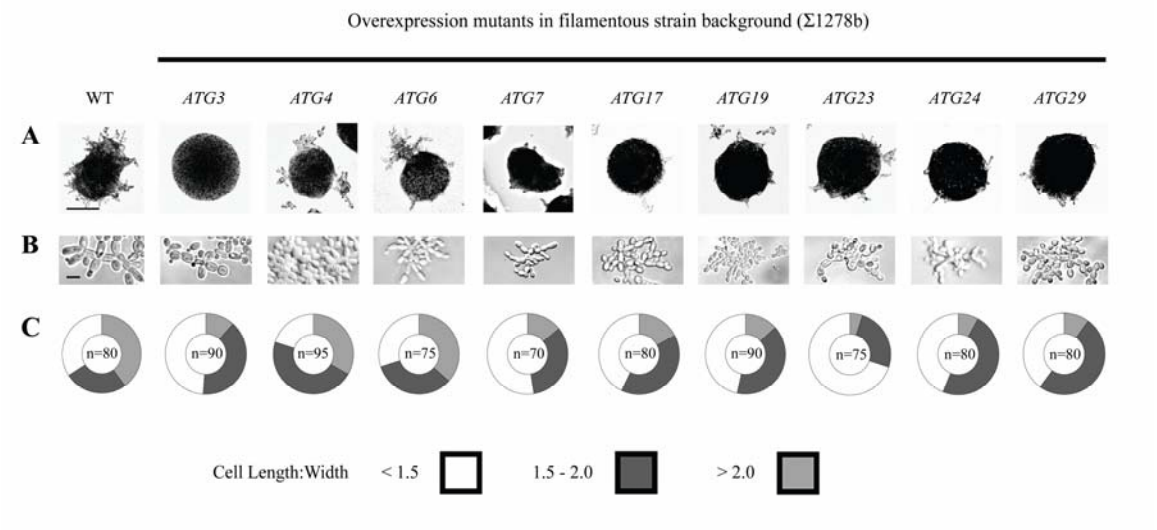
Overexpression mutants in filamentous strain background (Σ1278b)
WT
ATG3
ATG4
ATG6
ATG7
ATG17
ATG19
ATG23
ATG24
ATG29
A
B
C
n=80
n=90
n=95
n=75
n=70
n=80
n=90
n=75
n=80
n=80
Cell Length:Width
< 1.5
1.5 - 2.0
> 2.0

Figure 3.2. Activity of the autophagy pathway upon overexpression of *ATG1*. (A) For this study, we expressed *ATG1* from the copper-inducible *CUP1* promoter carried on a low-copy yeast shuttle vector, resulting in 2-3 fold gene overexpression in medium lacking exogenously supplied copper sulfate. This construct was introduced into the Σ1278b strain of yeast, carrying a plasmid-borne GFP-*ATG8* allele, for analysis of autophagic activity after 10, 20, and 30 minutes of nitrogen stress. Cell images obtained by differential interference contrast microscopy are included below each fluorescence micrograph. Vacuolar fluorescence indicates autophagic activity. The corresponding wild-type (B) and *atg1*Δ (C) strains are included for comparison. The kinetics and overall levels of autophagic activity in the *ATG1* overexpression and wild-type strains are comparable, with pathway activity clearly evident upon 20 and 30 minutes nitrogen stress in both strains. Activity of the autophagy pathway is inhibited in the *atg1*Δ strain. The scale bar indicates 5 μm.

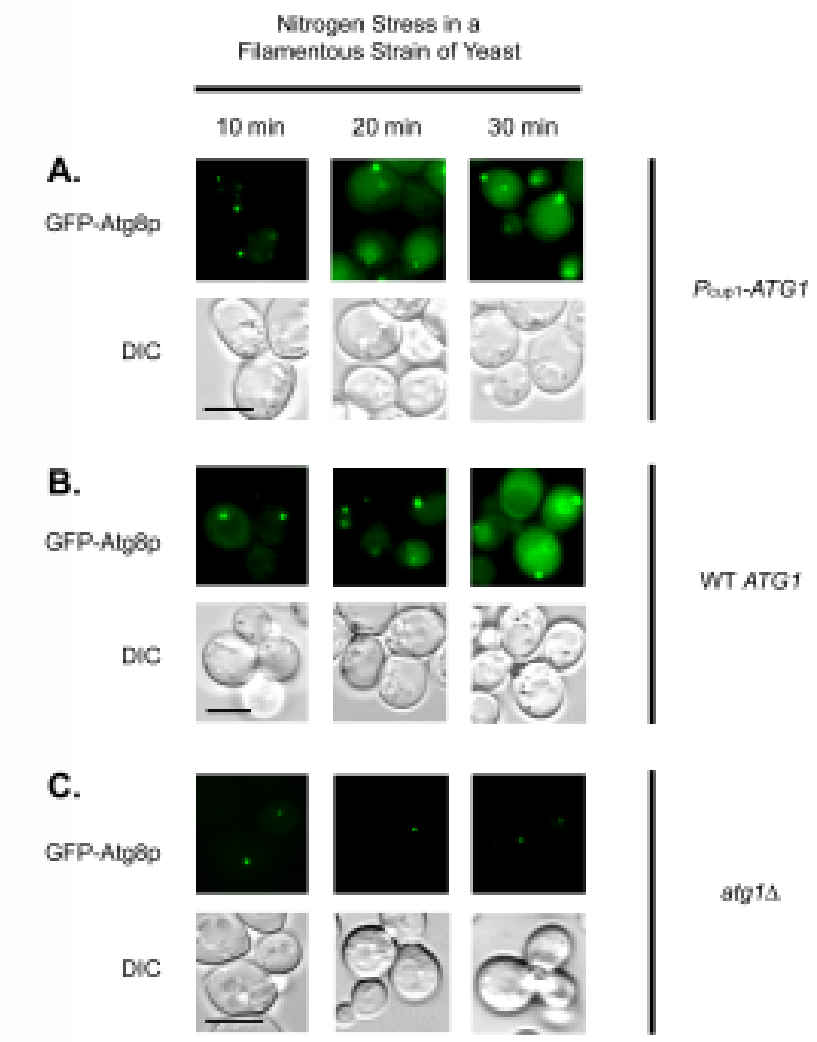
Nitrogen Stress in a
Filamentous Strain of Yeast
10 min
20 min
30 min
A.
GFP-Atg8p
DIC
P_{Cup1}-ATG1
B.
GFP-Atg8p
DIC
WT ATG1
C.
GFP-Atg8p
DIC
atg1Δ

Figure 3.3. Model describing the interrelationship between autophagy and filamentous growth in the budding yeast. Autophagy and filamentous growth are both induced in response to nitrogen stress. Autophagy contributes more to the available cellular nitrogen pool, as indicated by the larger arrow. The nitrogen pool is sensed by cell machinery that feeds back to inhibit the processes of autophagy and filamentous growth through as of yet undefined mechanisms. The overexpression studies presented here highlight an additional level of negative regulatory control of filamentous growth by autophagy.

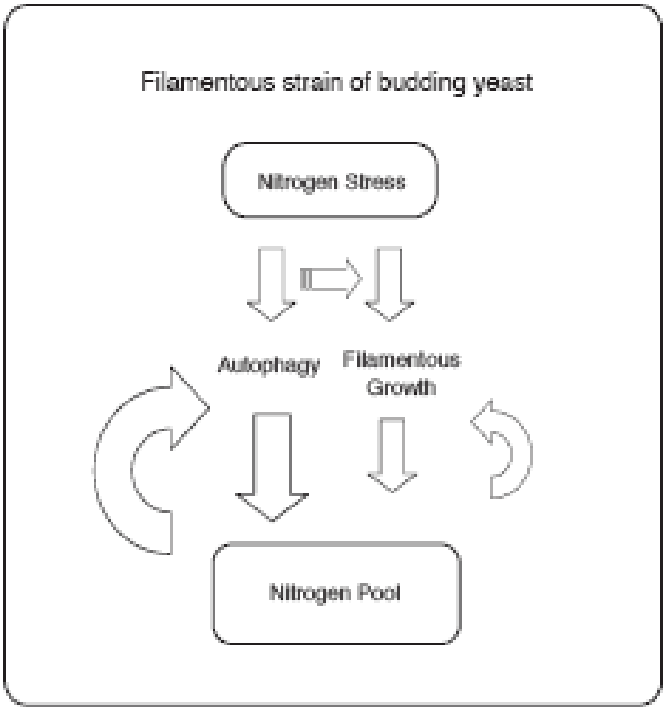
Filamentous strain of budding yeast
Nitrogen Stress
Autophagy
Filamentous Growth
Nitrogen Pool

Table 3.1 Spreadsheet of filamentous growth phenotypes of overexpressed autophagy-related genes. Gene name, the function of this gene, the autophagy process this gene involved in and the overexprrsion phenotype of this gene are listed.

Table 1 **Filamentous growth phenotypes of overexpressed autophagy-related genes**

Gene	Autophagy Process	Protein Function / Description	Overexpression Phenotype
ATG1	Induction; Retrieval	Protein kinase	Decreased filamentous growth
ATG3	Vesicle expansion and completion	Conjugation enzyme	Decreased filamentous growth
ATG4	Vesicle expansion and completion	Cysteine protease	Wild-type filamentous growth
ATG6/VPS30	Vesicle nucleation	Phosphatidylinositol-3-phosphate (PI3P) binding	Wild-type filamentous growth
ATG7	Vesicle expansion and completion	Activating enzyme	Decreased filamentous growth
ATG17	Cargo packaging	Receptor protein	Decreased filamentous growth
ATG19	Induction	PI3P binding	Decreased filamentous growth
ATG23	Cvt pathway	PI3P binding	Decreased filamentous growth
ATG24/SNX4	Possibly functions in autophagic body breakdown	Vacuolar membrane protein	Decreased filamentous growth
ATG29	Peroxisome sequestration; Selective pexophagy in *Pichia pastoris*	UDP-glucose:sterol glucosyltransferase-containing GRAM domain	Decreased filamentous growth

References

Cutler NS, Pan X, Heitman J, Cardenas ME. The TOR signal transduction cascade controls cellular differentiation in response to nutrients. Mol Biol Cell 2001; 12:4103-13.Gancedo JM. Control of pseudohyphae formation in *Saccharomyces cerevisiae*. FEMS Microbiol Rev 2001; 25:107-23.

Gimeno CJ, Fink GR. Induction of pseudohyphal growth by overexpression of *PHD1*, a *Saccharomyces cerevisiae* gene related to transcriptional regulators of fungal development. Mol Cell Biol 1994; 14:2100-12.

Gimeno CJ, Ljungdahl PO, Styles CA, Fink GR. Unipolar cell divisions in the yeast *S. cerevisiae* lead to filamentous growth: regulation by starvation and RAS. Cell 1992; 68:1077-90.

He C, Klionsky DJ. Atg9 trafficking in autophagy-related pathways. Autophagy 2007; 3:271-4.

Ichimura Y, Kirisako T, Takao T, Satomi Y, Shimonishi Y, Ishihara N, Mizushima N, Tanida I, Kominami E, Ohsumi M, Noda T, Ohsumi Y. A ubiquitin-like system mediates protein lipidation. Nature 2000; 408:488-92.

Ito H, Y. Fukuda, K. Murata, and A. Kimura. Transformation of intact yeast cells treated with alkali cations. J Bacteriol 1983; 153:163-8.

Kamada Y, Funakoshi T, Shintani T, Nagano K, Ohsumi M, Ohsumi Y. Tor-mediated induction of autophagy via an Apg1 protein kinase complex. J Cell Biol 2000; 150:1507-13.

Kametaka S, Okano T, Ohsumi M, Ohsumi Y. Apg14p and Apg6/Vps30p form a protein complex essential for autophagy in the yeast, *Saccharomyces cerevisiae*. J Biol Chem 1998; 273:22284-91.

Kim J, Huang WP, Klionsky DJ. Membrane recruitment of Aut7p in the autophagy and cytoplasm to vacuole targeting pathways requires Aut1p, Aut2p, and the autophagy conjugation complex. J Cell Biol 2001; 152:51-64.

Kirisako T, Baba M, Ishihara N, Miyazawa K, Ohsumi M, Yoshimori T, Noda T, Ohsumi Y. Formation process of autophagosome is traced with Apg8/Aut7p in yeast. J Cell Biol 1999; 147:435-46.

Klionsky DJ, Kumar A. A systems biology approach to learning autophagy. Autophagy 2006; 2:12-23.

Klionsky DJ. The molecular machinery of autophagy: Unanswered questions. J Cell Sci 2005; 118:7-18.

Kolch W. Coordinating ERK/MAPK signalling through scaffolds and inhibitors. Nat Rev Mol Cell Biol 2005; 6:827-37.

Kron SJ, Styles CA, Fink GR. Symmetric cell division in pseudohyphae of the yeast *Saccharomyces cerevisiae*. Mol Biol Cell 1994; 5:1003-22.

Kron SJ. Filamentous growth in budding yeast. Trends Microbiol 1997; 5:450-4.

Kumar A. Where do all the proteins go? Drug Discovery Today: Targets 2003; 2:237-44.

Kumar A, Agarwal S, Heyman JA, Matson S, Heidtman M, Piccirillo S, Umansky L, Drawid A, Jansen R, Liu Y, Cheung KH, Miller P, Gerstein M, Roeder GS, Snyder M. Subcellular localization of the yeast proteome. Genes Dev 2002; 16:707-19.

Lengeler KB, Davidson RC, D'Souza C, Harashima T, Shen WC, Wang P, Pan X, Waugh M, Heitman J. Signal transduction cascades regulating fungal development and virulence. Microbiol Mol Biol Rev 2000; 64:746-85.

Lang T, Schaeffeler E, Bernreuther D, Bredschneider M, Wolf DH, Thumm M. Aut2p and Aut7p, two novel microtubule-associated proteins are essential for delivery of autophagic vesicles to the vacuole. EMBO J 1998; 17:3597-607.

Levine B, Klionsky DJ. Development by self-digestion: molecular mechanisms and biological functions of autophagy. Devel Cell 2004; 6:463-77.

Liu H, Styles CA, Fink GR. Elements of the yeast pheromone response pathway required for filamentous growth of diploids. Science 1993; 262:1741-4.

Lo WS, Dranginis AM. The cell surface flocculin Flo11 is required for pseudohyphae formation and invasion by *Saccharomyces cerevisiae*. Mol Biol Cell 1998; 9:161-71.

Lo HJ, Kohler J, DiDomenico B, Loebenberg D, Cacciapuoti A, Fink GR. Nonfilamentous *C. albicans* mutants are avirulent. Cell 1997; 90:939-49.

Lo WS, Raitses EI, Dranginis AM. Development of pseudohyphae by embedded haploid and diploid yeast. Curr Genet 1997; 32:197-202.

Lorenz MC, Cutler NS, Heitman J. Characterization of alcohol-induced filamentous growth in *Saccharomyces cerevisiae*. Mol Biol Cell 2000; 11:183-99.Madhani HD, Fink GR. The control of filamentous differentiation and virulence in fungi. Trends in Cell Biol 1998; 8:348-53.

Loewith R, Jacinto E, Wullschleger S, Lorberg A, Crespo JL, Bonenfant D, Oppliger W, Jenoe P, Hall MN. Two TOR complexes, only one of which is rapamycin sensitive, have distinct roles in cell growth control. Mol Cell 2002; 10:457-68.

Madhani HD, Styles CA, Fink GR. MAP kinases with distinct inhibitory functions impart signaling specificity during yeast differentiation. Cell 1997; 91:673-84.

Mosch HU, Roberts RL, Fink GR. Ras2 signals via the Cdc42/Ste20/mitogen-activated protein kinase module to induce filamentous growth in *Saccharomyces cerevisiae*. Proc Natl Acad Sci U S A 1996; 93:5352-6.

Nair U, Klionsky DJ. Molecular mechanisms and regulation of specific and nonspecific autophagy pathways in yeast. J Biol Chem 2005; 280:41785-8.

Pan X, Harashima T, Heitman J. Signal transduction cascades regulating pseudohyphal differentiation of *Saccharomyces cerevisiae*. Curr Opin Microbiol 2000; 3:567-72.

Reggiori F, Klionsky DJ. Autophagy in the eukaryotic cell. Eukaryot Cell 2002; 1:11-21.

Reggiori F, Klionsky DJ. Autophagosomes: biogenesis from scratch? Curr Opin Cell Biol 2005; 17:415-22.

Roberts RL, Fink GR. Elements of a single MAP kinase cascade in Saccharomyces cerevisiae mediate two developmental programs in the same cell type: mating and invasive growth. Genes Dev 1994; 8:2974-85.

Robertson LS, Fink GR. The three yeast A kinases have specific signaling functions in pseudohyphal growth. Proc Natl Acad Sci U S A 1998; 95:13783-7.

Seaman MN, Marcusson EG, Cereghino JL, Emr SD. Endosome to Golgi retrieval of the vacuolar protein sorting receptor, Vps10p, requires the function of the *VPS29*, *VPS30*, and *VPS35* gene products. J Cell Biol 1997; 137:79-92.

Shintani T, Klionsky DJ. Autophagy in health and disease: a double-edged sword. Science 2004; 306:990-5.

Stephan J, Herman PK. The regulation of autophagy in eukaryotic cells: do all roads pass through Atg1? Autophagy 2006; 2:146-8.
Madhani HD, Galitski T, Lander ES, Fink GR. Effectors of a developmental mitogen-activated protein kinase cascade revealed by expression signatures of signaling mutants. Proc Natl Acad Sci U S A 1999; 96:12530-5.
Matsuura A, Tsukada M, Wada Y, Ohsumi Y. Apg1p, a novel protein kinase required for the autophagic process in *Saccharomyces cerevisiae*. Gene 1997; 192:245-50.26.
Scott RC, Juhasz G, Neufeld TP. Direct induction of autophagy by Atg1 inhibits cell growth and induces apoptotic cell death. Curr Biol 2007; 17:1-11.27.
Shintani T, Klionsky DJ. Cargo proteins facilitate the formation of transport vesicles in the cytoplasm to vacuole targeting pathway. J Biol Chem 2004; 279:29889-94.28.
Zheng XF, Schreiber SL. Target of rapamycin proteins and their kinase activities are required for meiosis. Proc Natl Acad Sci U S A 1997; 94:3070-5.29.

Chapter 4

Localization of Autophagy-Related Proteins in Yeast Using a Versatile Plasmid-Based Resource of Fluorescent Protein Fusions

Introduction

In characterizing a given protein, an understanding of its subcellular localization can be very informative. Protein localization is a good indicator of function, and controlled protein localization often serves as a regulatory mechanism ensuring specificity and timing of activity (Kumar et al. 2002; O'Neill et al. 1996; Edgington et al. 2001). Furthermore, the loss of regulated protein localization in a mutant background (i.e., gene deletion mutant) may suggest regulatory interactions between proteins (He et al. 2006; Bharucha et al. 2008). Gene products within a pathway often co-localize, and localization data provide a means to identify putative pathway components, particularly through systematic analyses of protein sets. As evidenced by these latter two examples, the utility of protein localization data can be enhanced by systematically localizing sets of proteins in a variety of genetic backgrounds.

Despite this utility, localization data sets are incomplete at best for most organisms, having been generated piecemeal from independent studies of single proteins. In the budding yeast *Saccharomyces cerevisiae*, several groups have constructed reagent collections for large-scale studies of protein localization, resulting in a more extensive

catalog of localization data(Kumar et al. 2002; Ross-Macdonald et al. 1999; Huh et al. 2003).These reagents, however, have been generated largely as integrated alleles and are not readily amenable to analysis in multiple genetic backgrounds. Accordingly, a plasmid-based resource of fluorescent protein-fusions would be a strong complement to existing reagents for protein localization.

As suggested above, the functions of proteins within a pathway can often be clarified by analysis of their subcellular localization; the autophagy pathway in yeast provides a strong example. Autophagy is a catabolic process observed in all eukaryotes wherein long-lived proteins, organelles, and other components of the cytoplasm are non-selectively sequestered within a double-membrane bound vesicle, the autophagosome, for trafficking to the vacuole or lysosome (Klionsky et al. 2005). The contents of the autophagosome are degraded in the vacuole to re-supply the cell with nutrients for essential metabolic processes during starvation (Klionsky et al. 1999; Levine et al. 2004). Thus, autophagy is induced under conditions of nutrient deprivation, contributing to cell survival (Reggiori et al. 2002; Klionsky et al. 2000). In addition to its role as a cellular stress response, autophagy has been implicated in many developmental processes and diseases, including aging, programmed cell death, cellular remodeling, cell growth, cancer, neurodegenerative disorders, and pathogenic infection (reviewed in Cuervo (Cuervo et al. 2004)). Autophagy has been studied extensively in the budding yeast, resulting in the identification of approximately 30 autophagy-related (*ATG*) genes (Reggiori et al. 2005). Under conditions of nutrient starvation in yeast, many *ATG* gene products accumulate at a perivacuolar site, termed the pre-autophagosomal structure (PAS) (Kim et al. 2002; Suzuki et al. 2001). The autophagosome originates from the

PAS, a distinct physical structure that can be visualized by fluorescence microscopy of PAS-targeted fluorescent protein fusions (Suzuki et al. 2007).

To facilitate a broader variety of systematic protein localization studies, we present here a plasmid-based resource of fluorescent protein fusions for analysis in yeast. Specifically, we generated a collection of 384 plasmids, each with a yeast gene and its native promoter cloned as a cassette suitable for transfer by recombination into any of seven custom-designed fluorescent protein-containing vectors. Using these vectors, we constructed a sub-collection of 276 kinases, transcription factors, and signaling proteins as carboxy-terminal YFP fusions. These constructs can be used to systematically analyze protein localization in multiple genetic backgrounds, providing a means to examine protein functions and relationships between components in a pathway. As proof-of-principle, we utilized this collection to identify *ATG* gene products at the PAS in yeast, and to identify localization patterns in the absence of an *ATG* gene (*ATG11*). We further illustrated the utility of this approach in identifying regulatory interactions between proteins by localizing the integral membrane protein Atg9p in relevant mutant backgrounds. Collectively, this study presents a template for the application of these constructs towards a diversity of regulatory and pathway-based analyses in the budding yeast.

Materials and Methods

Yeast strains and growth conditions. In this study, *ATG* gene products were localizedin strain BY4742, a derivative of S288c with the genotype *MATa ura3*Δ *leu2*Δ*his3*Δ*lys2*Δ (Winzeler et al. 1999). The *atg1*Δ strain was also constructed in BY4742 using a one-step PCR gene disruption strategy with the G418 resistance cassette from plasmid pFA6a-KanMX6 (Baudin et al. 1993; Longtine et al. 1998). Atg11 overexpression was achieved using the pRS416-derived plasmid pCUP1-ATG11; this vector, containing *ATG11* under transcriptional control of the copper-inducible *CUP1* promoter, was introduced into S288c strain SEY6210 (*MAT*Δ *ura3-52 leu2-3,112 his3-*Δ*200 trp1-*Δ*901 lys2-801 suc2-*Δ*9 mel GAL*) (He et al. 2006).

Unless otherwise indicated, yeast cells were grown in SMD medium (0.67% yeast nitrogen base, 2% glucose, with appropriate amino acids and vitamins). Starvation conditions were induced by growth in SD-N medium (0.17% yeast nitrogen base without amino acids and 2% glucose). Yeast transformations were carried out by the standard lithium acetate-mediated protocol described in Ito *et al.* (Ito et al. 1983)

Recombination-based cloning. Fluorescent protein fusions were generated by recombination-based cloning using the Gateway system (Invitrogen Corporation, CA). For this purpose, we constructed a series of fluorescent protein-containing Gateway-compatible vectors derived from the centromeric yeast shuttle vector YCp50 (Rose et al. 1987). Briefly, the coding sequence of each fluorescent protein indicated in Figure 4.1C was amplified by PCR with forward and reverse primers containing *Sph*I and *Sal*I sites,

respectively. The amplified fluorescent proteins were introduced into corresponding sites in YCp50. The Ycp50 vector was subsequently digested with *Sph*I and was made blunt with T4 DNA polymerase (New England Biolabs, MA). Gateway cassette A, consisting of terminal *att*R sites, the counter-selectable *ccd*B gene, and a chloramphenicol resistance marker, was ligated into the blunt-ended vector. *Eco*RI digestion was used to confirm proper orientation of the cassette. Target genes encoding kinases, transcription factors, and signaling proteins were identified from annotated genes in the *Saccharomyces* Genome Database (www.yeastgenome.org). Associated Gene Ontology terms were screened to identify these genes, and custom primers were designed for the amplification of each gene with its native promoter. Primers for this project have been designed so as to incorporate modified *att*B sites into the termini of each resulting PCR product. Specifically, each PCR primer consists of a 4-nt GGGG tail followed by the 25-nt *att*B sequence and approximately 26-30 nt of gene-specific sequence. Gene-specific sequence within each reverse primer is fixed by the 3' sequence of each gene. The gene-specific sequence within each forward primer consists of promoter sequence roughly 1 kb upstream of the translational start codon for each gene; using custom primer design scripts, we scan each promoter for suitable primer sequence within a region 800 bp to 1.4 kb 5' of the initiator methionine. Following PCR amplification of yeast genomic DNA, subsequent cloning steps were performed according to protocols described previously (Walhout et al. 2000; Alberti et al. 2007). The donor vector pDONR221 is commercially available (Invitrogen, CA).

Live cell microscopy and induction of autophagy. Yeast cells with plasmid-based fluorescent protein fusions were grown in SMD medium until early log phase. To label the vacuolar membrane, cells were washed and resuspended in fresh medium at OD 600 of 1.0, and the vital stain FM4-64 was added to a final concentration of 8 μM. The culture was incubated for an additional 30 minutes; cells were subsequently pelleted and resuspended in fresh medium. To induce autophagy, cells were cultured in SMD medium supplemented with 0.2 μg/ml rapamycin at 30°C for 2 hours. Alternatively, SD-N medium was added to induce starvation conditions. After incubation for 2 hours in SMD, SMD with rapamycin, or SD-N, samples were examined using a DeltaVision Spectris microscope (Applied Precision, Issaquah, WA) fitted with differential interference contrast optics and Olympus camera IX-HLSH100 with softWoRx software (Applied Precision).

Results

A set of vectors for the generation of fluorescent protein fusions by recombination based cloning: To construct a plasmid collection of fluorescent protein fusions, we implemented a recombination-based cloning strategy using the Gateway system. As illustrated in Figure 4.1A, Gateway cloning exploits the bacteriophage lambda recombination system, which shuttles sequence site-specifically between plasmids bearing compatible recombination sites. Each target yeast open reading frame (yORF) along with 1 kb of upstream promoter sequence was amplified by PCR with primers

containing appropriately modified lambda *att*B sites (sequences presented in Materials and Methods). This PCR product was recombined with a "donor" vector containing the counterselectable *ccd*B gene flanked by *att*P sites, resulting in an "entry clone" containing the target promoter-yORF flanked by *att*L sites. This *att*L-flanked sequence can recombine with a "destination" vector containing the *ccd*B gene bounded by *att*R sites. The final "expression clone" contains the target promoter-yORF flanked by *att*B sites in the destination vector backbone.

For this study, we generated yeast destination vectors carrying fluorescent proteins such that *att*L-*att*R recombination results in an in-frame fusion between the 3´-end of the targeted yORF and the 5´-end of the fluorescent protein-encoding sequence. A map of the principal destination vector used in this study, pDEST-vYFP, is presented in Figure 4.1B. The pDEST- vYFP construct is derived from the yeast centromeric plasmid YCp50; it contains an *att*R-flanked cassette consisting of a gene encoding chloramphenicol resistance and the *ccd*B gene. The *ccd*B gene acts as a counterselectable marker, since the encoded *ccd*B gene product interferes with *E. coli* DNA gyrase, thereby inhibiting growth of most *E. coli* strains. Recombination between the *att*L-flanked promoter-yORF in an entry clone and pDEST-vYFP results in loss of the counterselectable *ccd*B marker. Upon expression and translation, the promoter-yORF expression clone generates a chimeric protein fused at its carboxy terminus to vYFP. Thus, the entry clone represents a recombination-ready template for reaction with any appropriate destination vector, while the pDEST-vYFP expression clone encodes a fluorescent protein fusion for localization analysis. To maximize flexibility for localization studies, we constructed a series of destination vectors following the design

indicated in pDEST-vYFP with the fluorescent protein/selectable marker combinations listed in Figure 4.1C. We present these vectors as a community resource; they are freely available upon request from the authors.

Constructing the yORF-vYFP plasmid collection: Using the Gateway compatible vectors described above, we constructed a plasmid-based collection of promoter-yORF-fluorescent protein fusions for a large set of yeast genes encoding kinases, transcription-related proteins, and signaling proteins. We selected these gene classes because their encoded protein products likely exhibit regulated localization and, accordingly, are particularly interesting for localization studies in mutant genetic backgrounds. From information in the *Saccharomyces* Genome Database (www.yeastgenome.org) as of August 2006, we identified 125 kinase genes, 307 genes with transcription-related functions, and 80 genes encoding signaling proteins. Target genes with native promoters were cloned by recombination-based approaches into the donor vector pDONR221 and subsequently into the destination vector pDEST-vYFP, carrying the Venus variant of yellow fluorescent protein (Nagai et al. 2002). We selected Venus YFP for use as our principal fluorescent reporter because it matures rapidly, fluoresces brightly, and works well in yeast (Muller et al. 2005).

As indicated in Figure 4.2, we cloned 384 promoter-yORFs into the donor vector pDONR221, representing a success rate of approximately 75% from two passes through the target set. This collection encompasses 119 kinase genes, 203 genes with transcription-related functions, and 62 genes encoding signaling proteins or components of cell pathways. This donor plasmid collection is a useful source of promoter-yORF

cassettes for easy recombination into any appropriate Gateway- compatible destination vector. This recombination-based transfer is technically less demanding than the initial cloning step; so, the entry clone collection can be introduced into any desired destination vector even without extensive technical expertise in Gateway cloning. In this study, we transferred 276 promoter-yORFs into pDEST-vYFP, generating a sub-collection of low-copy plasmids with promoter-yORF-vYFP fusions for localization analysis.

Analysis of Atg protein localization: Localization studies can be effective in identifying pathway components and in identifying relationships between these components; the autophagy pathway in yeast provides a good test subject to illustrate this point. During autophagy, the PAS acts as the organizing center for autophagosome formation, and many Atg proteins localize at the PAS. Specifically, Suzuki *et al.* (Suzuki et al., 2007) localized 11 Atg-GFP chimeras to the PAS during autophagy. To validate and build upon these results, we generated carboxy-terminal vYFP fusions of 14 *ATG* gene products (Figure 4.2), six of which overlap with those studied in Suzuki *et al.*, and analyzed these products for localization to the PAS. In particular, these genes were selected for study because their encoded products are expected to function/localize properly upon carboxy-terminal modification. The functions of these genes and their roles in autophagy are summarized in Table 4.1.

For analysis of protein localization, each plasmid bearing an *ATG* gene-vYFP fusion was introduced into a haploid strain of yeast, and vYFP fluorescence was monitored under conditions of normal vegetative growth and during rapamycin-induced

autophagy. Rapamycin is an established inducer of autophagy, acting through inhibition of the Tor protein kinases (Cutler et al. 2001). The localization of each protein upon rapamycin treatment is presented in Figure 4.3. Each Atgp-vYFP chimera was expressed from a low-copy plasmid under control of its native promoter, and Atg16p-vYFP was not evident above background under conditions of nutrient sufficiency or in response to rapamycin treatment. The remaining proteins localized to the PAS upon rapamycin treatment, with the exception of Atg4p-vYFP and Atg22p-vYFP. Atg4p is a cysteine protease contributing to vesicle expansion and completion; it cleaves Atg8p to a form required for the generation of autophagosomes and also mediates attachment of autophagosomes to microtubules (Kirisako et al. 2000). Atg22p is a vacuolar permease, (Yang et al. 2006) and, as such, is localized to the vacuolar rim. Our results are in agreement with those of Suzuki *et al.* for Atg1p, Atg2p, Atg5p, Atg9p, Atg16p, and Atg18p — the only proteins common to both studies. Analysis of Atg9p is presented later in this text.

Genetic perturbations can often affect protein localization, thereby suggesting regulatory and/or functional relationships between proteins. To illustrate this point in regards to the autophagy pathway, we reexamined the localization of Atg18p and Atg20p in the absence of *ATG11* (Figure 4.4). Atg11p is a peripheral membrane protein that interacts with numerous Atg proteins, connecting cargo molecules with components of the vesicle-forming machinery during selective autophagy of precursor Ape1p (prApe1p) and Ams1p (the cytoplasm-to-vacuole targeting, or Cvt, pathway) (Klionsky et al. 1992; Hutchins et al. 2001). Accordingly, the localization of many Atg proteins is perturbed in

an *atg11*Δ mutant background. Atg18p is a WD-40 repeat-containing protein that binds phosphatidylinositol (3,5)-bisphosphate and phosphatidylinositol 3-phosphate; it is required for both the autophagy and Cvt pathways (Reggiori et al. 2004). Atg18p localizes at the PAS in a wild-type strain of yeast under conditions of rapamycin treatment; however, this localization is lost in the *atg11*Δ background. Atg20p is a sorting nexin family member that binds phoshatidylinositol 3-phosphate and interacts with Atg24p. Atg20p is required for both the autophagy and Cvt pathways. As indicated in Figure 4.4, Atg20p remains at the PAS in the *atg11*Δ background in response to rapamycin treatment. These results are consistent with our understanding of Atg11p-mediated interactions and specifically illustrate the advantages in examining protein function by defining localization patterns in relevant mutant backgrounds.

Localization of Atg9p in *ATG1* and *ATG11* mutants: Atg9p is an integral membrane protein that may function as a membrane carrier for vesicle formation during bulk and selective autophagy The subcellular distribution of Atg9p is not restricted to the PAS; instead, Atg9p localizes to the mitochondria, PAS, and additional unidentified structures (Reggiori et al. 2004), making it an interesting target for localization analysis. As indicated in Table 1 and Figure 4.2, we cloned *ATG9* along with its native promoter into pDEST-vYFP and subsequently introduced this construct into a standard lab strain of yeast for analysis of Atg9p localization. The Atg9p-vYFP chimera exhibits wild-type localization under conditions of nutrient sufficiency as well as under conditions of nitrogen deprivation (Figure 4.5A); thus, the chimera does not display any localization artifacts when expressed from its native promoter on a low-copy plasmid.

Furthermore, construction of this *ATG9-vYFP* expression clone provides a means to corroborate previously identified Atg9p regulatory interactions. He *et al.* (He et al. 2006) have reported that overexpression of *ATG11* localizes Atg9p to the PAS. With our plasmid-based *ATG9-vYFP* fusion, we also observe localization of Atg9p at the PAS upon copper-induced overexpression of *ATG11* (Figure 4.5C). Similarly, Atg1p plays a role in retrograde transport of Atg9p from the PAS to the mitochondria, (He et al., 2006; Reggiori et al. 2005) and, accordingly, deletion of *ATG1* restricts Atg9p-vYFP to the PAS under conditions of normal nitrogen (Figure 4.5C).

Discussion

In this chapter, we present a plasmid-base resource of promoter-yORF-fluorescent protein fusions for the systematic analysis of protein localization in the budding yeast. These reagents complement existing collections of integrated GFP-fusions, providing a convenient means to generate fusions of a given protein to multiple fluorescent reporters and a labor saving toolkit for the analysis of protein localization in multiple genetic backgrounds. In total, we report a collection of 384 genes with native promoters cloned as entry clones and/or expression clones (fluorescent protein fusions). To illustrate the utility of this collection, we analyzed a large subset of autophagy-related gene products as vYFP chimeras, localizing these proteins under normal vegetative growth conditions and during autophagy in wild-type and mutant backgrounds.

Collectively, the results from our studies indicate that plasmid-based fluorescent protein fusions can be used to effectively localize proteins, identify pathway components,

and investigate intra-pathway protein relationships with comparable accuracy to data generated from integrated alleles. The plasmids constructed here are derived from a low-copy centromeric yeast shuttle vector, typically present at 1-2 copies per cell (Rose et al. 1987), and yeast genes were cloned along with 1 kb upstream sequence, sufficient to encompass most yeast promoters. As a result, target genes were expressed at near endogenous levels, minimizing overexpression-based artifacts. Vectors in this study were designed to yield chimeras of a fluorescent protein to the carboxy terminus of the target protein, and while this approach is likely to generate fewer localization artifacts than amino-terminal tags, carboxy terminal modification will affect the localization of some gene products. In particular, carboxy-terminal tagging is problematic in analyzing isoprenylated gene products and geranylgeranylated proteins (Bhattacharya et al. 1995), as well as proteins with palmitoyl and farnesyl groups (Roth et al., 2006; Sun et al., 2004). To accommodate such proteins, we are currently designing a complementary set of recombination-compatible destination vectors for amino-terminal fluorescent protein tagging.

As presented here, recombination-based cloning by the Gateway system offers many advantages over traditional restriction enzyme/ligase cloning methods, particularly for large-scale applications. By recombination-based cloning, a single uniform strategy may be employed to clone thousands of genes, rather than rational cloning strategies being developed individually for each desired gene and vector. Furthermore, cloned genes may be quickly transferred to a variety of vectors without laborious "cut-and-paste" techniques. With the suite of fluorescent protein destination vectors presented here,

individual yeast proteins can be easily analyzed as fusions to multiple fluorescent proteins, facilitating co-localization studies of protein pairs. Accordingly, we constructed the pDEST-cCFP and pDEST-mCherry vectors with the *LEU2* selectable marker, for ease of use with yeast cells already containing a pDEST-FP vector with *URA3*. The principal limitation of the Gateway technology lies in the fact that PCR products greater than 5 kb in length can be difficult to clone. In this study, we achieved a success rate of 75%, with large genes constituting the majority of targets refractory to Gateway cloning. In addition, Gateway reagents are expensive, particularly over the course of a large project. Large-scale protein localization studies have been implemented successfully in the budding yeast; however, these studies only represent an initial level of analysis. Protein localization is dynamic, and many proteins shuttle between cellular compartments in response to environmental or cellular signals. To identify such differentially localized proteins, it is often necessary to analyze non-standard genetic backgrounds, since S288c-derived strains are inappropriate for the analysis of some cellular responses (e.g., pseudohyphal growth). Plasmid-based reagents are easy to introduce into a variety of strains, facilitating those studies.

Furthermore, as evidenced here, the analysis of protein localization in mutant backgrounds is useful in identifying regulatory mechanisms and relationships between proteins. The suite of destination vectors presented here can be used to construct gene fusions to a variety of fluorescent reporters, potentially suitable for large-scale co-localization studies or assays of fluorescence resonance energy transfer (FRET). Thus, our plasmid collections of fluorescent protein fusions constitute singular resources for the

implementation of numerous large-scale localization studies -experimental designs that will likely take hold for the study of proteins in other tractable model organisms as well.

Acknowledgements

The authors would like to thank Daniel Klionsky for providing the *ATG11* overexpression plasmid. This work was supported by grants RSG-06-179-01-MBC from the American Cancer Society, DBI 0543017 from the National Science Foundation, and Basil O'Connor Award 5- FY05-1224 from the March of Dimes (to A.K.).

Figure 4.1. A suite of destination vectors for recombination-based cloning of yeast genes as fluorescent protein fusions. (A) Overview of Gateway cloning. By the approach employed here, each amplified PCR product was cloned into the donor vector pDONR221, generating an "entry" clone. A subset of the promoter-gene cassettes were subsequently introduced into a destination vector, generating an "expression" clone by the LR reaction indicated. The LR reaction is technically simpler than the initial cloning process; accordingly, the entry clone collection represents a useful resource for recombination-based subcloning, even without extensive experience in Gateway-based techniques. (B) Plasmid map of the destination vector pDEST-vYFP, derived from the centromeric yeast shuttle vector YCp50. Arrows indicate gene-coding sequences. (C) Listing of destination vectors constructed in this study. Each destination vector varies in its fluorescent reporter and selectable marker as indicated.

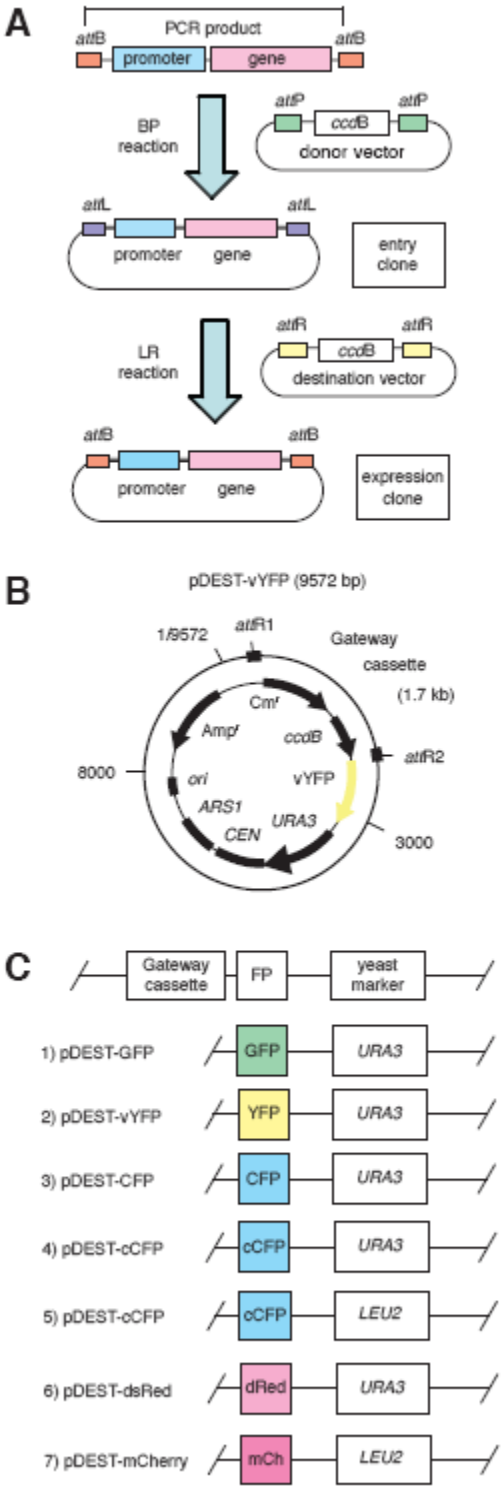
A
PCR product
attB
promoter
gene
attB
BP reaction
attP
ccdB
attP
donor vector
attL
promoter
gene
attL
entry clone
LR reaction
attR
ccdB
attR
destination vector
attB
promoter
gene
attB
expression clone
B
pDEST-vYFP (9572 bp)
1/9572
attR1
Gateway cassette
(1.7 kb)
Cmr
Ampr
ccdB
attR2
8000
ori
vYFP
ARS1
URA3
CEN
3000
C
Gateway cassette
FP
yeast marker
1) pDEST-GFP
GFP
URA3
2) pDEST-vYFP
YFP
URA3
3) pDEST-CFP
CFP
URA3
4) pDEST-cCFP
cCFP
URA3
5) pDEST-cCFP
cCFP
LEU2
6) pDEST-dsRed
dRed
URA3
7) pDEST-mCherry
mCh
LEU2

Figure 4.2. A plasmid-based collection of cloned promoter-gene cassettes. In total, 384 yeast genes with native promoters were cloned into the donor vector pDONR221; the cloned genes encompassed 119 kinase genes, 203 genes with transcription-related functions, and 62 genes encoding signaling proteins and/or components of cell pathways. A partial listing of these genes is presented here; genes listed in red have been subcloned into pDEST-vYFP. A full listing of genes is presented in Supplementary Table ST1 (with genes cloned as vYFP-fusions indicated in red).

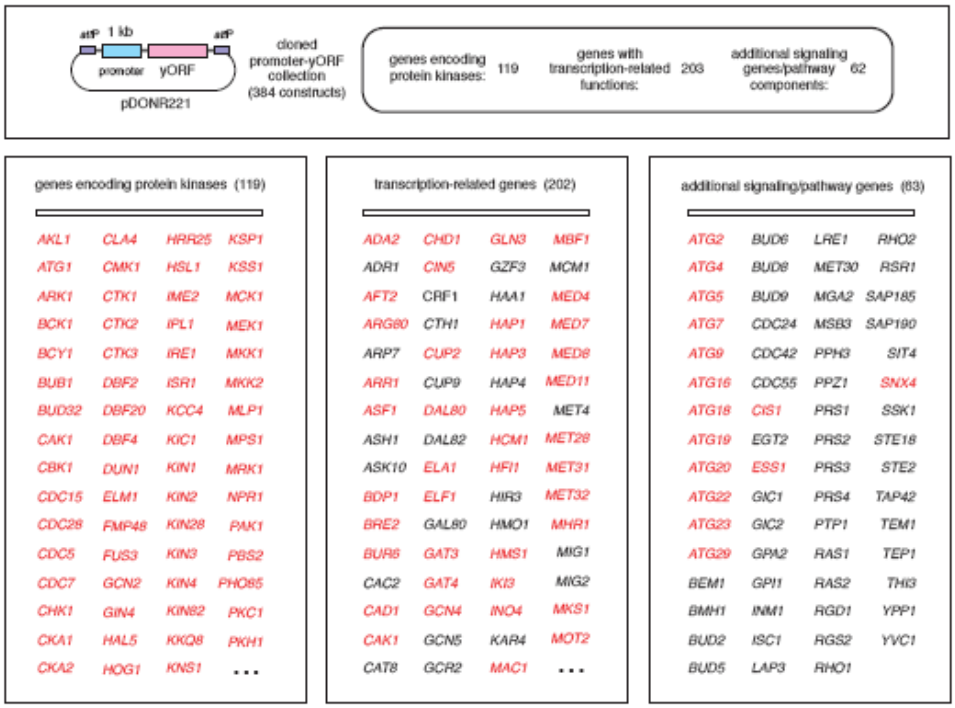
attP
1 kb
attP
promoter
yORF
pDONR221
cloned promoter-yORF collection (384 constructs)
genes encoding protein kinases: 119
genes with transcription-related functions: 203
additional signaling genes/pathway components: 62
genes encoding protein kinases (119)
AKL1 CLA4 HRR25 KSP1
ATG1 CMK1 HSL1 KSS1
ARK1 CTK1 IME2 MCK1
BCK1 CTK2 IPL1 MEK1
BCY1 CTK3 IRE1 MKK1
BUB1 DBF2 ISR1 MKK2
BUD32 DBF20 KCC4 MLP1
CAK1 DBF4 KIC1 MPS1
CBK1 DUN1 KIN1 MRK1
CDC15 ELM1 KIN2 NPR1
CDC28 FMP48 KIN28 PAK1
CDC5 FUS3 KIN3 PBS2
CDC7 GCN2 KIN4 PHO85
CHK1 GIN4 KIN82 PKC1
CKA1 HAL5 KKQ8 PKH1
CKA2 HOG1 KNS1 ...
transcription-related genes (202)
ADA2 CHD1 GLN3 MBF1
ADR1 CIN5 GZF3 MCM1
AFT2 CRF1 HAA1 MED4
ARG80 CTH1 HAP1 MED7
ARP7 CUP2 HAP3 MED8
ARR1 CUP9 HAP4 MED11
ASF1 DAL80 HAP5 MET4
ASH1 DAL82 HCM1 MET28
ASK10 ELA1 HFI1 MET31
BDP1 ELF1 HIR3 MET32
BRE2 GAL80 HMO1 MHR1
BUR6 GAT3 HMS1 MIG1
CAC2 GAT4 IKI3 MIG2
CAD1 GCN4 INO4 MKS1
CAK1 GCN5 KAR4 MOT2
CAT8 GCR2 MAC1 ...
additional signaling/pathway genes (63)
ATG2 BUD6 LRE1 RHO2
ATG4 BUD8 MET30 RSR1
ATG5 BUD9 MGA2 SAP185
ATG7 CDC24 MSB3 SAP190
ATG9 CDC42 PPH3 SIT4
ATG16 CDC55 PPZ1 SNX4
ATG18 CIS1 PRS1 SSK1
ATG19 EGT2 PRS2 STE18
ATG20 ESS1 PRS3 STE2
ATG22 GIC1 PRS4 TAP42
ATG23 GIC2 PTP1 TEM1
ATG29 GPA2 RAS1 TEP1
BEM1 GPI1 RAS2 THI3
BMH1 INM1 RGD1 YPP1
BUD2 ISC1 RGS2 YVC1
BUD5 LAP3 RHO1

Figure 4.3. Subcellular localization of Atg-vYFP chimeras in response to rapamycin treatment. Yeast cells were treated with rapamycin two hours prior to microscopy. The vital dye FM 4-64 was used as an indicator of the vacuolar membrane. Yeast cell morphology was visualized by differential interference contrast microscopy (DIC). Localization at the pre-autophagosomal structure (PAS +) and absence of this localization (PAS -) is indicated accordingly. Scale bar, 3 μm.

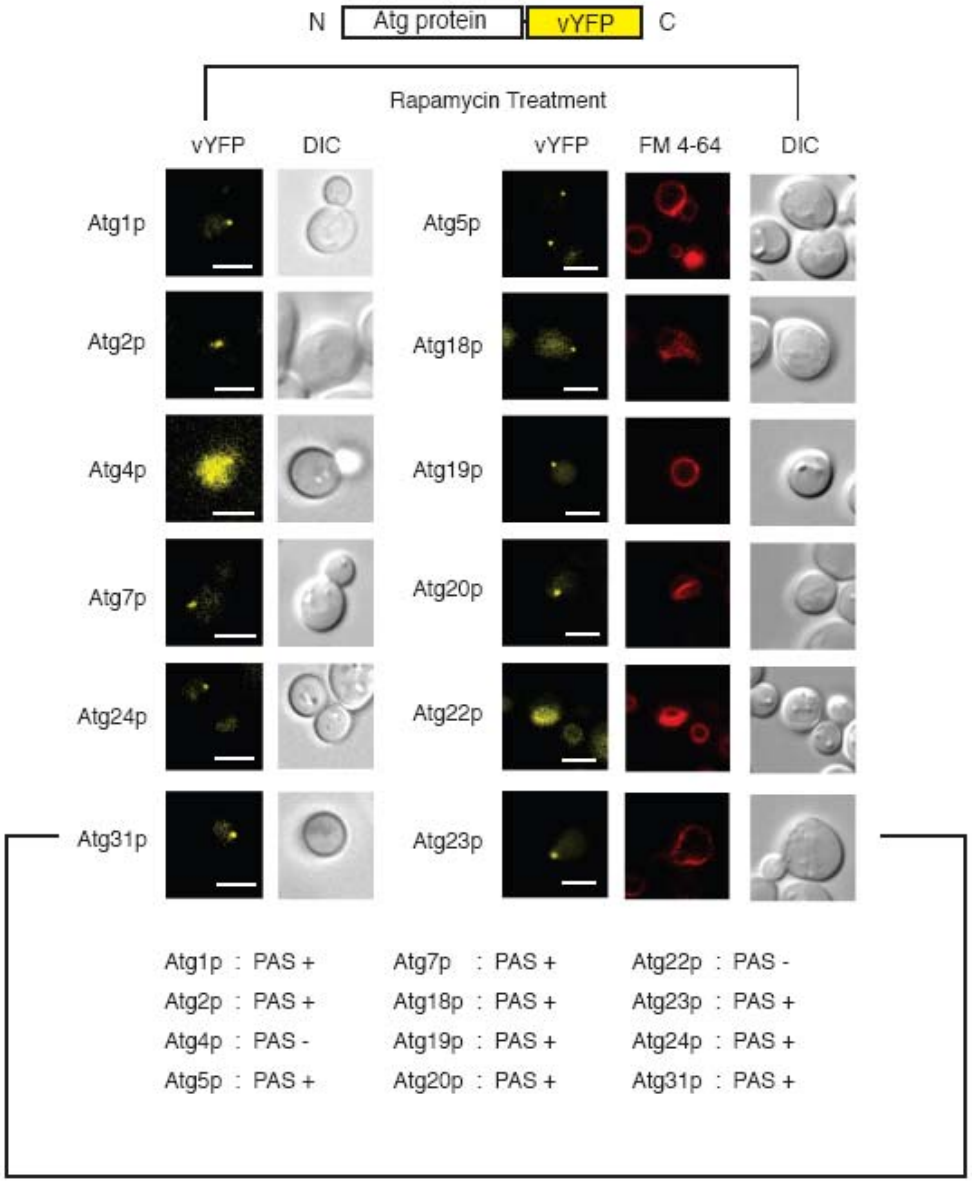
N
Atg protein
vYFP
C
Rapamycin Treatment
vYFP
DIC
vYFP
FM 4-64
DIC
Atg1p
Atg2p
Atg4p
Atg7p
Atg24p
Atg31p
Atg5p
Atg18p
Atg19p
Atg20p
Atg22p
Atg23p
Atg1p : PAS +
Atg2p : PAS +
Atg4p : PAS -
Atg5p : PAS +
Atg7p : PAS +
Atg18p : PAS +
Atg19p : PAS +
Atg20p : PAS +
Atg22p : PAS -
Atg23p : PAS +
Atg24p : PAS +
Atg31p : PAS +

Figure 4.4. Subcellular localization of Atg18p- and Atg20p-vYFP chimeras in a strain deleted for *ATG11*. The *atg11_* strain contains the kanMX6 cassette integrated at the *ATG11* locus. Autophagy was induced by rapamycin treatment for two hours. The vacuole was visualized by staining with FM 4-64; cell morphology was visualized by differential interference contrast microscopy (DIC). Localization at the pre-autophagosomal structure (PAS +) and absence of this localization (PAS -) is indicated. Scale bar, 3 μm.

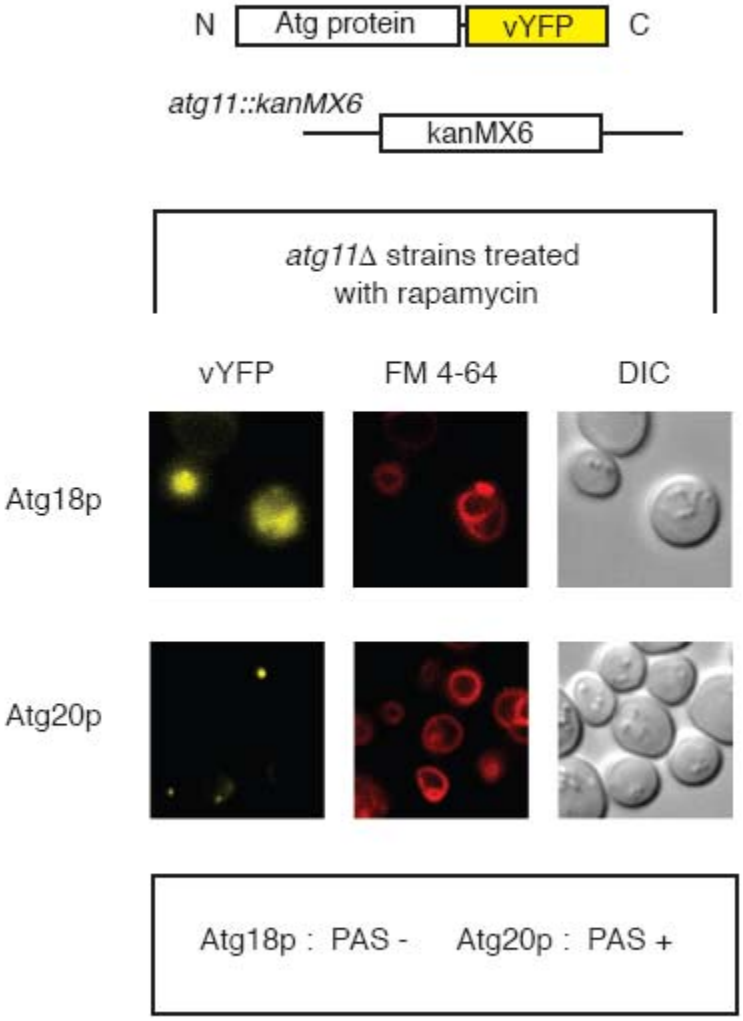
N
Atg protein
vYFP
C
atg11::kanMX6
kanMX6
atg11Δ strains treated with rapamycin
vYFP
FM 4-64
DIC
Atg18p
Atg20p
Atg18p : PAS -
Atg20p : PAS +

Figure 4.5. Overexpression of *ATG11* and deletion of *ATG1* drives Atg9p-vYFP to the PAS. (A) Subcellular localization of Atg9p-vYFP under conditions of normal vegetative growth and under conditions of nitrogen deprivation. The vacuole was visualized by staining with FM 4-64; cell morphology was visualized by differential interference contrast microscopy (DIC). The PAS is indicated in the cartoon at the right. (B) Localization of Atg9p-vYFP at the PAS in a strain overexpressing *ATG11* under normal growth conditions. (C) Localization of Atg9p-vYFP at the PAS in a strain deleted for *ATG1* under normal growth conditions. Scale bar, 3 μm.

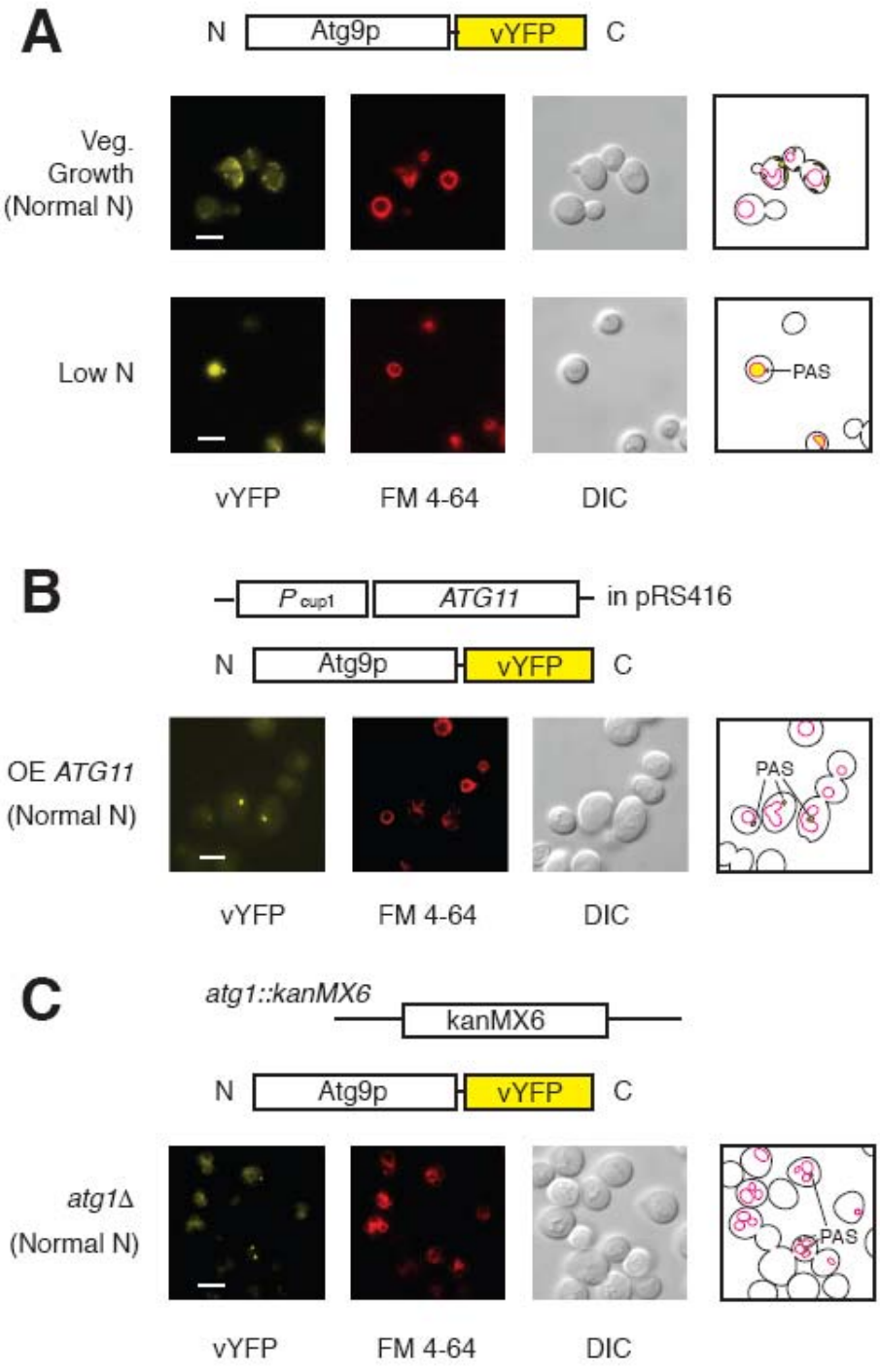
A
N
Atg9p
vYFP
C
Veg.
Growth
(Normal N)
Low N
PAS
vYFP
FM 4-64
DIC
B
Pcup1
ATG11
in pRS416
N
Atg9p
vYFP
C
OE ATG11
(Normal N)
PAS
vYFP
FM 4-64
DIC
C
atg1::kanMX6
kanMX6
N
Atg9p
vYFP
C
atg1Δ
(Normal N)
PAS
vYFP
FM 4-64
DIC

Table 4.1 Spreadsheet of Autophagy-related gene products analyzed as vYFP chimeras. The name of the gene, the autophagy process this gene involved in and the function of this gene are listed.

Table 1 **Autophagy-related (*ATG*) gene products analyzed as vYFP chimeras**

Gene	Process	Function/description
ATG1	Induction/retrieval	Serine/threonine protein kinase
ATG2	Retrieval	Peripheral membrane protein
ATG4	Vesicle expansion and completion	Cysteine protease
ATG5	Vesicle expansion and completion	Protein undergoes conjugation with Atg12p
ATG7	Vesicle expansion and completion	E1 ubiquitin-activating-like enzyme
ATG9	Vesicle expansion and completion	Integral membrane protein
ATG16	Vesicle expansion and completion	Protein multimerizes and links with Atg12p-Atg5p conjugate
ATG18	Retrieval	PI3P binding
ATG19	Cargo packaging (Cvt pathway)	Receptor protein
ATG20	Induction (Cvt pathway)	PI3P binding
ATG22	Macromolecular efflux from the vacuole/lysosome	Vacuole permease
ATG23	Vesicle expansion and completion	Interacts with Atg9
ATG24/SNX4	Induction	PI3P binding
ATG31/CIS1	Induction	Interacts with Atg17p for proper autophagosome formation

References

Alberti S, Gitler AD, Lindquist S. A suite of Gateway cloning vectors for high-throughput genetic analysis in Saccharomyces cerevisiae. Yeast 2007; 24:913-9.

Baudin A, Ozier-Kalogeropoulos O, Denouel A, Lacroute F, Cullin C. A simple and efficient method for direct gene deletion in *Saccharomyces cerevisiae*. Nucleic Acids Res 1993; 21:3329-30.

Bharucha N, Ma J, Dobry CJ, Lawson SK, Yang Z, Kumar A. Analysis of the Yeast Kinome Reveals a Network of Regulated Protein Localization During Filamentous Growth. Mol Biol Cell 2008.

Bhattacharya S, Chen L, Broach JR, Powers S. Ras membrane targeting is essential for glucose signaling but not for viability in yeast. Proc Natl Acad Sci U S A 1995; 92:2984-8.

Cuervo AM. Autophagy: in sickness and in health. Trends Cell Biol 2004; 14:70-7.

Cutler NS, Pan X, Heitman J, Cardenas ME. The TOR Signal Transduction Cascade Controls Cellular Differentiation in Response to Nutrients. Mol Biol Cell 2001; 12:4103-13.

Edgington NP, Futcher B. Relationship between the function and the location of G1 cyclins in S. cerevisiae. J Cell Sci 2001; 114:4599-611.

He C, Song H, Yorimitsu T, Monastyrska I, Yen WL, Legakis JE, Klionsky DJ. Recruitment of Atg9 to the preautophagosomal structure by Atg11 is essential for selective autophagy in budding yeast. J Cell Biol 2006; 175:925-35.

Huh WK, Falvo JV, Gerke LC, Carroll AS, Howson RW, Weissman JS, O'Shea EK. Global analysis of protein localization in budding yeast. Nature 2003; 425:686-91.

Hutchins MU, Klionsky DJ. Vacuolar localization of oligomeric alpha-mannosidase requires the cytoplasm to vacuole targeting and autophagy pathway components in Saccharomyces cerevisiae. J Biol Chem 2001; 276:20491-8.

Ito H, Y. Fukuda, K. Murata, and A. Kimura. Transformation of intact yeast cells treated with alkali cations. J Bacteriol 1983; 153:163-8.

Kim J, Huang WP, Stromhaug PE, Klionsky DJ. Convergence of multiple autophagy and cytoplasm to vacuole targeting components to a perivacuolar membrane compartment prior to de novo vesicle formation. J Biol Chem 2002; 277:763-73.

Kirisako T, Ichimura Y, Okada H, Kabeya Y, Mizushima N, Yoshimori T, Ohsumi M, Takao T, Noda T, Ohsumi Y. The reversible modification regulates the membrane-binding state of Apg8/Aut7 essential for autophagy and the cytoplasm to vacuole targeting pathway. J Cell Biol 2000; 151:263-76.

Klionsky DJ. The molecular machinery of autophagy: Unanswered questions. J Cell Sci 2005; 118:7-18.

Klionsky DJ, Cueva R, Yaver DS. Aminopeptidase I of Saccharomyces cerevisiae is localized to the vacuole independent of the secretory pathway. J Cell Biol 1992; 119:287-99.

Klionsky DJ, Emr SD. Autophagy as a regulated pathway of cellular degradation. Science 2000; Science:1717-21.

Klionsky DJ, Ohsumi Y. Vacuolar import of proteins and organelles from the cytoplasm. Annu Rev Cell Dev Biol 1999; 15:1-32.

Kumar A, Agarwal S, Heyman JA, Matson S, Heidtman M, Piccirillo S, Umansky L, Drawid A, Jansen R, Liu Y, Cheung KH, Miller P, Gerstein M, Roeder GS, Snyder M. Subcellular localization of the yeast proteome. Genes Dev 2002; 16:707-19.

Levine B, Klionsky DJ. Development by Self-Digestion: Molecular Mechanisms and Biological Functions of Autophagy. Devel Cell 2004; 6:463-77.

Longtine MS, McKenzie III A, Demarini DJ, Shah NG, Wach A, Brachat A, Philippsen P, Pringle JR. Additional Modules for Versatile and Economical PCR-based Gene Deletion and Modification in Saccharomyces cerevisiae. Yeast 1998; 14:953-61.

Muller EG, Snydsman BE, Novik I, Hailey DW, Gestaut DR, Niemann CA, O'Toole ET, Giddings TH, Jr., Sundin BA, Davis TN. The organization of the core proteins of the yeast spindle pole body. Mol Biol Cell 2005; 16:3341-52.

Nagai T, Ibata K, Park ES, Kubota M, Mikoshiba K, Miyawaki A. A variant of yellow fluorescent protein with fast and efficient maturation for cell-biological applications. Nat Biotechnol 2002; 20:87-90.

O'Neill EM, Kaffman A, Jolly ER, O'Shea EK**.** Regulation of PHO4 nuclear localization by the PHO80-PHO85 cyclin-CDK complex. Science 1996; 271:209-12.

Reggiori F, Klionsky DJ. Autophagy in the eukaryotic cell. Eukaryot Cell 2002; 1:11-21.

Reggiori F, Klionsky DJ. Autophagosomes: biogenesis from scratch? Curr Opin Cell Biol 2005; 17:415-22.

Reggiori F, Shintani T, Nair U, Klionsky DJ. Atg9 cycles between mitochondria and the pre- autophagosomal structure in yeasts. Autophagy 2005; 1:101-9.

Reggiori F, Tucker KA, Stromhaug PE, Klionsky DJ. The Atg1-Atg13 complex regulates Atg9 and Atg23 retrieval transport from the pre-autophagosomal structure. Devel Cell 2004; 6:79-90.

Roth AF, Wan J, Green WN, Yates JR, Davis NG. Proteomic identification of palmitoylated proteins. Methods 2006; 40:135-42.

Rose MD, Novick P, Thomas JH, Botstein D, Fink G. A Saccharomyces cerevisiae genomic plasmid bank based on a centromere-containing shuttle vector. Gene 1987; 60:237-43.

Ross-Macdonald P, Coelho PS, Roemer T, Agarwal S, Kumar A, Jansen R, Cheung KH, Sheehan A, Symoniatis D, Umansky L, Heidtman M, Nelson FK, Iwasaki H, Hager K, Gerstein M, Miller P, Roeder GS, Snyder M. Large-scale analysis of the yeast genome by transposon tagging and gene disruption. Nature 1999; 402:413-8.

Sun B, Chen L, Cao W, Roth AF, Davis NG. The yeast casein kinase Yck3p is palmitoylated, then sorted to the vacuolar membrane with AP-3-dependent recognition of a YXXPhi adaptin sorting signal. Mol Biol Cell 2004; 15:1397-406.

Suzuki K, Kirisako T, Kamada Y, Mizushima N, Noda T, Ohsumi Y. The pre-autophagosomal structure organized by concerted functions of APG genes is essential for autophagosome formation. EMBO J 2001; 20:5971-81.

Suzuki K, Kubota Y, Sekito T, Ohsumi Y. Hierarchy of Atg proteins in pre-autophagosomal structure organization. Genes Cells 2007; 12:209-18.

Walhout AJM, Temple GF, Brasch MA, Hartley JL, Lorson MA, Heuvel Svd, Vidal M. GATEWAY Recombinational Cloning: Application to the Cloning of Large Numbers of Open Reading Frames or ORFeomes. Methods Enzymol 2000; 328:575-92. Winzeler EA, Shoemaker DD, Astromoff A, Liang H, Anderson K, Andre B, Bangham R, Benito R, Boeke JD, Bussey H, Chu AM, Connelly C, Davis K, Dietrich F, Dow SW, Bakkoury ME, Foury F, Friend SH, Gentalen E, Giaever G, Hegemann JH, Laub TJM, Liao H, Liebundguth N, Lockhart DJ, Lucau-Danila A, Lussier M, M'Rabet N, Menard P, Mittmann M, Pai C, Rebischung C, Revuelta JL, Riles L, Roberts CJ, Ross-MacDonald P, Scherens B, Snyder M, Sookhai-Mahadeo S, Storms RK, Véronneau S, Voet M, Volckaert G, Ward TR, Wysocki R, Yen GS, Yu K, Zimmermann K, Philippsen P, Johnston M, Davis RW. Fuctional characterization of the *S. cerevisiae* genome by gene deletion and parallel analysis. Science 1999; 285:901-6.

Yang Z, Huang J, Geng J, Nair U, Klionsky DJ. Atg22 recycles amino acids to link the degradative and recycling functions of autophagy. Mol Biol Cell 2006; 17:5094-104.

Chapter 5

An Unconventional Genomic Architecture in the Budding Yeast Masks the Nested Antisense Gene NAG1

Introduction

Eukaryotic gene organization is routinely presumed to follow a collinear design, wherein protein-coding genes are ordered at discrete, non-overlapping points along a given chromosome (Kapranov et al. 2007). This organizational model is manifestly evident in the genome of the budding yeast *Saccharomyces cerevisiae*. The *S. cerevisiae* genome was sequenced in 1996, and its 13-Mb sequence was subsequently annotated for genes using a combination of existing genetic information and straightforward computational approaches (Mewes et al. 1997). As part of this process, putative protein-coding open reading frames (ORFs) were predicted by gene-finding algorithms, employing a set of criteria based upon ORF size and spatial organization. Specifically, any ORF greater than 100 codons in length was annotated as a gene, provided it did not significantly overlap a longer ORF. If two ORFs overlapped, the longer of the two sequences was annotated as a gene, and the other was discarded (Mewes et al. 1997; Philippsen et al. 1997). Perhaps in part because of this gene prediction strategy, to date, no verified, completely overlapping protein-coding genes have been identified in the yeast genome.

Recently, several lines of evidence have raised doubts concerning the presumed

collinear organization of protein-coding genes in eukaryotic genomes. In the budding yeast, David *et al.* (David et al. 2006) have employed a high-density oligonucleotide tiling array to profile RNA expression on both DNA strands over the entire genome; this study highlights a considerable degree of antisense transcription in the yeast genome - that is, transcripts overlapping known genes in an antisense orientation. In addition, Havilio *et al.* (Havilio et al. 2005) mined microarray expression data in yeast to identify a significant body of transcripts oriented antisense to known genes. This level of antisense transcription, however, may reflect some degree of "leaky" transcription or a potential regulatory mechanism in *S. cerevisiae* (Hongay et al. 2006), and does not conclusively indicate that protein-coding sequences can exist antisense to other protein-coding genes. In fact, the only confirmed report of entirely overlapping genes in yeast was presented by Coelho *et al.* (Coelho et al. 2002), describing the mitochondrial protein Tar1p, which is encoded antisense to the 25S rRNA gene in the nuclear rDNA repeat region of chromosome XII. Tar1p, however, is not oriented opposite a protein-coding gene, but rather a structural RNA.

In this chapter, we present the first report of a yeast protein-coding gene nested opposite another protein-coding gene. The yeast open reading frame *YGR031C-A* is nested antisense and opposite the known gene *YGR031W*, the latter encoding a mitochondrial protein of unknown function. Genome-wide transposon-tagging studies had previously suggested that the *YGR031C-A* ORF may encode a protein, and, in this study, we established that this ORF (herein renamed *NAG1*) does encode a 19-kDa protein that localizes to the yeast cell periphery, contains putative transmembrane domains, and co-fractionates with known plasma membrane proteins. Sequence analysis

revealed that *NAG1* is conserved among fungi as a unit oriented opposite an ortholog of *YGR031W*. Consistent with its conservation in fungi, *NAG1* contributes to cell wall synthesis and maintenance in *S. cerevisiae*. Disruption of *NAG1* results in cell sensitivity to Calcofluor white and altered transcriptional levels for many cell wall biosynthesis / maintenance genes.

Furthermore, Nag1p levels increase upon Calcofluor white treatment, and *NAG1* expression is dependent upon the Slt2p mitogen-activated protein kinase (MAPK) pathway and its key downstream transcription factor Rlm1p. In total, these results identify a new protein contributing to cell wall function in yeast, while highlighting both the existence of nested protein-coding genes and the likelihood that other such genes exist in the eukaryotic kingdom.

Materials And Methods

Yeast strains and growth conditions. Yeast strains containing the *nag1*::*mTn* allele were generated in the genetic background BY4742 (Winzeler et al. 1999). The W303 genetic background was obtained from the Yeast Genetics Stock Center (Berkeley, CA). The *slt2*Δ and *rlm1*Δ mutants were from the yeast deletion collection (Winzeler et al. 1999) generated in the BY4742 background referenced above. Growth media and basic genetic manipulation were as described previously (Guthrie et al. 1991). The *slt2*Δ mutant was grown at 25°C to accommodate its cell wall defect. The *nag1*::*mTn* allele was carried on plasmid pHSS6 (Seifert et al. 1986); this plasmid was digested with *Not*I, and the transposon-mutagenized genomic DNA fragment was introduced into BY4742 by

standard methods of DNA transformation (Ito et al. 1983). The BY4742 strain containing *NAG1-3xHA* was constructed using the PCR-based epitope-tagging method of Longtine *et al.* (Longtine et al. 1998) using an integration cassette amplified from pFA6a-3HA-kanMX6 with PCR primers containing 40 bp flanking sequence homology.

Sequence alignments. Sequence similarity searches were performed using tBLASTn with Nag1p amino acid sequence against a six-frame translation of the NCBI non-redundant nucleotide database (Ye et al. 2006). All searches were repeated with the BLOSUM62 and BLOSUM45 scoring matrices, coupled with default parameters, and optimal sequence alignments were generated using CLUSTALW (Thompson et al., 1994).

Western blotting. The hemagglutinin (HA) tag was integrated at the 3′-end of *NAG1* using the KanMX6 selection cassette from plasmid pFA6a-3HA-KanMX6 (Longtime et al. 1998). Transformants were selected on YPD plates containing 200 μg/ml G418. Correct integration was verified by PCR.

For Western blotting, yeast strains were grown at 30°C to mid-log phase in YPD medium unless otherwise noted. The cells were then converted into spheroplasts and subjected to subcellular fractionation based on previously described protocols (Kim et al. 1999). Unlysed spheroplasts were removed by centrifugation at 1500 *g* for 5 min at 4°C. The total lysate was centrifuged at 13,000 *g* for 5 min at 4°C to separate supernatant and pellet factions (S13 and P13, respectively). Aliquots of each fraction were precipitated with 10% trichloroacetic acid on ice for 30 minutes, washed with 100% acetone, and air-

dried. The dried pellets were resuspended in SDS sample buffer. Aliquots were resolved by SDS-PAGE and probed with anti-3xHA antibody (Santa Cruz Biotechnology).

Fluorescence microscopy. The *NAG1* and *YGR031W* coding sequences along with 1-kb upstream sequence were cloned into a derivative of the centromeric plasmid YCp50 such that each formed an in-frame 3′-fusion to sequence encoding the Venus variant of yellow fluorescent protein (vYFP) (Nagai et al. 2002). Plasmids carrying *NAG1-vYFP* and *YGR031W-vYFP*, respectively, were transformed into BY4742. Yeast cultures were grown in SD-Ura medium until mid-log phase before examination. To label mitochondria, Mito Fluor Red 594 (Molecular Probes) was added to a final concentration of 5 μM, and the culture was incubated for an additional 30 minutes prior to microscopy. Cells were washed once before examination using the DeltaVision Spectris inverted microscope (Applied Precision, Issaquah, WA).

Generation of the *nag1-1* site-directed mutant. The *nag1-1* mutant contains a nonsense mutation at codon 41 of *NAG1* (TAT to TAA) that is silent with respect to *YGR031W*, constructed by site-directed mutagenesis of a low-copy plasmid carrying the *YGR031W* locus. Specifically, we first constructed a Gateway-compatible yeast vector for recombination-based cloning of yeast genomic DNA. This gateway vector was constructed from the centromeric yeast shuttle vector YCp50. YCp50 was digested with *Sph*I and made blunt with T 4 DNA Polymerase (New England Biolabs, MA). Gateway cassette A (Invitrogen Corporation, CA) was ligated with the blunt-ended vector, and *Eco*RI was used to identify the orientation of the cassette. To maintain an intact promoter

region for both *YGR031W* and *NAG1*, we amplified the *YGR031W* open reading frame along with 1 kb of sequence upstream of its start codon and 1 kb downstream of its stop codon; this genomic DNA was introduced into YCp50 by recombination-based cloning (Walhout et al. 2000). The *nag1-1* mutant was generated using the QuikChange Site-DirectedMutagenesis Kit (Stratagene, La Jolla, CA) and the following primers: forward primer, 5′- CGTTCTTCGAATGTATAAGACGACACAGACG-3′; reverse primer, 5′-CGTCTGTGTCGTCTTATACATTCGAAGAACG-3′. This construct was subsequently introduced into the yeast deletion strain *ygr031w*Δ by standard methods of yeast transformation (Ito et al. 1983).

DNA microarray analysis. To reduce background variances in gene expression, transcriptional profiles were generated from *ygr031w*Δ bearing either wild-type *NAG1* (in the YCp50 derivative described above) or *nag1-1* (the identical plasmid after site-directed mutagenesis). Thus, the single difference between the strains lies in the point mutation described above. Yeast strains were cultured to mid-log phase in SD-Ura medium prior to RNA extraction. RNA was prepared according to standard protocols using the Poly(A) Purist kit (Ambion, Austin, TX). RNA concentration and purity were determined spectrophotometrically and by gel electrophoresis. Microarray hybridization was performed with the Yeast Genome S98 Array using standard protocols (Affymetrix, Inc, Santa Clara, CA). All microarray experiments were performed in quadruplicate (four biological replicates) for each strain. Differentially expressed genes were identified by significance analysis of microarrays (SAM) (Rieger et al. 2004; Tusher et al. 2001) according to protocols described in Ma *et al.* (Ma et al. 2007).

Calcofluor white sensitivity. Cell wall-related mutant phenotypes were scored on solid medium as described below. A freshly prepared stock solution of 1% (w/v) Calcofluor white was added to sterile selection medium at a final concentration of 10 μg/ml. This medium was adjusted to pH 6.0 with NaOH prior to pouring plates. Wild type and *nag1-1* mutant strains were grown at 30°C in selection medium to log phase. A five-fold dilution series of each cell suspension was made, and 3 μl of each dilution was spotted onto Calcofluor white-containing plates. Growth was monitored after two days incubation at 30°C. This phenotypic assay was repeated for the *nag1-1* mutant in both S288c- and W303-derived strains.

β-galactosidase assays. β-galactosidase assays were performed using the Yeast ß-Galactosidase Assay Kit (Pierce, Rockford, IL) according to standard methods. Mean activities were averaged from three parallel assays. Strains treated with Calcofluor white were grown in liquid medium to mid-log phase; cell cultures were incubated for an additional five hours before β-galactosidase activity was measured.

Results

Identification of the *NAG1* gene nested antisense and opposite *YGR031W*: In a previous study, we utilized a transposon-based gene trap to identify putative protein-coding sequences in the yeast genome (Kumar et al. 2002). This gene trap is diagrammed in Figure 5.1A; it contains a 5′-truncated *lacZ* reporter lacking its promoter and start

codon, such that transposon insertion only results in β- galactosidase activity if the transposon lands in-frame with yeast protein-coding sequence (Ross-Macdonald et al. 1999; Ross-Macdonald et al. 1997). By random transposon mutagenesis with this gene trap, we identified a set of previously non-annotated ORFs that putatively encode proteins, including a set of 54 ORFs positioned opposite and antisense of annotated yeast genes (Kumar et al. 2002). Within this gene set, we were particularly interested in the ORF designated *YGR031C-A* since it is greater than 100 codons in length, is oriented opposite an ORF that putatively encodes a protein, and exhibited easily detected levels of expression during vegetative growth.

The *YGR031C-A* ORF is positioned antisense and opposite the gene *YGR031W* on yeast chromosome VII as indicated in Figure 5.1B. The *YGR031W* gene is functionally uncharacterized but known to encode a mitochondrial protein (Huh et al. 2003; Reinders et al. 2006). *YGR031C-A* consists of a single exon 163 codons in length nested on the opposite strand, but completely within, the *YGR031W* genomic locus. The *YGR031W* gene is more than twice the size of *YGR031C-A*, and both ORFs are relatively well separated from other upstream and downstream genes. Because of this unusual genetic organization, we hereafter refer to *YGR031C-A* as *NAG1* (for Nested Antisense Gene).

To establish that *NAG1* encodes a protein, we first sought to confirm expression of *NAG1*::*mTn* as a β-galactosidase chimera. By PCR amplification of the transposon insertion junction and DNA sequencing of this PCR product, we verified integration of our mini- transposon gene trap at codon 52 of *NAG1* (Figure 5.1B and C). Using quantitative liquid assays, we detected an approximately 9-fold increase in β-galactosidase activity under conditions of vegetative growth in a diploid yeast strain

harboring one transposon-mutagenized copy of *NAG1* relative to the same strain containing an integrated transposon insertion in an intergenic region of noncoding DNA (Figure 5.1C). To validate further the protein-coding potential of *NAG1*, we generated a HA-tagged allele of this gene by integration of a 3xHA-G418 drug-resistance cassette at the *NAG1* 3´-terminus. Cell lysates were extracted from this strain under normal growth conditions for Western blotting with anti-HA antibodies, and this analysis revealed a protein product of approximately 19 kDa, corresponding to the predicted molecular mass of Nag1p-3HA. Thus, the *NAG1* gene does encode protein, and the size of this protein is consistent with its predicted mass as derived from the *NAG1* coding sequence.

***NAG1* is part of an evolutionarily conserved unit in fungi:** The predicted Nag1p sequence (Figure 5.2A) is 163 amino acids in length and exhibits no obvious functional motifs. Similarity searches with this sequence indicated putative *NAG1* orthologs in several bacterial species and numerous fungi (Figure 5.2B). In particular, Nag1p sequence conservation is strongest over a region of 35 residues extending from amino acid 108 to 142. An optimized alignment of this region highlights a strongly conserved Pro-Ile-Glu-Cys-Pro sequence in Nag1p (residues 134 to 138) as well as invariant Gly, Ala, Ser, and Gly residues at positions 109, 110, 112, and 122, respectively.

Interestingly, the *NAG1* gene is conserved as a unit with *YGR031W*: in each organism carrying a putative ortholog of *NAG1*, the *NAG1* sequence is nested antisense an obvious ortholog of *YGR031W* (Figure 5.2C). The *YGR031W* gene itself is highly conserved in organisms ranging from prokaryotes to humans; however, *NAG1* is not present opposite orthologs of *YGR031W* in higher eukaryotes, but instead is specific for

prokaryotes and fungi. While these alignments indicate sequence similarity, we cannot conclusively assign functions to any putative *NAG1* orthologs without experimental analysis of each sequence in each organism.

Subcellular localization of Nag1p: As a means of assessing the subcellular distribution of Nag1p, we cloned the *NAG1* gene along with 1 kb of upstream promoter sequence into a low- copy yeast shuttle vector such that the 3′-end of *NAG1* forms an in-frame fusion with sequence encoding the Venus variant of yellow fluorescent protein (vYFP). As shown in Figure 5.3A, this carboxy-terminal Nag1p-vYFP chimera localized to the yeast cell periphery under conditions of vegetative growth. Nag1p did not localize to the endoplasmic reticulum; the integral membrane protein Spo7p serves as a marker for the nuclear envelope-endoplasmic reticulum network (Siniossoglou et al. 1998), and the carboxy-terminal Spo7p-RFP chimera (Figure 5.3A) did not co-localize with Nag1p-vYFP. The localization of Nag1p was also distinct from that of Ygr031wp. As mentioned above, *YGR031W* encodes a mitochondrial protein, as determined in a large-scale study of yeast protein localization (Huh et al. 2003) and in a separate mass spectrometry-based study of yeast mitochondrial proteins (Reinders et al. 2006). To confirm these results, we generated a carboxy-terminal Ygr031wp-vYFP chimera and found this protein localized to the mitochondria under conditions of vegetative growth (Figure 5.3B).

Computational analysis of the Nag1p amino acid sequence revealed two putative transmembrane domains of roughly 20 residues positioned towards the center and carboxy terminus of the protein (Figure 5.3C). Predictions of transmembrane segments were obtained from the programs HMMTOP (Tusnady et al. 2001), PHDhtm (Rost et al.

1996), TopPred (Charos et al. 1994), TMpred (Ikeda et al. 2992), and TMHMM (Krogh et al. 2001). Each program highlighted transmembrane segments of slightly different lengths, but residues 77- 94 and 135-152 were identified unanimously (Figure 5.3C). These putative transmembrane domains flank the region of strong sequence conservation presented in Figure 5.2B, although the carboxy-terminal putative transmembrane segment does overlap this conserved region by 8 bp. In corollary to the studies above, we also examined the possible membrane association of Nag1p by subcellular fractionation. Lysed sheroplasts were prepared from yeast cells carrying HA-tagged Nag1p expressed from its native promoter under conditions of vegetative growth; cell lysates were subjected to centrifugation at 16,000 *g* (13,000 rpm). As visualized by Western blotting, HA-tagged Nag1p was present in the pellet fraction following low-speed centrifugation, co-fractionating with other known membrane proteins (Figure 5.3D).

Thus, Nag1p localizes to the cell periphery, is predicted to contain two transmembrane domains, fractionates with membrane proteins, and does not co-localize with ER markers — properties consistent with those of a plasma membrane protein.

Phenotypic characterization of *NAG1*: To investigate *NAG1* function, we generated a point mutation (*nag1-1*) disrupting *NAG1*, but silent with respect to the opposite gene *YGR031W* (Figure 5.4A). Specifically, we mutated *NAG1* codon 41 (TAT encoding tyrosine) to a stop codon (TAA); this single base change does not affect the amino acid composition of the YGR031W protein, since the complementary TCA to TCT substitution at codon 247 still encodes serine. The *nag1-1* mutation truncates *NAG1* coding sequence at approximately 25% its full length. Deletion of the entire *NAG1*

coding sequence in *ygr031w*Δ generates a comparable phenotype to *nag1-1* in the assays applied here; thus, *nag1-1* mimics a null allele in our studies.

With no *a priori* indication of a process to which *NAG1* contributes, we decided to implement a global strategy, profiling gene expression in *nag1-1* by microarray analysis (Figure 5.4B). By this approach, biological processes impaired in *nag1-1* should be evident from altered gene expression profiles. Transcriptional profiling of *nag1-1* against a wild-type strain under conditions of vegetative growth revealed differential expression of 262 genes. In particular, 149 genes exhibited decreased transcript levels in *nag1-1*; this gene set was statistically enriched (*p*-value of 4.85×10^{-5}) for genes contributing to cell wall organization and biogenesis (GO Cellular Process ID 7047). Furthermore, the set of 262 genes as a whole was enriched (*p*-value of 1.19×10^{-5}) for genes encoding proteins associated with the plasma membrane (GO Cell Component ID 5886). No other gene subsets were statistically overrepresented in this microarray data set.

The decrease in cell wall-related gene transcription evident in the *nag1-1* mutant is unusual for a gene contributing to cell wall biogenesis. More typically, the deletion of a cell wall-related gene leads to an increase in cell wall gene transcription as a compensatory response (Jung et al. 1999). Of course, most cell wall associated genes are involved in the biosynthesis or structural organization of the cell wall, and loss of function leads directly to a structural defect that requires a compensatory response to maintain integrity. Since *nag1-1* exhibited the opposite effect on cell wall gene transcription, we next asked if *nag1-1* displayed phenotypes consistent with an altered cell wall structure. Towards this end, we compared the growth of *nag1-1* with a wild

type strain in the presence of a set of cell wall perturbants including Calcofluor white, Congo red, caffeine, and caspofungin. As indicated in Figure 5.4C, *nag1-1* is sensitive to Calcofluor white but showed no apparent growth defects with any of the other drugs. Calcofluor white is a negatively charged fluorescent dye that binds nascent chains of chitin and, to a lesser degree, glucan; as a result, Calcofluor white prevents microfibril assembly, thereby interfering with cell wall organization (Elorza et al. 1983; Lussier et al. 1997). Calcofluor white hypersensitivity has been observed as a pleiotropic phenotype associated with many yeast cell wall mutants (Hampsey et al. 1997; Lussier et al., 1997), and the *nag1-1* mutant exhibits sensitivity to Calcofluor white at 37ºC. A similar phenotype is observed for *nag1-1* at 30ºC, although the severity is decreased. These phenotypes are consistent across multiple independent transformants in the BY4742 genetic background. To consider further the function of Nag1p in cell wall biogenesis, we introduced the *nag1-1* allele into the yeast strain W303. The wild-type W303 strain is defective for the gene *SSD1*, encoding a protein involved in the maintenance of cellular integrity (Kaeberlein et al. 2002); therefore, cell wall-related phenotypes are often exacerbated in the W303 genetic background. Accordingly, the *nag1-1* mutant yields a more pronounced Calcofluor white phenotype at both 30ºC and 37ºC in the W303 background, as assayed in multiple independent tranformants. In some Calcofluor white hypersensitive mutants, cell wall chitin is increased, resulting in increased Calcofluor white staining. The *nag1-1* mutant, however, did not display either an increased amount or abnormal distribution of Calcofluor white staining at 25°C or 37°C (data not shown).

Observed *nag1-1* phenotypes are specific to cell wall function. The *nag1-1* mutant is viable at both 30ºC and 37ºC, without obvious fitness defects under conditions

of vegetative growth at either temperature. In addition, analysis of *nag1-1* for growth sensitivity under conditions of nutritional stress, alternative carbon source, nitrogen stress, and high osmolarity did not reveal mutant phenotypes (data not shown).

Nag1p production is regulated by the Slt2p cell wall integrity pathway: Since many proteins contributing to cell wall function are induced upon treatment with cell wall perturbing agents, we examined the response of Nag1p upon treatment with Calcofluor white in the W303 genetic background (Figure. 5.4D). Using a Nag1p-β-galactosidase chimera, we investigated Nag1p protein levels under conditions of vegetative growth and in identical growth medium supplemented with Calcofluor white. Calcofluor white treatment resulted in a 1.4-fold increase in Nag1p levels relative to those observed during vegetative growth, further supporting its role in cell wall-related processes.

In yeast, cell wall integrity is maintained, in part, through a signaling pathway encompassing the Slt2p/Mpk1p mitogen-activated protein kinase (MAPK) cascade (Figure. 5.5A). The Slt2p pathway is activated in response to numerous environmental stimuli, including conditions of hypoosmotic stress, exposure to mating pheromone, and treatment with agents causing cell wall stress (de Nobel et al. 2000; Ketela et al. 1999; Lee et al. 1993; Zarzov et al. 1996). These stimuli are transduced into signals activating the GDP/GTP exchange factor Rom2p and the small GTP-binding protein Rho1p (Philip et al. 2001). Rho1p binds and activates Pkc1p, which in turn elicits serial activation of a MAPK cascade consisting of the MAPKKK Bck1p, the MAPKKs Mkk1p and Mkk2p, and the MAPK Slt2p/Mpk1p (Heinisch et al. 1999). The transcription factor Rlm1p acts downstream of Slt2p (Dodou et al. 1997), and Rlm1p activates expression of at least 20

genes, the majority of which contribute to yeast cell wall biogenesis (Jung et al. 1999) (Figure. 5.5A).

Interestingly, transcription of both *SLT2* and *RLM1* was downregulated in the *nag1-1* site-directed mutant (Figure. 5.4B). To investigate a possible role for Nag1p acting downstream of the Slt2p pathway, we assayed protein levels of a Nag1p-β-galactosidase chimera in *slt2*Δ and *rlm1*Δ deletion strains under conditions of vegetative growth and Calcofluor white treatment (Figure 5.5B).

Nag1p levels were diminished during vegetative growth in both deletion strains, but with a more pronounced decrease evident in the *rlm1*Δ mutant. Consistent with a role for Rlm1p in the transcriptional activation of Nag1p, a Rlm1p binding site consensus sequence (CTA(T/A) 4 TA (Dodou et al. 1997; Jung et al. 2002)); is present 430 nt upstream of the presumed *NAG1* start codon. Interestingly, this putative, palindromic Rlm1p binding site is shared with the promoter of *GSC2*, the inducible subunit of 1,3-β-glucan synthase and a gene that is upregulated by cell wall stress. Upon exposure to Calcofluor white, the overall levels of *NAG1* expression were decreased in both *slt2*Δ and *rlm1*Δ mutants relative to wild type. However, exposure to Calcofluor white increased *NAG1* expression in both mutants relative to the untreated cells, suggesting that Slt2p-independent cell wall response pathways may also contribute to Nag1p expression (Levin et al., 2005). Based on this analysis, we conclude that the cell wall stress-induced production of Nag1p is partially dependent upon Slt2p and Rlm1p.

Discussion

In this chapter, we present an unusual orientation of protein-coding genes in the yeast genome, identifying a previously overlooked gene, *NAG1*, nested antisense and opposite another protein-coding gene *YGR031W*. This gene superstructure represents an evolutionary unit conserved among many fungal species. The strongly conserved *YGR031W* gene encodes a mitochondrial protein, while *NAG1* encodes a 19-kDa membrane protein localized to the yeast cell periphery.

To study *NAG1* function, we constructed a point mutation disrupting *NAG1* but silent with respect to *YGR031W*; this mutant exhibited hypersensitivity to Calcofluor white and altered transcript levels for a significant subset of genes mediating cell wall biogenesis. Furthermore, Nag1p levels were increased upon Calcofluor white treatment and reduced in strains deleted for *SLT2* and *RLM1*, key components of the yeast MAPK cell wall integrity pathway. Collectively, this study highlights a role for Nag1p in maintaining yeast cell wall integrity and function, while validating the protein-coding potential of this nested gene.

In particular, the nested organization of genes at the *NAG1* locus holds interesting evolutionary implications. Overlapping genes have been found commonly in viruses and microorganisms, where this type of interleaved and nested gene organization presumably contributes to the maintenance of a compact genome — a beneficial characteristic, since genome size in these organisms is limited by the size of the viral particle or cell (Krakauer et al., 2000). Eukaryotic genomes, of course, do not face this constraint, and, in this light, two points regarding *NAG1* are noteworthy. First, putative *NAG1* orthologs

are exclusively found opposite an ortholog of *YGR031W*. Second, *YGR031W* encodes a mitochondrial protein. Mitochondria are thought to have evolved from purple non-sulfur bacteria (Cavalier-Smith et al., 2006), wherein this type of nested gene organization might not be uncommon. Extrapolating from this, we can speculate that the *NAG1* locus may represent the remnants of an ancient genetic unit, possibly even tracing back to symbiont gene transfer during mitochondrial evolution. *YGR031W* is strongly conserved in prokaryotes and eukaryotes alike, but, over evolutionary time, *NAG1* function may have been lost in organisms lacking a cell wall. Consistent with this possibility, putative *NAG1* orthologs are present only in prokaryotes and fungi (Figure 5.2), although further studies would be necessary to determine if these orthologs are functional.

The cell wall-related function of Nag1p is supported by three lines of evidence. First, and most striking, is the fact that the *nag1-1* mutation leads to a significant decrease in the expression of a large set of cell wall genes during vegetative growth. This is opposite to the more common phenomenon whereby deletion of a cell wall gene causes an up-regulation of cell wall gene transcription to compensate for the resulting cell wall defects. The negative effect of *nag1-1* on cell wall gene expression is more consistent with Nag1p functioning as a type of regulatory protein as opposed to having a direct role in cell wall structure or biosynthesis. This analysis is further supported by the relatively mild cell wall phenotype displayed by *nag1-1*. However, it is important to note that mutation of a number of cell wall-related genes causes Calcofluor white hypersensitivity as their only discernible cell wall phenotype; therefore, this second set of observations supporting a cell wall role for Nag1p is consistent with other bona fide cell wall proteins. Third, the effect of cell wall stress and the cell wall integrity MAPK signaling pathway

on *NAG1* expression provides compelling support for the cell wall-related function of Nag1p. As is the case for many cell wall-related genes, cell wall stress such as Calcofluor white treatment induces a modest increase in Nag1p levels. *NAG1* may share its promoter region with *GSC2* (Figure 5.1B), the stress-inducible subunit of 1,3-β-glucan synthase, and, therefore, *NAG1* expression could be regulated by processes that also regulate *GSC2*. Indeed, this region contains a consensus binding site for Rlm1p, a transcription factor regulated by the cell wall integrity MAPK signaling pathway. Since the Rlm1p binding site is palindromic, it should control transcription of appropriately oriented open reading frames on either the Watson or Crick strands. Consistent with this analysis, *NAG1* expression is dependent on both Slt2p and Rlm1p in a significant but not exclusive fashion. Intriguingly, the effect of Slt2p and Rlm1p on *NAG1* expression is quite apparent during vegetative growth. Although the cell wall integrity pathway is more commonly thought of as a stress-response cascade, it is activated during specific periods of the cell cycle (Levin et al. 2005). Therefore, *NAG1* expression may be controlled through basal signaling of the cell wall integrity pathway. We speculate that this pattern of expression may relate to the positive effect of Nag1p on the transcription of other cell wall genes during vegetative growth. Obviously, a more extensive characterization of Nag1p will be required to confirm this assertion. However, it is clear from our data that Nag1p is a functional protein involved in yeast cell wall integrity.

Here, we have referred to *NAG1* as being unique, but, in fact, *NAG1* may actually represent the first identified gene of a larger class: the potential certainly exists for other nested antisense genes in yeast. By transposon mutagenesis using a simple gene trap reporter, we previously identified a set of at least 54 putative nested genes in yeast

(Kumar et al. 2002). While we expect that some, and perhaps the majority, of these nested ORFs do not encode protein, additional studies may uncover other nested protein-coding genes previously overlooked in the yeast genome. These overlooked genes potentially represent a wealth of unexplored yeast biology, with implications impacting gene predictions and gene-finding studies in other eukaryotes as well. As a result, the example set by *NAG1* may prove useful in refining annotation efforts applied to other genomes, separate from the relevance of this gene as an interesting component of the signaling pathways and networks contributing to yeast cell surface biology.

Acknowledgements

We thank Dan Klionsky for providing reagents and for helpful comments regarding this manuscript. This work was supported by NIH grant K08A1062978 (to D.J.K.) and grants RSG- 06-179-01-MBC from the American Cancer Society, DBI 0543017 from the National Science Foundation, and Basil O'Connor Award 5-FY05-1224 from the March of Dimes (to A.K.).

Figure 5.1 The *NAG1* gene is nested opposite *YGR031W* and encodes a protein product. (A) Schematic of the transposon-based gene trap used to identify *YGR031C-A*/*NAG1*. The *lacZ* reporter lacks its start codon and promoter, so β-galactosidase (β-gal) is only produced if the transposon inserts in genomic DNA such that the *lacZ* coding sequence is in frame with a host gene. The transposon-encoded *lacZ* fusion will be separated from host gene coding sequence by the Tn*3*L terminal sequence and *loxR* site. (B) Diagrammatic representation of the *YGR031W* locus, indicating *YGR031C-A*/*NAG1* nested antisense to *YGR031W* on the opposite strand. The circle inset indicates the exact transposon insertion identifying *NAG1*. (C) β-gal assay of the Nag1p-β-gal protein product; the Nag1p chimera consists of the N-terminal 52 amino acids of Nag1p, the Tn*3*L and *loxR* sequences, and β-galactosidase from the second amino acid onwards. For comparison, the β-gal level from a transposon insertion in non-coding DNA (chromosome XV, coordinate 216,878) is indicated. (D) Western blot identifying Nag1p tagged at its carboxy- terminus with three copies of the HA epitope. Protein extract from an untagged strain is also included as a control; both extracts were prepared from cells undergoing vegetative growth. Levels of Pgk1p, 3-phosphoglycerate kinase, were analyzed to ensure comparability between protein samples.

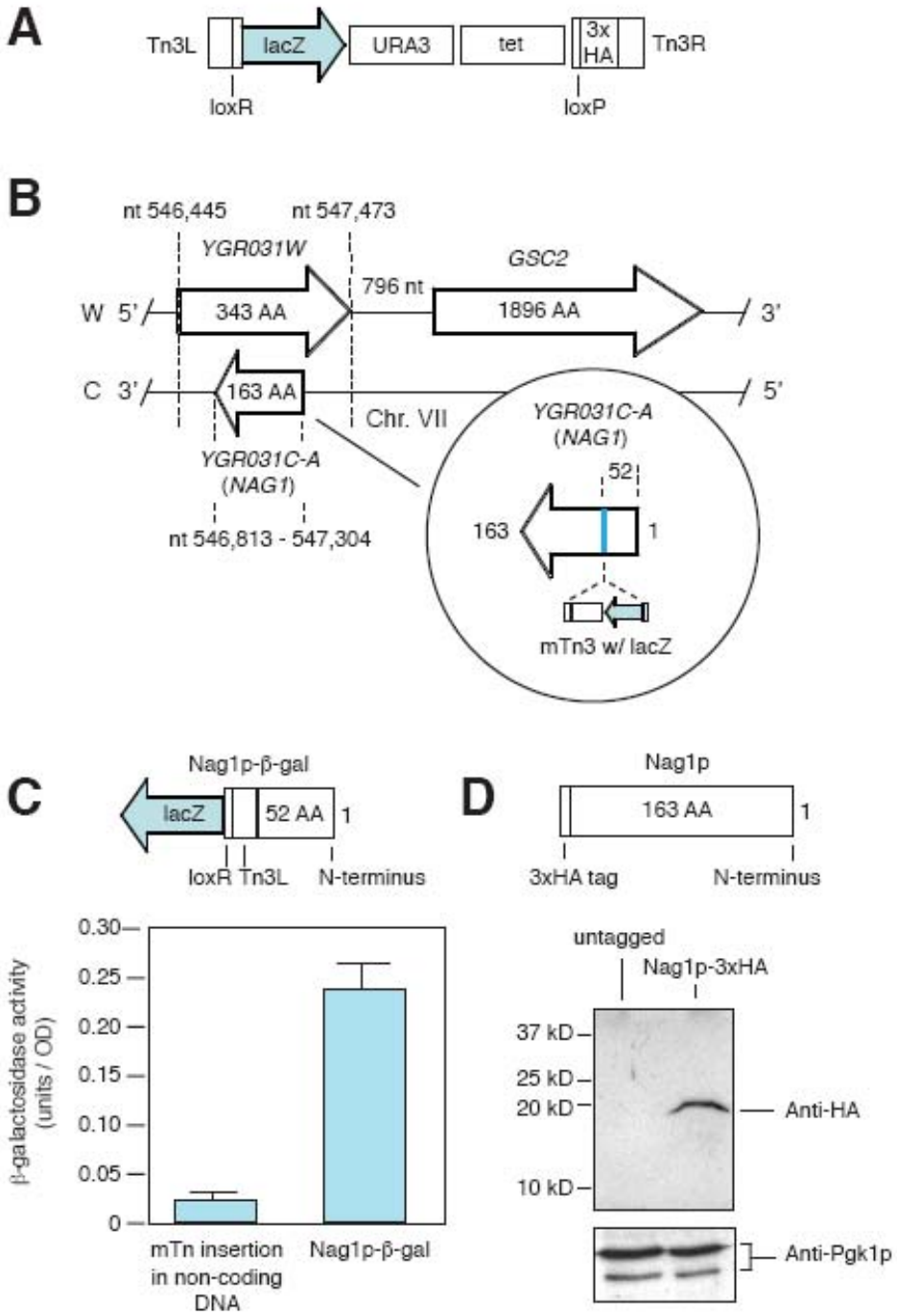
A
Tn3L
lacZ
URA3
tet
3x HA
Tn3R
loxR
loxP
B
nt 546,445
nt 547,473
YGR031W
GSC2
796 nt
W 5'
343 AA
1896 AA
3'
C 3'
163 AA
5'
Chr. VII
YGR031C-A (NAG1)
nt 546,813 - 547,304
52
163
1
mTn3 w/ lacZ
C
Nag1p-β-gal
lacZ
52 AA
1
loxR Tn3L
N-terminus
β-galactosidase activity (units / OD)
0.30
0.25
0.20
0.15
0.10
0.05
0
mTn insertion in non-coding DNA
Nag1p-β-gal
D
Nag1p
163 AA
1
3xHA tag
N-terminus
untagged
Nag1p-3xHA
37 kD
25 kD
20 kD
10 kD
Anti-HA
Anti-Pgk1p

Figure 5.2 *NAG1* is conserved as a unit with *YGR031W* in bacteria and fungi. (A) Amino acid sequence of Nag1p as predicted by conceptual translation. (B) Putative *NAG1* orthologs from prokaryotic and fungal species. Schematic diagram illustrating conserved regions within the identified set of putative *NAG1* orthologs. Each line represents the full length of the orthologous sequence; gaps in the multiple sequence alignment are indicated as such in the figure. The inset rectangle highlights the most strongly conserved region of the alignment. Identical residues are indicated as white on black, and similar residues are shown as black on gray. (C) Since Nag1p has not been recognized previously as a protein, neither its sequence nor the sequence of any ortholog is present in a protein database; thus, the Nag1p amino acid sequence was searched against a six-frame translation of genomic DNA sequence. The coordinates of each putative orthologous gene are indicated here, relative to each indicated database accession ID. In each instance, putative orthologs of *NAG1* are found opposite orthologs of *YGR031W*; thus, the nested organization of *NAG1* relative to *YGR031W* is conserved as an evolutionary unit.

A

Nag1p Amino Acid Sequence:

```
1         10         20         30         40         50         60
MNSAGRVHRSRAGSRGHAAISPLTMASFSVARGIRSSNVYDDTDDELSILTFFSAVRRNR
61        70         80         90         100        110        120
LTSSLPPILSARCSSACFSVRIVLPLSLTISISALMYSTNSALGRKLTGAFSIQTNIEQS
121       130        140        150        160
CGFFRTSIMATLPPIECPIIIGPPLVFNSCFVIKCFTSSDMTS*
```

B

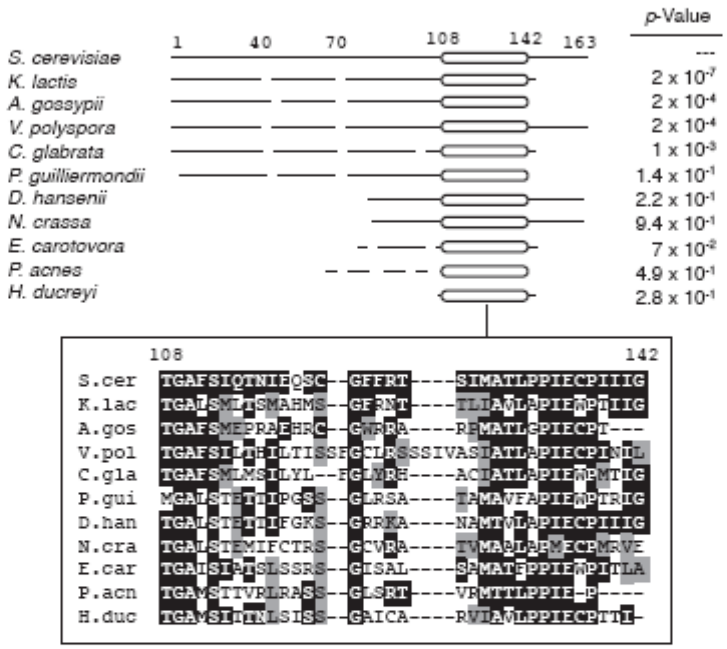

C

Genus / Species	Kingdom / Superkingdom	Database ID	nt Seq. Coordinates	Opposite ORF:
S. cerevisiae	Fungi	gbIAF479950.1	1-489	YGR031W
K. lactis	Fungi	refIXM_451797.1	863-456	YGR031W ortholog
A. gossypii	Fungi	gbIAE016816.2	47021-47413	YGR031W ortholog
V. polyspora	Fungi	refIXM_001642751.1	758-291	YGR031W ortholog
C. glabrata	Fungi	emblCR380957.1	370088-369708	YGR031W ortholog
P. guilliermondii	Fungi	refIXM_001481991.1	827-441	YGR031W ortholog
D. hansenii	Fungi	emblCR382135.1	620-462	YGR031W ortholog
N. crassa	Fungi	refIXM_950749.1	593-402	YGR031W ortholog
E. carotovora	Bacteria	emblBX950851.1	1511222-1511419	YGR031W ortholog
P. acnes	Bacteria	gbIAE017283.1	1192677-1192862	YGR031W ortholog
H. ducreyi	Bacteria	gbIAE017143.1	1030374-1030478	YGR031W ortholog

Figure 5.3 Nag1p localizes to the yeast cell periphery, distinct from Ygr031wp, and exhibits properties consistent with a plasma membrane protein. (A) Fluorescence microscopy of a Nag1p- vYFP chimera expressed from its native promoter under conditions of vegetative growth. The Spo7p-RFP chimera serves as a marker for the nuclear envelope and endoplasmic reticulum (middle image), and yeast cell morphology was visualized by differential interference contrast (DIC) microscopy (right image). (B) Fluorescence microscopy of Ygr031wp-vYFP indicates its localization to the mitochondria. The MitoFluor stain was used to confirm co-localization with mitochondria (middle image), and a DIC image is provided (right). (C) Diagram illustrating predicted Nag1p transmembrane domains. Each putative transmembrane segment is shaded gray in the Nag1p schematic, and the primary sequence of each segment along with its amino acid coordinates are indicated. (D) Western blots indicating the presence of Nag1p-3xHA in the pellet fraction (P13) after centrifugation of total cell lysates (T) at 13,000 rpm (16,000 *g*). The known plasma membrane protein Pma1p was also found in the P13 fraction, as indicated by Western blotting with antibody directed against native Pma1p. As a further control, we used antibody directed against 3-phopshoglycerate kinase, Pgk1p, to confirm the presence of this protein in the supernatent fraction (S13) following centrifugation.

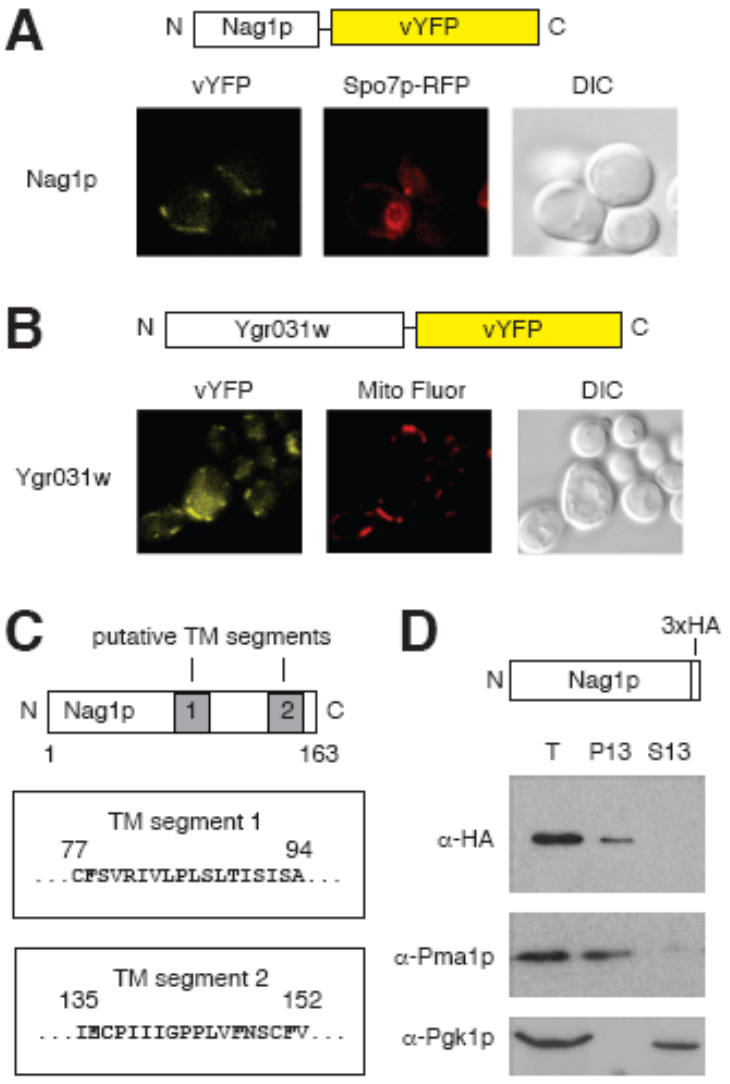
A
N
Nag1p
vYFP
C
vYFP
Spo7p-RFP
DIC
Nag1p
B
N
Ygr031w
vYFP
C
vYFP
Mito Fluor
DIC
Ygr031w
C
putative TM segments
N
Nag1p
1
2
C
1
163
TM segment 1
77
94
...CFSVRIVLPLSLTISISA...
TM segment 2
135
152
...IMCPIIIGPPLVFNSCFV...
D
3xHA
N
Nag1p
T
P13
S13
α-HA
α-Pma1p
α-Pgk1p

Figure 5.4 *NAG1* contributes to yeast cell wall biogenesis. (A) The *nag1-1* point mutation introduces a nonsense mutation at codon 41, without altering the predicted amino acid sequence of the Ygr031wp protein product. (B) DNA microarray analysis of the *nag1-1* mutant under conditions of vegetative growth. Details of this experimental design are presented in Materials and Methods. The total number of differentially expressed genes in *nag1-1* relative to the wild- type strain is indicated. Genes associated with the GO Cellular Process term 7047 (Cell Wall Organization / Biogenesis) were statistically enriched in the set of genes with decreased transcript levels in *nag1-1*; these genes are shown under this GO term in the middle box. Genes associated with the GO Cell Component term 5886 (Plasma membrane) were statistically enriched in the total set of genes identified by microarray analysis (both with increased and decreased transcript levels); these genes are also shown below the GO term. The majority of these cell surface-related genes are indicated in the heat map to the left with corresponding t-statistics and *p*-values. (C) The *nag1-1* mutant is sensitive to Calcofluor white. For the assay shown here, we introduced a plasmid carrying the *nag1-1* allele in the *YGR031W* genomic DNA locus into a strain of the W303 genetic background deleted for *YGR031W*. The resulting *nag1-1* mutant was hypersensitive to Calcofluor white, with increased severity at elevated temperature (37°C). (D) Nag1p protein levels are increased upon Calcofluor white treatment, as evidenced by increased β-gal activity from a Nag1p-β-gal chimera.

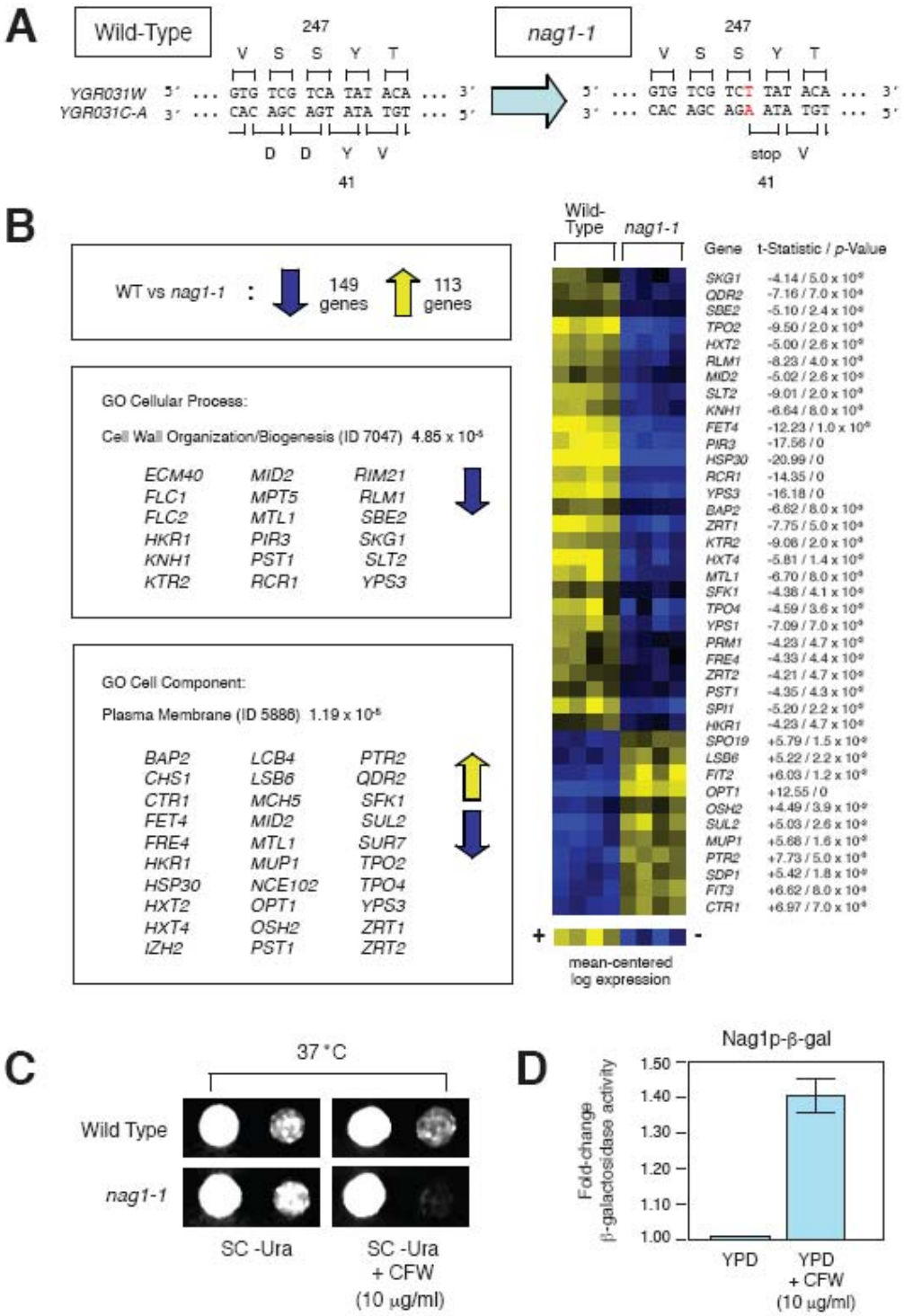
A
Wild-Type
247
V S S Y T
YGR031W 5′ ... GTG TCG TCA TAT ACA ... 3′
YGR031C-A 3′ ... CAC AGC AGT ATA TGT ... 5′
D D Y V
41
nag1-1
247
V S S Y T
5′ ... GTG TCG TCT TAT ACA ... 3′
3′ ... CAC AGC AGA ATA TGT ... 5′
stop V
41
B
WT vs nag1-1 : 149 genes 113 genes
GO Cellular Process:
Cell Wall Organization/Biogenesis (ID 7047) 4.85 x 10-5
ECM40 MID2 RIM21
FLC1 MPT5 RLM1
FLC2 MTL1 SBE2
HKR1 PIR3 SKG1
KNH1 PST1 SLT2
KTR2 RCR1 YPS3
GO Cell Component:
Plasma Membrane (ID 5886) 1.19 x 10-5
BAP2 LCB4 PTR2
CHS1 LSB6 QDR2
CTR1 MCH5 SFK1
FET4 MID2 SUL2
FRE4 MTL1 SUR7
HKR1 MUP1 TPO2
HSP30 NCE102 TPO4
HXT2 OPT1 YPS3
HXT4 OSH2 ZRT1
IZH2 PST1 ZRT2
Wild-Type
nag1-1
Gene t-Statistic / p-Value
SKG1 -4.14 / 5.0 x 10-5
QDR2 -7.16 / 7.0 x 10-9
SBE2 -5.10 / 2.4 x 10-6
TPO2 -9.50 / 2.0 x 10-9
HXT2 -5.00 / 2.6 x 10-6
RLM1 -8.23 / 4.0 x 10-9
MID2 -5.02 / 2.6 x 10-6
SLT2 -9.01 / 2.0 x 10-9
KNH1 -6.64 / 8.0 x 10-9
FET4 -12.23 / 1.0 x 10-9
PIR3 -17.56 / 0
HSP30 -20.99 / 0
RCR1 -14.35 / 0
YPS3 -16.18 / 0
BAP2 -6.62 / 8.0 x 10-9
ZRT1 -7.75 / 5.0 x 10-9
KTR2 -9.06 / 2.0 x 10-9
HXT4 -5.81 / 1.4 x 10-6
MTL1 -6.70 / 8.0 x 10-9
SFK1 -4.38 / 4.1 x 10-5
TPO4 -4.59 / 3.6 x 10-5
YPS1 -7.09 / 7.0 x 10-9
PRM1 -4.23 / 4.7 x 10-5
FRE4 -4.33 / 4.4 x 10-5
ZRT2 -4.21 / 4.7 x 10-5
PST1 -4.35 / 4.3 x 10-5
SPI1 -5.20 / 2.2 x 10-5
HKR1 -4.23 / 4.7 x 10-5
SPO19 +5.79 / 1.5 x 10-9
LSB6 +5.22 / 2.2 x 10-5
FIT2 +6.03 / 1.2 x 10-9
OPT1 +12.55 / 0
OSH2 +4.49 / 3.9 x 10-5
SUL2 +5.03 / 2.6 x 10-9
MUP1 +5.68 / 1.6 x 10-9
PTR2 +7.73 / 5.0 x 10-9
SDP1 +5.42 / 1.8 x 10-9
FIT3 +6.62 / 8.0 x 10-9
CTR1 +6.97 / 7.0 x 10-9
+
-
mean-centered log expression
C
37 °C
Wild Type
nag1-1
SC -Ura
SC -Ura + CFW (10 μg/ml)
D
Nag1p-β-gal
Fold-change β-galactosidase activity
1.50
1.40
1.30
1.20
1.10
1.00
YPD
YPD + CFW (10 μg/ml)

Figure 5.5 Nag1p production is dependent upon the MAPK Slt2p and the transcription factor Rlm1p. (A) Simplified overview of the yeast Slt2p MAPK cell wall integrity pathway. Rlm1p acts as a key transcriptional regulator downstream of Slt2p. (B) β-gal assays of the Nag1p-β-gal chimera during vegetative growth and in response to Calcofluor white treatment in strains deleted for *SLT2* and *RLM1*, respectively. Fold-change from wild type β-gal levels are presented for each mutant under the indicated growth conditions. All β-gal assay results were normalized per yeast cell optical density unit.

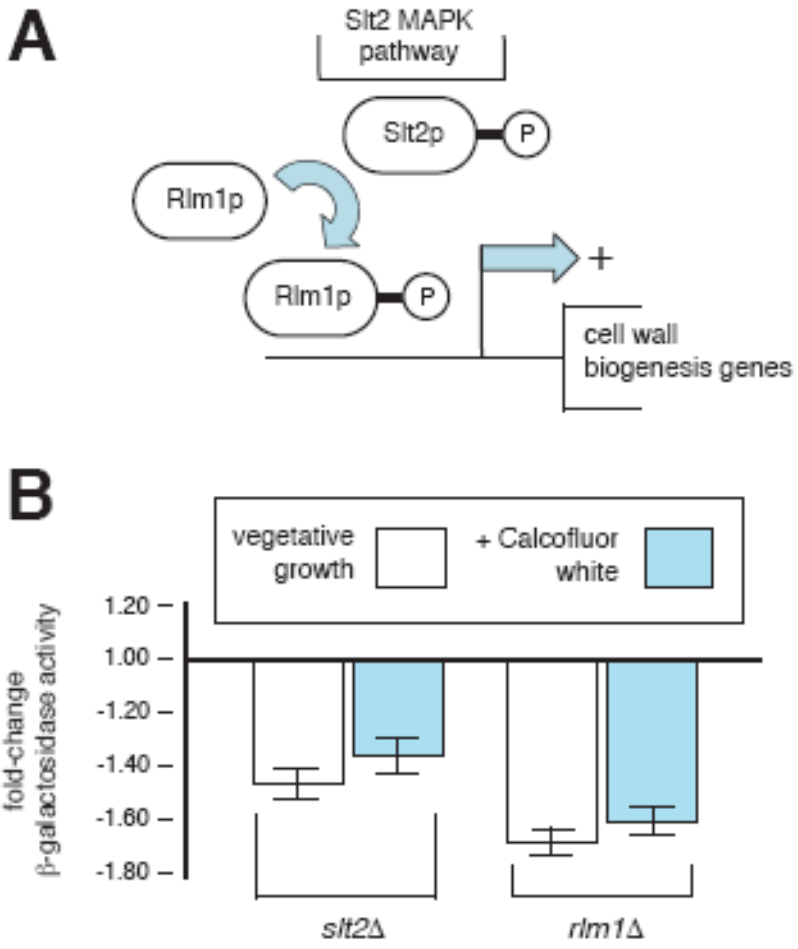
A
Slt2 MAPK pathway
Slt2p
P
Rlm1p
Rlm1p
P
+
cell wall biogenesis genes
B
vegetative growth
+ Calcofluor white
fold-change β-galactosidase activity
1.20
1.00
-1.20
-1.40
-1.60
-1.80
slt2Δ
rlm1Δ

References

Cavalier-Smith, T. 2006. Origin of mitochondria by intracellular enslavement of a photosynthetic purple bacterium. Proc Biol Sci **273**:1943-1952.

Claros, M. G., and G. von Heijne. 1994. TopPred II: an improved software for membrane protein structure predictions. Comput Appl Biosci **10**:685-686.

Coelho , P. S., A. C. Bryan, A. Kumar, G. S. Shadel, and M. Snyder. 2002. A novel mitochondrial protein, Tar1p, is encoded on the antisense strand of the nuclear 25S rDNA. Genes Dev **16**:2755-2760.

David, L., W. Huber, M. Granovskaia, J. Toedling, C. J. Palm, L. Bofkin, T. Jones, R. W. Davis, and L. M. Steinmetz. 2006. A high-resolution map of transcription in the yeast genome. Proc Natl Acad Sci U S A **103**:5320-5325.

de Nobel, H., C. Ruiz, H. Martin, W. Morris, S. Brul, M. Molina, and F. M. Klis. 2000. Cell wall perturbation in yeast results in dual phosphorylation of the Slt2/Mpk1 MAP kinase and in an Slt2-mediated increase in FKS2-lacZ expression, glucanase resistance and thermotolerance. Microbiology **146 (Pt 9)**:2121-2132.

Dodou, E., and R. Treisman. 1997. The Saccharomyces cerevisiae MADS-box transcription factor Rlm1 is a target for the Mpk1 mitogen-activated protein kinase pathway. Mol Cell Biol **17**:1848-1859.

Elorza, M. V., H. Rico, and R. Sentandreu. 1983. Calcofluor white alters the assembly of chitin fibrils in Saccharomyces cerevisiae and Candida albicans cells. J Gen Microbiol **129**:1577-1582.

Guthrie, C., and G. Fink. 1991. Guide to Yeast Genetics and Molecular Biology. Academic Press, San Diego, CA.

Hampsey, M. 1997. A review of phenotypes in *Saccharomyces cerevisiae*. Yeast **13**:1099- 1133.

Havilio, M., E. Y. Levanon, G. Lerman, M. Kupiec, and E. Eisenberg. 2005. Evidence for abundant transcription of non-coding regions in the Saccharomyces cerevisiae genome. BMC Genomics **6**:93.

Heinisch, J. J., A. Lorberg, H. P. Schmitz, and J. J. Jacoby. 1999. The protein kinase C-mediated MAP kinase pathway involved in the maintenance of cellular integrity in Saccharomyces cerevisiae. Mol Microbiol **32**:671-680.

Hongay, C. F., P. L. Grisafi, T. Galitski, and G. R. Fink. 2006. Antisense transcription controls cell fate in Saccharomyces cerevisiae. Cell **127**:735-745.

Huh, W. K., J. V. Falvo, L. C. Gerke, A. S. Carroll, R. W. Howson, J. S. Weissman, and E. K. O'Shea. 2003. Global analysis of protein localization in budding yeast. Nature **425**:686- 691.

Ikeda, M., M. Arai, D. M. Lao, and T. Shimizu. 2002. Transmembrane topology prediction methods: a re-assessment and improvement by a consensus method using a dataset of experimentally-characterized transmembrane topologies. In Silico Biol **2**:19-33.

Ito, H., Y. Fukuda, K. Murata, and A. Kimura. 1983. Transformation of intact yeast cells treated with alkali cations. J. Bacteriol. **153**:163-168.

Jung, U. S., and D. E. Levin. 1999. Genome-wide analysis of gene expression regulated

by the yeast cell wall integrity signalling pathway. Mol Microbiol **34**:1049-1057.
Jung, U. S., A. K. Sobering, M. J. Romeo, and D. E. Levin. 2002. Regulation of the yeast Rlm1 transcription factor by the Mpk1 cell wall integrity MAP kinase. Mol Microbiol **46**:781- 789.
Kaeberlein, M., and L. Guarente. 2002. Saccharomyces cerevisiae MPT5 and SSD1 function in parallel pathways to promote cell wall integrity. Genetics **160**:83-95.
Kapranov, P., A. T. Willingham, and T. R. Gingeras. 2007. Genome-wide transcription and the implications for genomic organization. Nat Rev Genet **8**:413-423.
Ketela, T., R. Green, and H. Bussey. 1999. Saccharomyces cerevisiae mid2p is a potential cell wall stress sensor and upstream activator of the PKC1-MPK1 cell integrity pathway. J Bacteriol **181**:3330-3340.
Kim, J., V. M. Dalton, K. P. Eggerton, S. V. Scott, and D. J. Klionsky. 1999. Apg7p/Cvt2p is required for the cytoplasm-to-vacuole targeting, macroautophagy, and peroxisome degradation pathways. Mol Biol Cell **10**:1337-1351.
Krakauer, D. C. 2000. Stability and evolution of overlapping genes. Evolution Int J Org Evolution **54**:731-739.
Krogh, A., B. Larsson, G. von Heijne, and E. L. Sonnhammer. 2001. Predicting Transmembrane protein topology with a hidden Markov model: application to complete genomes. J Mol Biol **305**:567-580.
Kumar, A., P. M. Harrison, K. H. Cheung, N. Lan, N. Echols, P. Bertone, P. Miller, M. B. Gerstein, and M. Snyder. 2002. An integrated approach for finding overlooked genes in yeast. Nat Biotechnol **20**:58-63.
Lee, K. S., K. Irie, Y. Gotoh, Y. Watanabe, H. Araki, E. Nishida, K. Matsumoto, and D. E. Levin. 1993. A yeast mitogen-activated protein kinase homolog (Mpk1p) mediates signalling by protein kinase C. Mol Cell Biol **13**:3067-3075.
Levin, D. E. 2005. Cell wall integrity signaling in Saccharomyces cerevisiae. Microbiol Mol Biol Rev **69**:262-291.
Longtine, M. S., A. McKenzie III, D. J. Demarini, N. G. Shah, A. Wach, A. Brachat, P. Philippsen, and J. R. Pringle. 1998. Additional Modules for Versatile and Economical PCR- based Gene Deletion and Modification in Saccharomyces cerevisiae. Yeast **14**:953-961.
Lussier, M., A.-M. White, J. Sheraton, T. d. Paulo, J. Treadwell, S. B. Southard, C. I. Horenstein, J. Chen-Weiner, A. F. J. Ram, J. C. Kapteyn, T. W. Roemer, D. H. Vo, D. C. Bondoc, J. Hall, W. W. Zhong, A.-M. Sdicu, J. Davies, F. M. Klis, P. W. Robbins, and H. Bussey. 1997. Large Scale identification of genes involved in cell surface biosynthesis and architecture in *Saccharomyces cerevisiae*. Genetics **147**:435-450.
Ma, J., R. Jin, X. Jia, C. J. Dobry, L. Wang, F. Reggiori, J. Zhu, and A. Kumar. 2007. An interrelationship between autophagy and filamentous growth in budding yeast. Genetics **177**:205-214.
Mewes, H. W., K. Albermann, M. Bahr, D. Frishman, A. Gleissner, J. Hani, K. Heumann, K. Kleine, A. Maierl, S. G. Oliver, F. Pfeiffer, and A. Zollner. 1997. Overview of the yeast genome. Nature **387**:7-65.
Nagai, T., K. Ibata, E. S. Park, M. Kubota, K. Mikoshiba, and A. Miyawaki. 2002. A variant of yellow fluorescent protein with fast and efficient maturation for cell-biological applications. Nat Biotechnol **20**:87-90.

Philip, B., and D. E. Levin. 2001. Wsc1 and Mid2 are cell surface sensors for cell wall integrity signaling that act through Rom2, a guanine nucleotide exchange factor for Rho1. Mol Cell Biol **21**:271-280.

Philippsen, P., K. Kleine, R. Pohlmann, A. Dusterhoft, K. Hamberg, J. H. Hegemann, B. Obermaier, L. A. Urrestarazu, R. Aert, K. Albermann, R. Altmann, B. Andre, V. Baladron, J. P. Ballesta, A. M. Becam, J. Beinhauer, J. Boskovic, M. J. Buitrago, F. Bussereau, F. Coster, M. Crouzet, M. D'Angelo, F. Dal Pero, A. De Antoni, and J. Hani. 1997. The nucleotide sequence of Saccharomyces cerevisiae chromosome XIV and its evolutionary implications. Nature **387**:93-98.

Reinders, J., R. P. Zahedi, N. Pfanner, C. Meisinger, and A. Sickmann. 2006. Toward the complete yeast mitochondrial proteome: multidimensional separation techniques for mitochondrial proteomics. J Proteome Res **5**:1543-1554.

Rieger, K. E., and G. Chu. 2004. Portrait of transcriptional responses to ultraviolet and ionizing radiation in human cells. Nucleic Acids Res **32**:4786-4803.

Ross-Macdonald, P., P. S. Coelho, T. Roemer, S. Agarwal, A. Kumar, R. Jansen, K. H. Cheung, A. Sheehan, D. Symoniatis, L. Umansky, M. Heidtman, F. K. Nelson, H. Iwasaki, K. Hager, M. Gerstein, P. Miller, G. S. Roeder, and M. Snyder. 1999. Large- scale analysis of the yeast genome by transposon tagging and gene disruption. Nature **402**:413-418.

Ross-Macdonald, P., A. Sheehan, G. S. Roeder, and M. Snyder. 1997. A multipurpose transposon system for analyzing protein production, localization, and function in *Saccharomyces cerevisiae*. *Proc. Natl. Acad. Sci. USA* **94**:190-195.

Rost, B., P. Fariselli, and R. Casadio. 1996. Topology prediction for helical transmembrane proteins at 86% accuracy. Protein Sci **5**:1704-1718.

Seifert, H. S., E. Y. Chen, M. So, and F. Heffron. 1986. Shuttle mutagenesis: a method of transposon mutagenesis for Saccharomyces cerevisiae. Proc Natl Acad Sci U S A **83**:735-739.

Siniossoglou, S., H. Santos-Rosa, J. Rappsilber, M. Mann, and E. Hurt. 1998. A novel complex of membrane proteins required for formation of a spherical nucleus. EMBO J **17**:6449-6464.

Thompson, J. D., D. G. Higgins, and T. J. Gibson. 1994. CLUSTAL W: improving the sensitivity of progressive multiple sequence alignment through sequence weighting, position-specific gap penalties and weight matrix choice. Nucleic Acids Res **22**:4673-4680.

Tusher, V. G., R. Tibshirani, and G. Chu. 2001. Significance analysis of microarrays applied to the ionizing radiation response. Proc Natl Acad Sci U S A **98**:5116-5121.

Tusnady, G. E., and I. Simon. 2001. The HMMTOP transmembrane topology prediction server. Bioinformatics **17**:849-850.

Walhout, A. J. M., G. F. Temple, M. A. Brasch, J. L. Hartley, M. A. Lorson, S. v. d. Heuvel, and M. Vidal. 2000. GATEWAY Recombinational Cloning: Application to the Cloning of Large Numbers of Open Reading Frames or ORFeomes. Methods Enzymol **328**:575-592.

Winzeler, E. A., D. D. Shoemaker, A. Astromoff, H. Liang, K. Anderson, B. Andre, R. Bangham, R. Benito, J. D. Boeke, H. Bussey, A. M. Chu, C. Connelly, K. Davis, F. Dietrich, S. W. Dow, M. E. Bakkoury, F. Foury, S. H. Friend, E. Gentalen, G.

Giaever, J. H. Hegemann, T. J. M. Laub, H. Liao, N. Liebundguth, D. J. Lockhart, A. Lucau-Danila, M. Lussier, N. M'Rabet, P. Menard, M. Mittmann, C. Pai, C. Rebischung, J. L. Revuelta, L. Riles, C. J. Roberts, P. Ross-MacDonald, B. Scherens, M. Snyder, S. Sookhai-Mahadeo, R. K. Storms, S. Véronneau, M. Voet, G. Volckaert, T. R. Ward, R. Wysocki, G. S. Yen, K. Yu, K. Zimmermann, P. Philippsen, M. Johnston, and R. W. Davis. 1999. Fuctional characterization of the *S. cerevisiae* genome by gene deletion and parallel analysis. Science **285**:901-906.

Ye, J., S. McGinnis, and T. L. Madden. 2006. BLAST: improvements for better sequence analysis. Nucleic Acids Res **34**:W6-9.

Zarzov, P., C. Mazzoni, and C. Mann. 1996. The SLT2(MPK1) MAP kinase is activated during periods of polarized cell growth in yeast. EMBO J **15**:83-91.

Chapter 6

Conclusions and future directions

How does a cell react to changes in its extracellular environment? This seemingly simple question can lead to some very complicated answers, far beyond the scope of a single thesis. As described in Chapter 1, nutritional controls of yeast metabolism involve overlapping inputs through a sensor system, modification of cell morphology to adapt to the new environment, and a reprogramming of cellular pathways. Although specific components of each pathway have been heavily investigated, previous studies partly disregarded the connections among the pieces of this puzzle. In fact, all pathways simultaneously receive nutrient signals that are integrated into the control of an overlapping set of cellular processes. Elucidating this integration and crosstalk between pathways is very important for the correct understanding of cellular processes.

Upon the transition from nutrient-rich to nutrient-limited medium, yeast cells initiate a morphological change, forming filaments as a means of foraging for a better nutrient supply. Autophagy serves as another mechanism by which cells can survive nutrient stress. The relationship of these two pathways has not been investigated previously, in part because normal lab strains do not undergo filamentous growth. In Chapter 2, our studies show that both pathways are active under conditions of nitrogen deprivation. The inhibition of autophagy results in exaggerated filamentous growth. Our model suggests that both autophagy and filamentous growth mutually mitigate the effects

of nutrient stress, contributing positively to the available pool of nitrogen in the cell. Furthermore, the overexpression of autophagy-related genes can inhibit filamentous growth as shown in Chapter 3, which indicates that, in addition to its role in regulating the nitrogen pool, autophagy might also impact the regulation of filamentous growth. However, the molecular mechanisms underlying this phenomenon are not as clear as the phenotype itself. Our results indicate certain components within the autophagy pathway or other proteins involved in nutrient sensing and signaling might function as links between filamentous growth and autophagy. The direct link is still waiting to be identified, and, given the complexity of the processes, this task will not be easy.

Several lines of evidence from previous research by other groups may guide us in investigating the connection between autophagy and filamentous growth. In Cutler *et al*. (Cutler, Pan, et al, 2001), a novel role for Tor signaling in regulating the transition to filamentous growth was revealed. The Tor protein kinases, Tor1p and Tor2p, play an essential role in nutrient response. The functions of the Tor kinases are inhibited by rapamycin, which will induce the expression of genes required for the utilization of poor nitrogen sources and autophagy. Sublethal concentrations of rapamycin inhibit pseudohyphal differentiation of yeast cells in response to nitrogen limitation. Components of the Tor kinase pathway, Tor1p,Tor2p,Tap42p and Sit4p, are involved in regulating this process. Pseudohyphaal growth can be restored by activation of the MAP kinase and cAMP signaling cascades. Since rapamycin causes the induction of autophagy, these results are consistent with our model (Figure 2.6). Our survival analysis indicates that autophagy plays the major role in facilitating cell survival under conditions of nitrogen deprivation (Figure 2.5). Therefore, slight increases in autophagic activity (or

slight decreases in Tor activity) by sublethal concentrations of rapamycin could relieve cells from the threshold levels needed to activate filamentous growth. Instead, cells can use alternative methods to adapt to the environment, such as expression of the nitrogen catabolite repression (NCR) transcriptional response. The constitutive activation of NCR-regulated genes can block pseudohyphal growth (Lorenz, and Heitman, 1998).

Based on a study from Budovskaya and colleagues (Budovskaya, Stephan, et al, 2004), Ras/PKA signaling, which is one of the major pathways functioning in filamentous growth, has a negative role on the control of autophagy. Elevated levels of Ras/PKA activity were found to result in a complete block of autophagy. Interestingly, the mutational inactivation of the Ras/PKA pathway led to an induction of autophagy activity even in rich growth media that normally inhibit autophagy. This result indicates there might be a threshold for the induction of autophagy as well, and this threshold control might be related to the level of Ras/PKA pathway activity. Ras/PKA has been suggested to function as a key component of a growth checkpoint mechanism in *S.cerevisiae* to ensure that the overall metabolic rate is balanced with the available nutrient supply (Herman, 2002).

Again, the methods appropriate for the study of an individual pathway may not be effective in analyzing a phenotype resulting from the coordination of several pathways, involving fine tuned networks of kinases, transcription factors and downstream targets. Traditional approaches in molecular biology are limited as methods for the study of cellular processes as a whole system. Therefore, the parallel progress of fundamental experimental research and state-of-the-art systems biology is essential for addressing quantitative descriptions of how the different pathways interact with one another. This

level of research requires an integrated resource of quantitative information on a much larger scale, such as expression levels of mRNA and protein, rate constants and stoichiometry of biochemical reactions. The integration of these information sets and the subsequent generation of a pathway network require rigorous mathematical modeling and computational simulation.

A recent paper by Vinod *et al*. (Vinod, Sengupta, et al, 2008) serves as a good example of the approaches through which the yeast nutrient response network can be analyzed on a systematic level. Our study has shown that pseudohyphal growth is a graded response, with increased filamentous growth correlated with decreasing available nitrogen (Figure 2.4). It is reasonable to speculate that yeast cells initiate dynamic changes in response to varying concentrations of available nitrogen source. In the study by Vinod *et al*., the authors investigated how variations in the availability of ammonium sulfate are sensed and transduced by an integrative network comprising cAMP-PKA, MAPK and TOR pathways using experimental and steady-state modeling approach. The expression of *FLO11(also called MUC1)* was quantified as an indicator of filamentous growth. Their findings show that yeast switched from increasing expression of *FLO11* to the accumulation of storage carbohydrate trehalose, with decreased concentrations of ammonium sulfate from limiting conditions (25μM to 300μM) to conditions of complete starvation (below 25μM). Cells prefer initiating filamentous growth under conditions of nitrogen limitation, while preferring the accumulation of trehalose under conditions of nitrogen starvation. A strong double-negative feedback loop in the TOR pathway might be responsible for the *FLO11* bistable response in respect to the concentration of ammonium sulfate. Their model indicates that the cAMP-PKA, MAPK and TOR

pathways function in parallel to integrate signals on the *FLO11* promoter, thereby affecting filamentous growth.

Another layer of complexity comes from the ability of yeast cells to sense the concentration of nutrients, both inside and outside of cells. Obviously, appropriate cellular adjustments can only be made in cells that precisely sense the nutrient status surrounding them. While under conditions of moderate nutrient limitation, cells may initiate autophagy and filamentous growth to get more nutrients. Under conditions of severe nutrient depletion, cells may just enter into stationary phase, thereby lowering metabolic activity for purposes of survival. Yeast cells possess both intracellular sensors and plasma membrane-localized sensors to obtain information regarding the concentrations of amino acids, ammonium and glucose. The Tor kinase acts as part of a signal transduction pathway that senses intracellular nutrients. Intracellular glutamine activates the TOR pathway to promote growth, whereas glutamine depletion inhibits TOR to arrest growth. In addition to its role in ammonium uptake, Ammonium permease Mep2 has been suggested as an ammonium sensor that generates signal required for the induction of filamentous growth. The study by Vinod and colleagues (Vinod, Sengupta, et al, 2008) indicates that the sensitivity of these sensors may be different, with Mep2p exhibiting higher sensitivity towards concentrations of ammonium sulfate than Tor. It remains unclear how the sensors coordinate their activities to set the respective thresholds for initiation of diverse actions.

A protein's localization is typically related to its function, and an understanding of the localization of a protein is regarded as an important step towards the full

understanding of its physiological role. In addition to where a protein is found, the timing and dynamics of its subcellular distribution can be very informative. As I discussed above, the dynamic movements of proteins can help us understand cellular networks more completely. With sequencing of the yeast genome, protein localization can now be pursued on a large-scale.

Compared with transposon-mediated random epitope-tagging followed by immunofluorescence and homologous recombination-based insertion of GFP into genomic loci, our plasmid-based promoter-yORF-fluorescent protein fusion collection has its own advantage. The Gateway system is very useful for high-throughput cloning, since it allows for the automation of otherwise time-consuming cloning processes. After optimization of the protocol, the efficiency of this cloning is high. More than 90% of ORFs with a size less than 4Kb can be cloned into a donor vector on the first try. More efforts are needed to clone larger ORFs. Reagents for the Gateway system are not cheap,; however, the total cost of this process can be lowered by using smaller quantities of reagents without affecting the efficiency of the system. Upon insertion of the promoter-yORF into a donor vector, the resulting entry plasmid can be inserted into any destination vector. In our study described in Chapter 4, a set of destination vectors containing fluorescent proteins was generated. Destination vectors with other epitopes have been generated as well. So it is conveniently possible to generate a plasmid collection with the desired modification(s). The biggest advantage of such a plasmid-based collection lies in its ability to be transformed into diverse genetic backgrounds. Since it can be preferable to study a broad set of genes functioning in the same pathway or within similar functional categories instead of just focusing on several proteins, our collection can serve as a

toolbox to facilitate the study of dynamic protein localization in any number of mutant backgrounds.

In Chapter 4, the localization of ATG genes in a wild type strain and atg11 mutant strain has been checked to show the utility of our collection in identifying regulatory interactions among proteins. Another study conducted in our lab using a kinase-vYFP collection also reveals interesting relationship between these proteins. Bharucha *et al*. (Bharucha, Ma, et al, 2008)have screened all protein kinases in the budding yeast for differential localization during filamentous growth. Our analysis showed six kinases localized evenly across the cell during vegetative growth but localized predominantly in the nucleus under conditions of filamentous growth (Bharucha, Ma, et al, 2008).Further localization-based epistasis studies indicate the existence of an interdependent network formed by these kinases. Using deletion mutants and kinase-dead alleles, we showed that kinase translocation normally requires the presence/activity of another kinase. Several novel filamentous growth-related genes were also discovered in this study. Our current collection contains kinases, transcription factors and selected signaling proteins. One reason to choose these categories for initial study is that the translocalization from cytosol to nucleus or to plasma membrane is relative easy to observe. More sophisticated processes, such as protein trafficking, need more sophisticated approaches, like FRET, which can be used to suggest protein-protein interactions in living cells. Although our collection is definitely applicable to this kind of study, the intensity of fluorescence needs to be enhanced and stabilized to achieve reliable results. By comparing and combining protein localization data with other large datasets on protein function, the knowledge gained from individual studies can be enhanced greatly.

New experimental strategies combined with complete genomic information and automated technologies are moving biological research to a higher systematic level. As more efficient high throughput functional genomic and proteomic technologies are invented, new bioinformatic and statistical approaches will be needed to analyze these data as well.

With improved understanding of the yeast genome, some previously overlooked groups of functionally important DNA sequences are starting to emerge, such as small ORFs, overlapping ORFs, and noncoding RNAs. The discovery of these genome features depends mainly on homology searches across several species and high throughput, high-resolution array-based experiments, including SAGE, DNA microarray analysis, transposon-based gene-trapping studies, mass-spectrometry, etc… In a study by Kastenmayer and colleagues (Kastenmayer, Ni, et al, 2006), the properties of sORFs (small open reading frames, <100 amino acids) were investigated. They discovered that a similar percentage of sORFs are annotated in multiple eukaryotes and that many of the *S.cerevisiae* sORFs have potential orthologs in other eukaryotes (Kastenmayer, Ni, et al, 2006).The idea of overlapping genes or nested genes is not new. These genes were originally discovered in viruses, mitochondria, and other extrachromosomal nuclear elements, which are evolutionarily stable and thought to be involved in genome size minimization. Recently, overlapping genes have been found in the chromosomal DNA of microbes and higher organisms. This genomic structure has been demonstrated to be potentially important for the transcriptional and translational regulation of gene expression and to influence the evolution of genes.

In the human genome, nested genes are frequently found completed within the boundaries of an intron of the host gene, and often in opposite orientation (Yu et al, 2005). More specifically, the majority of the antiparallel overlap occurred between the UTR region of one coding gene and a noncoding RNA on the opposite strand. Although no overrepresented functional classes were detected, some studies suggested that the majority of antisense genes participate in translational regulation instead of functioning as signal transducers. In a high-resolution tiling array study of the yeast transcriptome by David *et al.* (David, Huber, et al, 2006),a group of nonannotated antisense transcripts were highlighted. The authors identified many genes with antisense transcripts functioning in the meiotic cell cycle and in transcriptional regulation. More antisense transcripts overlapped 3' untranslated regions (UTRs) than 5' UTRs, UTRs that had overlapping antisense transcripts were longer than UTRs that did not. However, the function of the majority of these antisense genes is still not clear. In contrast to gene organization observed in the human genome, only 4% of yeast ORFs have introns. Instead of residing opposite to introns, protein-coding sequences have been identified overlapping sequences encoding ribosomal RNA (rRNA). TAR1 has been shown nested opposite the 25S rRNA gene in the rDNA repeat region of Chromosome XII (Coelho, Bryan, et al, 2002). Tar1p localizes to the mitochondria and has a putative role as a mitochondrial protein. Furthermore, the TAR1 ORF is highly conserved among very diverse yeast species. In Chapter 5, I described the identification and characterization of another nested gene *NAG1*, which is located antisense to a protein-coding gene. *NAG1* encodes a protein that localizes to the plasma membrane, and Nag1p is involved in cell wall biogenesis. *NAG1* is conserved among fungi as a unit oriented opposite an ortholog

of the mitochondrial protein YGR031W. It will be interesting to check the potential interactions of the nested and the host gene. Topics such as whether there is correlation of transcription, and what is the real-time transcriptional timing and regulation for a pair of genes, will give us more insightful information on this unusual type of gene organization.

Reference

Bharucha, N., Ma, J., Dobry, C.J., Lawson, S.K., Yang, Z., and Kumar, A. (2008). Analysis of the Yeast Kinome Reveals a Network of Regulated Protein Localization During Filamentous Growth. Mol. Biol. Cell

Budovskaya, Y.V., Stephan, J.S., Reggiori, F., Klionsky, D.J., and Herman, P.K. (2004). The Ras/cAMP-dependent protein kinase signaling pathway regulates an early step of the autophagy process in Saccharomyces cerevisiae. J. Biol. Chem. *279,* 20663-20671.

Coelho, P.S., Bryan, A.C., Kumar, A., Shadel, G.S., and Snyder, M. (2002). A novel mitochondrial protein, Tar1p, is encoded on the antisense strand of the nuclear 25S rDNA. Genes Dev. *16,* 2755-2760.

Cutler, N.S., Pan, X., Heitman, J., and Cardenas, M.E. (2001). The TOR signal transduction cascade controls cellular differentiation in response to nutrients. Mol. Biol. Cell *12,* 4103-4113.

David, L., Huber, W., Granovskaia, M., Toedling, J., Palm, C.J., Bofkin, L., Jones, T., Davis, R.W., and Steinmetz, L.M. (2006). A high-resolution map of transcription in the yeast genome. Proc. Natl. Acad. Sci. U. S. A. *103,* 5320-5325.

Herman, P.K. (2002). Stationary phase in yeast. Curr. Opin. Microbiol. *5,* 602-607.

Kastenmayer, J.P., Ni, L., Chu, A., Kitchen, L.E., Au, W.C., Yang, H., Carter, C.D., Wheeler, D., Davis, R.W., Boeke, J.D., Snyder, M.A., and Basrai, M.A. (2006). Functional genomics of genes with small open reading frames (sORFs) in S. cerevisiae. Genome Res. *16,* 365-373.

Lorenz, M.C., and Heitman, J. (1998). Regulators of pseudohyphal differentiation in Saccharomyces cerevisiae identified through multicopy suppressor analysis in ammonium permease mutant strains. Genetics *150,* 1443-1457.

Vinod, P.K., Sengupta, N., Bhat, P.J., and Venkatesh, K.V. (2008). Integration of global signaling pathways, cAMP-PKA, MAPK and TOR in the regulation of FLO11. PLoS ONE *3,* e1663.

Yu, P., Ma, D., and Xu, M. (2005). Nested genes in the human genome. Genomics *86,* 414-422.